The Pyrylium Dyes: A New Class of Biolabels.

Synthesis, Spectroscopy, and Application as Labels and in

General Protein Assay

Dissertation zur Erlangung des

Doktorgrades der Naturwissenschaften

(Dr. rer. nat.)

der Fakultät Chemie und Pharmazie

der Universität Regensburg

vorgelegt von

Dipl. Chem. Bianca K. Höfelschweiger

aus Hohenthann, Landshut

im Juni 2005

Danksagung

Promotionsgesuch eingereicht am: 02.06.2005

Diese Arbeit wurde angeleitet von Prof. Dr. Wolfbeis.

Kolloquiumstermin: 14.07.2005

Prüfungsausschuß:

Vorsitzender: Prof. Dr. Kunz

Erstgutachter: Prof. Dr. Wolfbeis

Zweitgutachter: Prof. Dr. Dick

Drittprüferin: Prof. Dr. Steinem

Table of Contents

1. Introduction

Fluorescence and the closely related area of phosphorescence have become firmly established and widely used tools in analytical chemistry. In most bioanalytical assays it is not the intrinsic fluorescence of the analyte that is measured. There are many cases where the molecule of interest is non-fluorescent (like DNA), or where the intrinsic fluorescence is not adequate for the desired experiment.

Intrinsic protein fluorescence originates from the aromatic amino acids tryptophan, tyrosine, and phenylalanine. Their emission maxima are in the range of 280-350 nm. In case of proteins it is frequently advantageous to label them with chromophores which have longer excitation and emission wavelength than the aromatic amino acids, in order to separate the signal from the background and intrinsic fluorescence of other biocompounds [1]. These chromophores can be attached covalently or noncovalently to the biomolecules. Many different methods are known [2]. In most cases of covalent labeling the reactive moiety of the label is not part of the chromophoric system, or in other words, the dye has to be activated in an additional synthesis step to become a reactive label.

1.1. Fluorophores and Labels

In general, labels can be divided into three main groups, radioactive labels, enzymatic labels, and luminescent labels.

Radioactive labels are the smallest labels available with the advantage of no steric hindrance. They allow nearly background-free measurements, making these labels very sensitive so that even single particles can be detected. Unfortunately, they sometimes possess a limited working life due to radioactive decomposition. But more seriously, the handling and disposal of radioactive material requires a high degree of safety monitoring and leads to high costs. Reduction of volume quantities is necessary for new assay platforms (e.g. high throughput systems, HTS), but means reducing the concentration of radioisotopes. This extends detection times, and, as radiodecay is irreversible, and the biological system limits the concentration of radioactive tracer, the method has proven challenging [3].

Enzymes are the most widespread labels. The most familiar assay type using enzymatic labels is the ELISA assay. Examples of often used enzymatic labels include peroxidase (POx) and alkaline phosphatases (APases) because of their stability, turnover number and lack of interferences. An enzymatic assay has a high sensitivity since the detectable reaction product

is continuously generated enzymatically. The main disadvantages of enzymatic assays are the need to add reagents, the requirement of repeated washing steps, and a time-consuming incubation, which can lead to the denaturation of proteins. Finally, the use of large proteins may cause steric hindrance of binding events.

Luminescent, in particular fluorescent, labels have gained tremendous popularity during the last years. They possess a very high sensitivity since each binding event continuously generates a signal due to a regeneration of the emitted photons. Furthermore, a host of luminescent dyes is commercially available at various wavelengths. When using luminescent labels in assays, the measurements of several parameters become feasible: luminescence intensity, lifetime τ, anisotropy or emission spectra [3].

Fluorophores are the structural parts of a dye where the fluorescence originates from. A reactive fluorophore which can covalently or noncovalently interact with biomolecular material is called a label. A fluorescent label has the ability to absorb photons and can return to the ground state with emission of fluorescence. According to Stokes' Law, the emission wavelength is always longer and thus of lower energy than the wavelength of excitation. The characteristics of fluorescence (spectrum, quantum yield, lifetime), which are affected by any excited-state process involving interactions of the excited molecule with its close environment, can then provide information on such a microenvironment [4].

There are several requirements for fluorescent biolabels. An ideal luminescent label should possess the following properties [5]. The fluorophore is expected to have a high molar absorbance. Charged groups (usually anionic) are often introduced into the biolabel to avoid undesired electrostatic attraction to the biomolecule. The fluorophore should be stable and soluble in organic solvents and in water. The fluorescence of the label should be weak in its unconjugated form and high if bound to the target (a large quantum yield in order to obtain a high light intensity). Fluorescence is expected to be pH-independent in the physiological range between pH 5 and 9. Besides, a high photostability and at least one reactive group for coupling to the target at ambient temperature under mild reaction conditions are required.

The number of fluorophores has increased dramatically during the past decade. Numerous fluorophores are available for covalent labeling of biomolecules. Fluorescein has an absorption maximum around 490 nm which nicely matches the Argon-laser line. Most fluorescein derivatives display low photostability and their fluorescence is pH dependent. Oregon Green, one of these derivatives, has a better photostability, and its fluorescence is independent in the pH range above 5 (fig. 1.1., left structure).

Coumarines are another extensively investigated and commercially significant group of fluorescent dyes. Alexa dyes are developed as fluorescent, photostable and pH-insensitive dyes with bright emission that is retained on conjugation [6]. Their structures are based on coumarines or rhodamines.
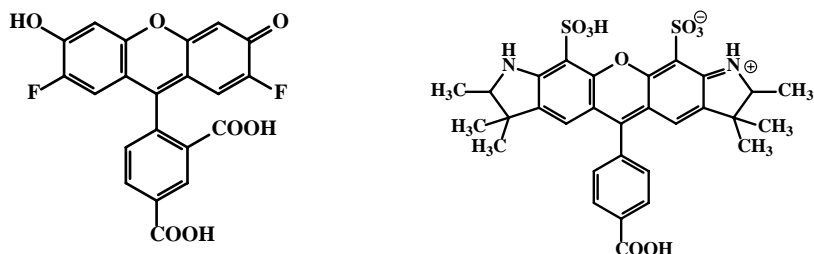
Fig. 1.1.   Chemical structure of Oregon Green (λ_{exc} 490 nm, λ_{em} 514 nm, left structure) and Alexa532 (λ_{exc} 530 nm, λ_{em} 554 nm, right structure).

Another class of dyes, the so called Bodipy-dye, was introduced for the replacement of fluoresceins and rodamines. These dyes are based on an unusual boron-containing fluorophore. They compensate the disadvantages of fluorescein, but have a very small Stokes' shift of 10 nm (fig. 1.2., left structure).

The cyanine dyes were established as long-wavelength dyes. They display absorption and emission wavelengths of 530-750 nm with a small Stokes' Shift. Charged side chains are used for improved water solubility and to prevent self-association, which is a common cause of self-quenching, a tail in the spectra and a multi-exponential decay time [1]. Prominent examples are Cy3 and Cy5 (fig. 1.2., right structure).
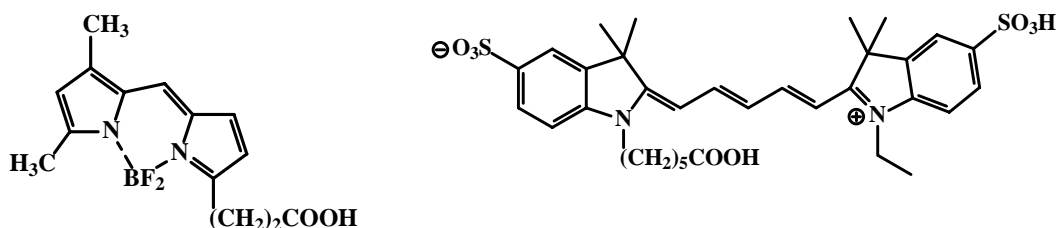
Fig. 1.2.   Structure of Bodipy®FL (λ_{exc} 505 nm, λ_{em} 513 nm, left structure) and Cy5 (λ_{exc} 635 nm, λ_{exc} 665 nm, right structure).

Phthalocyanine dyes contain a central metal and a porphyrin ring system. Most of them are very poorly water soluble. They have attracted interest for their potential use in optical and conductive materials (fig. 1.3., left).

Ruthenium complexes are representatives for metal-ligand based fluorophores. The dyes consist of a central transition metal ion with one or more diimine ligands. These complexes

display luminescence decay times ranging from 100 ns to several µs. Therefore, gated fluorescence intensity measurements are one of their important application fields. They are also found in applications as polarization labels.
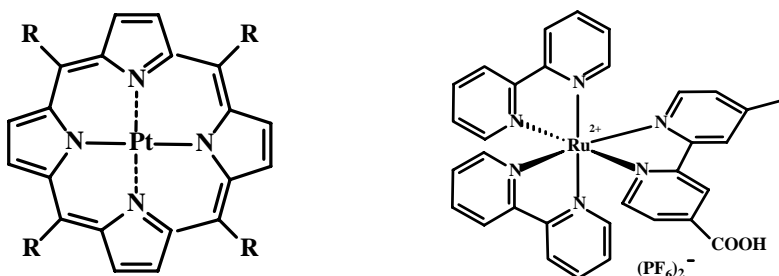
Fig. 1.3.   General structure of a metal porphyrin complex and the structure of Ru-tris-(bipyridine).

Fluorescent proteins, e.g. phycobiliprotein, which can be isolated from a variety of algae, exhibit extremely high absorptivities, high quantum efficiency, and excitation and emission bands across the visible spectrum. These stable, hydrophilic proteins can easily be linked to antibodies by conventional protein cross-linking reagents [7]. They are sensitive to elevated temperatures and extreme pH values. Of course there are several other classes of dyes besides those mentioned above, but the most important classes are named.

1.2. Labeling Techniques

The interest in bioanalysis focuses on analytes such as proteins and nucleic acids (DNA/RNA). They are not detectable in the visible range of light. Therefore labels, especially fluorescent labels, can be attached for detection. The conjugation process involves the reaction of one functional group with another, resulting in the formation of a covalent bond [2]. In the following chapters some labeling techniques for proteins and amino-modified oligonucleotides are shown in brief.

1.2.1. Common Labeling Techniques for Proteins

Functional groups at the side chains as well as at the C and at the N terminal ends of the peptide chain of proteins can be used for labeling. A reactive group in proteins in neutral or basic aqueous solution is the thiol group of the amino acid cystein. The iodacetamide, the maleimide, and the disulfide exchange method are the most frequently used methods for thiol labeling (fig. 1.4.).
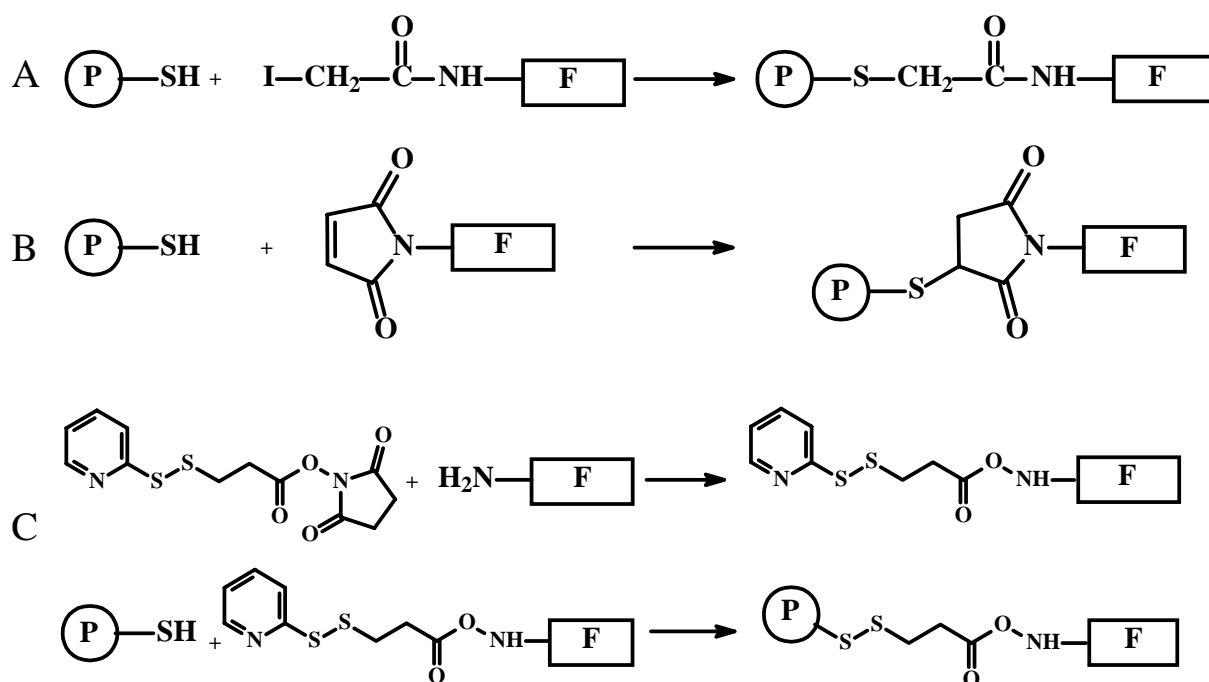
Fig. 1.4.   Common methods for thiol labeling. (A) the iodacetamide, (B) the maleimide, and (C) the disulfide exchange method. P denotes a protein, F a fluorophore.

The most common functional group for cross-linking or for modification of proteins, peptides or a host of other macromolecules is the amino-group [2]. Reactive esters, especially oxysuccinimide (OSI) esters, are some of the most frequently used reagents for amino group labeling. The labeling reaction competes with hydrolysis of the active ester but the rates of both reactions depend on the pH. Most labeling reactions with active esters are carried out between 8.5 and 9.5 over a period between 15 min to several hours (fig 1.5., A). There are, however, several drawbacks to the use of OSI esters as labeling agents of proteins. As they are uncharged, they are often insoluble in water, requiring the use of an amount of organic cosolvent for solubilization. This can cause damages to some proteins and can induce denaturation. Furthermore, the modification of proteins by OSI esters involves a change in the global charge of the protein which in turn changes its solubility properties [8].

Isothiocyanates are amine modifying reagents of intermediate reactivity. They are somewhat more stable in water than the OSI esters and react optimally with proteins at pH 9.0 – 9.5 (fig. 1.5., B). Sulfonylchlorides are highly reactive labels. They are unstable in water but form extremely stable sulfonamide bonds which can survive even amino acid hydrolysis (fig 1.5., C).
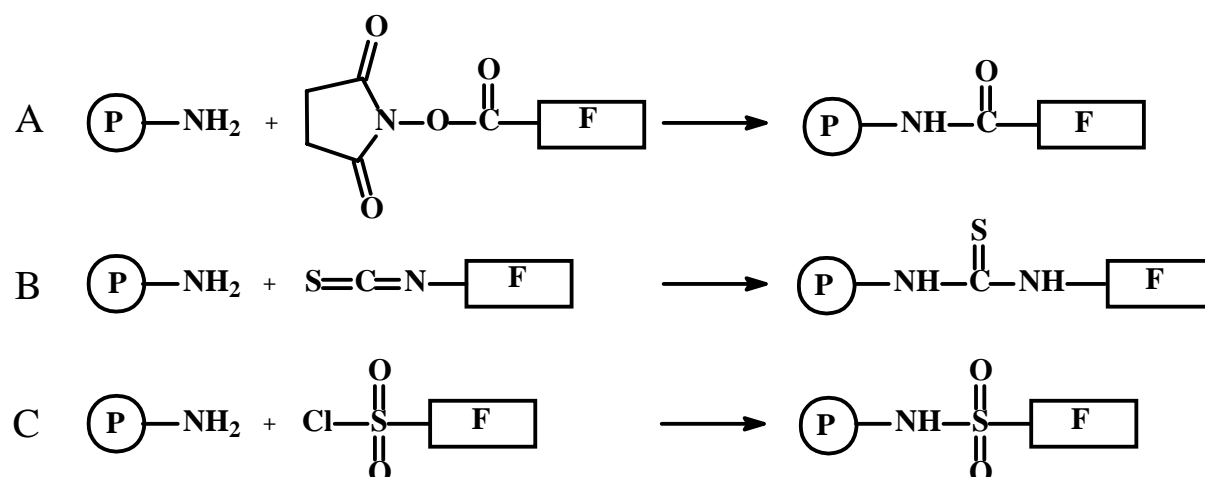
Fig. 1.5.   Common methods for labeling amino groups. (A) the succinimidyl active ester method, (B) the isothiocyanate method and (C) the sulfonylchloride method. P denotes a biomolecule, for example a protein, F a fluorophore.

For completion it has to be noted that carboxy acid groups and hydroxy groups of biomolecules, for example aspartic acid, glutamic acid, serine and threonine in polypeptides play a under part role for labeling. In aqueous solution, the carboxylated functional groups display rather low nucleophilicity and therefore reactivity.

1.2.2. Pyrylium as an Amine-Reactive Group

Pyrylium ions are heterocyclic aromatic compounds that have been shown to react in a specific manner and under very mild conditions with protein amino groups by exchange of oxygen to nitrogen to form positively charged N-substituted pyridinium adducts [9]. The mechanism of the pyrylium-pyridinium conversion has been thoroughly studied (fig. 1.6.).
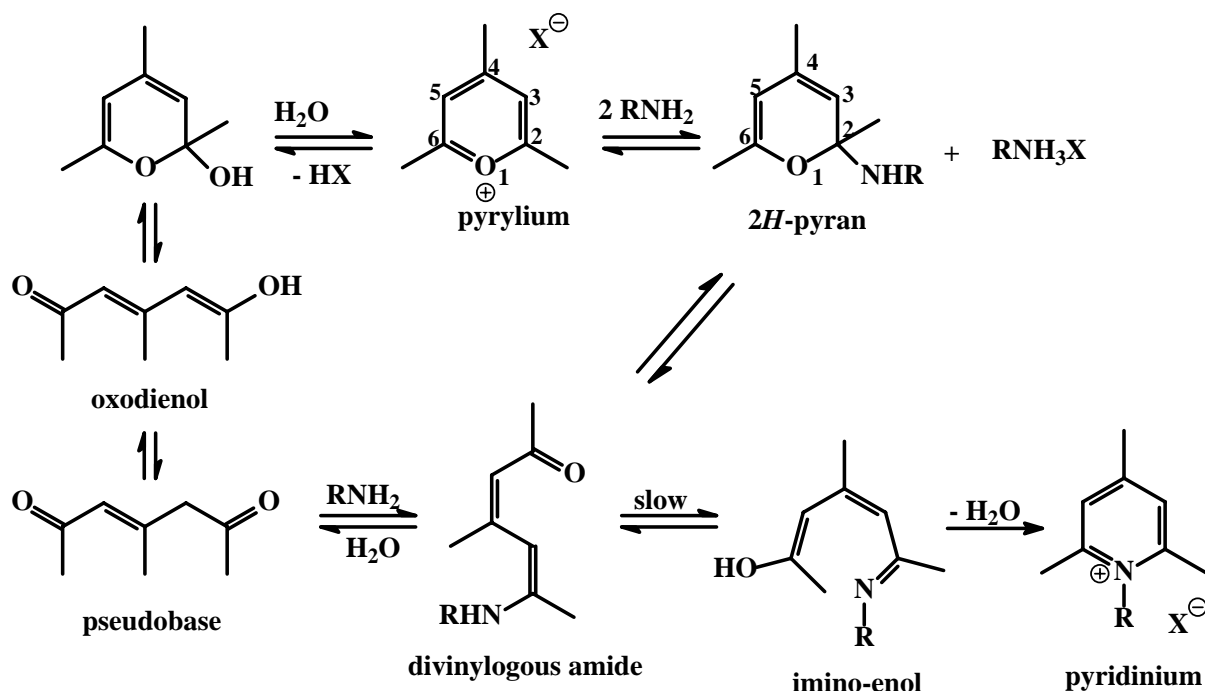
Fig. 1.6.   General mechanism of the reaction of pyrylium ions with primary amines

Addition of amine occurs at position 2 and 6 and yields the first intermediate 2*H*-pyran, which generally has a very short lifetime. This ring spontaneously opens to form the second intermediate, a divinylogous amide, which is usually more stable. This divinylogous amide tautomerises into an imino-enol, which rapidly cyclises into the pyridinium product. The rate determining step is the conversion of the divinylogous amide to the pyridinium product.

The rate of formation of the pyridinium species is depending on the substituents in ortho and para position to the oxygen in the pyrylium salt. The lower steric crowding of for example two methyl groups instead of two phenyl groups in ortho-position leads to an increasing rate of reaction, but causes also a less stability of the pyrylium in aqueous solution. Additional steric substituents in the para-position to the pyrylium oxygen also decrease the rate of reaction, which could be due to an increase of the steric crowding in the transition state. Stability of a pyrylium salt in aqueous medium of different pHs is dependent on the equilibration of the pseudobase via 2*H*-pyran and oxodienol intermediates [9].

Figure 1.7. shows the reaction mechanism of labeling a protein with a chromophore via a reactive pyrylium group. The advantage of this new reactivity is that the pyrylium is part of the chromophoric system, which means that no extra activation step of the dye as with an OSI ester is necessary.
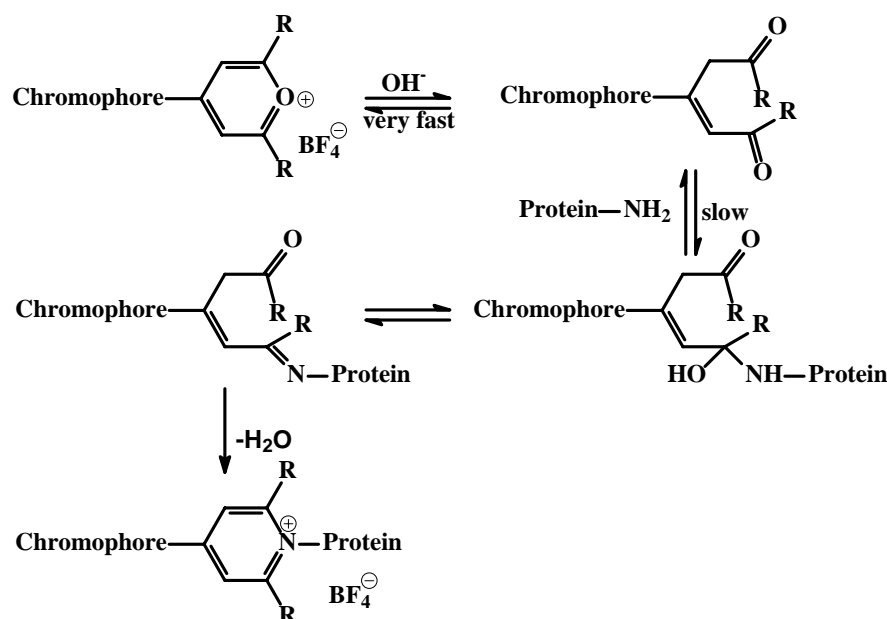
Fig.1.7.   Mechanism scheme of the reaction of a Py label with a primary amine of a protein.

In addition, the labeling with a pyrylium reactive dye does not change the charge of the protein. The amino-groups in proteins at neutral pH are protonated, which means they have a positive charge, and after covalent labeling with the dye this positive change is preserved.

1.3. Motivation and Aim of Work

Pyrylium was introduced as a reactive group in the 1970s, but only in 2000 it became known for fluorescence labeling techniques. A reactive pyrylium group can be introduced into numerous organic or metal organic compounds.

In the presented work, a new class of dyes, the Py labels, are introduced and characterized. A range of representatives was synthesized and examined according to synthesis and yield, chemical and photophysical behavior, spectral characteristics, reactivity and usefulness in bioanalytical applications. Attention is focused especially on the new reactivity. Py labels need no further activation step. The reactive moiety is part of the label. Py labels react with primary amino groups to form a covalent bond. The spectral differences of the dyes in the reactive label form, and the label bound to a primary amino group of several aliphatic compounds and biomolecules is another new feature of these labels. This effect was used in bioanalytical applications described in chapter 4.

1.4. References

[1] J.R. Lakowicz, Principles of Fluorescence Spectroscopie (2nd edition), Kluwer Academic/Plenum Publisher, New York **1999**.

[2] G.T. Hermanson, Bioconjugate Techniques, Academic Press, New York **1996**.

[3] P. Gribbon, A. Sewing, Fluorescence Readouts on HTS: No Gain without Pain, DDT **2003**, 8, 1035-1043.

[4] B. Valeur, Molecular Fluorescence, Principles and Application, Wiley-VCH, Weinheim **2002**.

[5] T. Soukka, J. Paukkunen, H. Härmä, S. Lönnberg, H. Lindroos, T. Lövgren, Supersensitive Time-resolved Immunofluorometric Assay of Free Prostate-specific Antigen with Nanoparticle Label Technology, Clinical Chem. **2001**, 47, 1269-1278.

[6] N. Panchuk-Voloshina, R.P. Haugland, J. Bishop-Stewart, M.K. Bhalgat, P.J. Millard, F. Mao, W. Leung, R.P. Haugland, Alexa Dyes, a Series of New Fluorescent Dyes that Yield Exceptionally Bright, Photostable Conjugates, J. Histochem. Cytochem. **1999**, 47, 1179-1188.

[7] M.N. Kronick, P.D. Grossman, Immunoassay Techniques with Fluorescent Phycobiliprotein Conjugates, Clin. Chem. **1983**, 29(9), 1582-1586.

[8] M. Salmain, K.L. Malisza, S. Top, G. Jaouen, M.-C. Sénéchal-Tocquer, D. Sénéchal, B. Caro, [η^5-Cyclopentadienyl]metal Tricarbonyl Pyrylium Salts: Novel Reagents for the Specific Conjugation of Proteins with Transition Organometallic Labels, Bioconj. Chem. **1994**, 5, 655-659.

[9] B. Caro, F. Le Guen-Robin, M. Salmain, G. Jaouen, 4-Bechrotrenyl Pyrylium Salts as Protein Organometallic Labelling Reagents, Tetrahedron **2000**, 56, 257-263.

2. Background

2.1. Methods of Protein Determination

The analysis of a protein pattern, its temporal changes, and the interpretation of its function is one of the most fascinating technologies at present. It is often referred to as proteomics [1, 2]. The *proteom* can be defined as all proteins expressed by a cell at a particular time and under specific conditions. Proteomics is the study of all the proteins, which requires identification of the proteins and analyzing their role in physiology as well as the pathologic state. The growth of proteomics can be illustrated in a plot showing the number of citations in each year (fig. 2.1.). The increasing number of citations (search parameter "proteome*" in the DCBI database) shows the interest in the proteomics field.
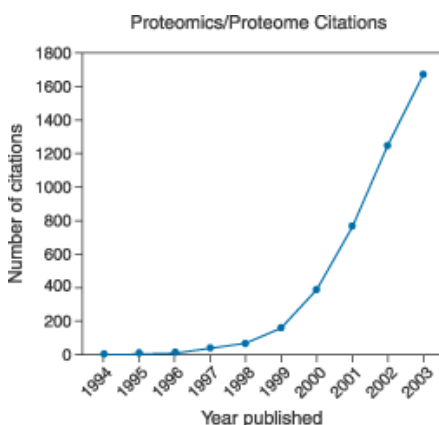
Fig. 2.1.   Growth of proteomics. Figure from literature [3].

2.1.1. Separation and Staining of Proteins in SDS Gel Electrophoreses

Protein patterns can be analyzed by a variety of methods including gel electrophoresis, blotting, or via so-called biochips. While biochips (and protein arrays) are preferably applied to systems of known protein composition to identify specific proteins, electrophoresis in 1- or 2-dimensional form is readily applied to unknown samples [4, 5].

For decades, polyacrylamide gel electrophoresis and related blotting techniques have formed the core of technologies for protein analysis [6]. Gel electrophoresis is commonly used to analyze the composition of complex protein mixtures and to determine the relative abundance of particular protein or polypeptide species in such preparations [7]. Electrophoresis of denatured reduced proteins in the presence of SDS on polyacrylamide gels (SDS PAGE) is particularly useful for estimating the size and purity of polypeptides.
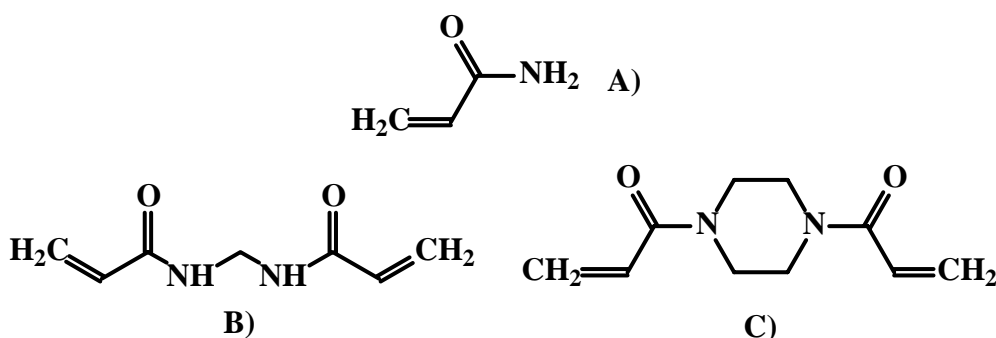
Fig. 2.2.   Structure of monomeric acrylamide (A) and of the cross linking agents: (B) N,N'-methylene-bis-acrylamide (bis) and (C) diacrylylpiperazine.

Figure 2.2. shows the structure of the monomer acrylamide for polyacrylamide gels and two cross linking agents B) and C). The pore size in a polyacrylamide gel is dependent on the total concentration of acrylamide and the cross linking agent and described via T and C:

$$T = \frac{m(\text{acrylamide}) + m(\text{bis}) \bullet 100}{mL(\text{solution})} [\%]$$

$$C = \frac{m(\text{bis}) \bullet 100}{m(\text{acrylamide}) + m(\text{bis})} [\%]$$

With increasing T the pore size in the gel decreases. The smallest pores appear with C between 2 and 5%. The polymerization of acrylamide is started with ammonium persulfate (AP) and N,N'-tetramethylenediamine (TEMED) as the basic component for promotion of the decomposition of AP to a radical. An acrylamide gradient gel (for example 5% at the top to 20% at the botton) is especially useful, when small to very large proteins should be separated on one gel [8]. The detergent SDS (sodium dodecylsulfate) forms complexes with most proteins, coating the protein surface with SDS molecules in a ratio of 1.4 mg SDS per mg protein. These large negatively charged aggregates can be separated according to their size which correlates well with their molecular weight. This separation of denatured proteins in a gel is called SDS-PAGE.

The methods chosen for the detection of proteins after electrophoresis may depend on the amount and type of proteins in the gel, as well as on the subsequent use of the identified polypeptide(s), and on the requirements for quantitation or storage of information from the gel [7]. Standard methods for visualization include silver staining or staining with dyes such as Coomassie Brilliant Blue or Amido Black B [9-11].

Fluorescent methods for staining and visualization of proteins have experienced particular interest because of the sensitivity of (laser-induced) fluorescence which meanwhile

has reached the nano- and picomole (if not zeptomole or single molecule) level, at least for solutions.

Two types of fluorescent protein stains need to be distinguished: The first involves non-covalent protein-probe interaction, the second involves covalent linkage of the stain to a functional group of a protein (such as amino or thiol). Both have their merits.

2.1.1.1. Noncovalent Staining of Proteins in SDS PAGE

Since its introduction nearly 40 years ago, Coomassie Brilliant Blue (CBB) staining of polyacrylamide gels in an aqueous solution of methanol and acetic acid followed by destaining in a similar solution lacking dye has proven as a popular protein detection technique. The sensitivity of CBB staining techniques is relatively poor.
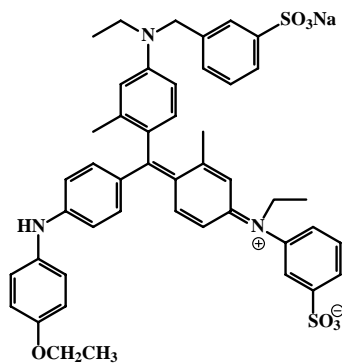
Fig. 2.3.   Structure of Coomassie Brilliant Blue (CBB) R250 (λ_{max}^{abs} 580 nm).

Silver staining methods are considerably more sensitive than CBB staining procedures, often permitting the detection of low nanogram amounts of protein [12]. Despite its complicated and poor defined binding mechanism, it is well known that silver has variable binding characteristics towards many proteins and a relatively low dynamic range (1-60 ng on 1-D gels) [12, 13].

The measurement of light emission is intrinsically more sensitive than measurement of light absorbance, however, as absorption is limited by the molar extinction coefficient of the colored complex. Thus fluorescent protein stains often provide greater sensitivity and broader linear dynamic responses when compared to their colorimetric counterparts. The widespread adoption of ethidium bromide, SYPRO Green and SYPRO Gold stain for fluorescence detection of nucleic acids has bolstered acceptance of fluorescent stains as tools for the routine analysis of proteins [14, 15]. The use of fluorescence based approaches for protein detection has become more common in the recent years.

Typical non-covalent protein stains include the SYPRO dyes (certain organic or metal-organic fluorochromes) that give red or pink emissions [7, 12, 14]. The stains bind to the SDS coat of the proteins with high affinity which then can be determined in gels in quantities of 2 – 10 ng/band. The hydrophobic dye 1,8-ANS (1-anilinonaphthalene-8-sulfonic acid) and Bis-ANS (4,4'-dianilino-1,1'-binaphthyl-5,5'-disulfonic acid) are used for noncovalently protein binding after SDS-PAGE, resulting in fluorescence staining with a sensitivity roughly equivalent or even more sensitive than CBB [7].

2.1.1.2. Covalent Staining and Pre-Staining of Proteins in SDS-PAGE

A covalent linkage to the protein is stable (i.e. the tag cannot be washed out), while non-covalent labeling enables, for example, mass spectroscopy to be performed, because no change in the total mass of the protein occurs on staining. The stain can be removed from the proteins in the gel after detection and before determination in MS [16].

Covalent fluorescent labeling is also widely used in polyacrylamide gel electrophoresis (PAGE) or protein blotting techniques. Conjugation is achieved by either pre-staining or after electrophoresis. The reactive dye forms a covalent bond with a specific group of the protein, e.g. the amine or thiol group. A variety of covalent labels are known [7, 12, 14, 17-19]. BODIPY dyes are used as permanent protein blot stains [6]. Covalent fluorescent labeling with rhodamine B isothiocyanate, fluorescamine or with carboxytetramethylrhodamine succinimidyl ester results in very sensitive protein detection but changes the electrophoretic mobility of the proteins labeled before the run. The sensitivity of covalent fluorophores is always a function of the number of available primary amines or thiols. However, all of these labels have spectral properties that are identical (within a few nm) with those of the labeled protein. This requires, however, that – in case of staining after electrophoresis - excess label has to be washed out very carefully from the gel or blot in order to minimize fluorescent background.

2.1.2. Quantitative Protein Determination in Solution

Biogenic amines and proteins are among the most frequently analyzed species in biosciences. Not surprisingly, numerous photometric and fluorimetric methods for quantitative protein assay do exist (see table 2.1.).

Table 2.1.   Schedule of common methods for quantitative protein determination in solution.

Assay Method	Useful Range	Comments
BCA method[a]	0.5 µg/mL to 1.5 mg/mL	redox reaction (with proteins) generates Cu^+, which forms with BCA a purple complex [20]
Bradford assay [a]	1 µg/mL to 1.5 mg/mL	CBB is bound to a protein and its λ_{max} shifts from 465 to 595 nm [20]
Lowry assay [a]	1 µg/mL to 1.5 mg/mL	Cu^+ reduces the yellow Folin-Ciocalteu reagent to a deep blue color [20]
absorbance at 280 nm [a]	50 µg/mL to 2 mg/mL	determination of absorbance of some aromatic amino acids (Phe, Tyr, Trp) at 280 nm, strong interference by several other biomolecules [20]
NanoOrange assay [b]	10 ng/mL to 10 µg/mL	dye interacts with the protein and gives a strong fluorescence, exc/em 470/570 nm [6]
ATTO-TAG CBQCA protein quantitation kit	100 ng/mL to 1.5 mg/mL[c]	non fluorescent component forms a fluorescent conjugate with a protein and KCN, which can be excited between 430-490 nm and the emission detected at 525-600 nm
Py-1 assay	$LOD_{fluorimetric}$ 60 ng/mL[d] $LOD_{photometric}$ 1.2 µg/mL[d]	amine reactive dye forms a fluorescent conjugate with proteins in buffered solution and can be excited around 500 nm and displays a strong fluorescence over 600 nm [21] (see chapter 4.1.2)

[a] Product information, Molecular Probes, N-6666

[b] calculated using the data given in the product information (www.probes.com)

[c] calculated using the data given in literature [6, 22]; the graph in the catalog gives 10 ng, but this is for a 100 µL assay; thus the LOD is 100 ng/mL

[d] preliminary data (see chapter 4.1.2.)

2.1.2.1. Photometric Detection

Photometric approaches are based on either the intrinsic absorbance at 280 nm [23], or on reagent-based assays such as the Lowry assay [24], bicinchoninic acid (BCA) [25] and Bradford assay [26], but these suffer from limited sensitivity and often from tedious procedures [22]. The direct photometric assay, in turn, is heavily interfered by any substance also absorbing at 280 nm (e.g. amino acids).

2.1.2.2. Fluorescence Detection

Fluorimetric protein assays have been reported and are generally more sensitive than photometric assays. They include methods based on endpoint detection of enzymatic reactions [27] or on fluorogenic reagents such as fluorescamine, *ortho*-phthalaldehyde (OPA), NanoOrange, or another quinolinoic acid reagent refered to as ATTO-TAG™ CBQCA [22, 27-29].
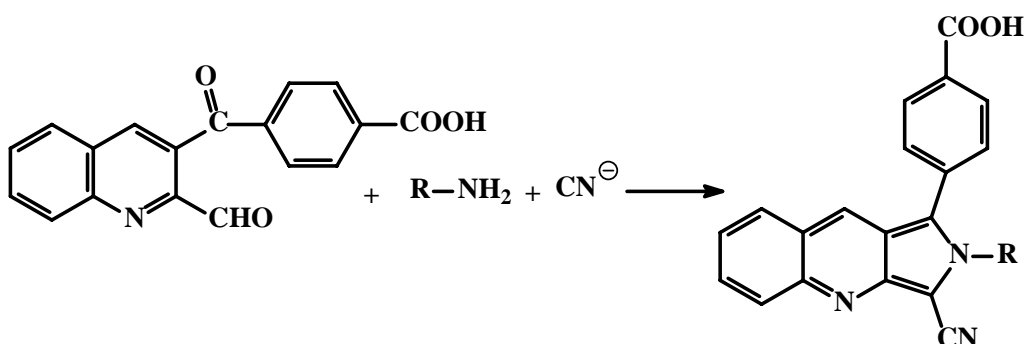
Fig. 2.4.   Fluorogenic amine derivatization reaction of 3-(4-carboxy-benzoyl)quinoline-2-carboxaldehyde (CBQCA) with proteins (exc/em 430-490/525-600 nm).

Fluorescamine has to be used in a large excess and suffers from a high rate of hydrolysis, which results in high blanks. The OPA method requires the addition of mercaptoethanol (with its characteristic smell) and requires excitation at 340 nm, which causes substantial fluorescence background by almost any biological matter. The CBQCA protein assay (fig. 2.4.) needs the addition of potassium cyanide but yields a product that can be excited at longer wavelengths (between 430 and 490 nm) than that of OPA. Reactions typically are complete after 30 to 90 min at room temperature.

2.2. Methods of Optical Immunoassays

2.2.1. ELISA Based Immunoassay

Immunoassays constitute a large and diverse family of assays. The most commonly used immunoassay format is the enzyme-linked immunosorbent assay (ELISA) owing to its high sensitivity and applicability to a wide range of antigens. ELISA is described as a heterogeneous assay. The most simple ELISA is, when the antigen is attached to the surface of a microplate, the antibody against this antigen is linked to an enzyme, dissolved in buffer and added to the antigen. Excess of antibody is washed away and the antigen/antibody-enzyme complex is detected via a substrate, which is converted by the enzyme and affects a chromogenic dye solution. This is a so called direct ELISA. The other two basic systems used for ELISA are indirect ELISA, and Sandwich ELISA. The indirect ELISA needs one additional specific antibody. The first antibody is specific against the antigen, the wells are washed and any bound antibody is detected by addition of antispecies antibody to which an enzyme is linked covalently. Such antibodies are specific for species, in which the first antibodies added were produced [30].

The sandwich ELISA is similar to the other two methods described before. The sandwich ELISA can also be direct or indirect, but this system exploits antibodies attached to a solid phase to capture antigen. The antigen is then detected using a second specific antibody labeled with enzyme. The antigen must have at least two different antigenic sites.

The indirect detection is done by adding a third antibody, which is labeled with an enzyme and binds to the second (detection) antibody specifically, but not to the capture antibody. Here the sandwich consists of the first antibody bound to the surface, the antigen, the second antibody and the third antibody, labeled with the enzyme.

2.2.2. FRET Based Immunoassays

Fluorescence resonance energy transfer (FRET) immunoassays are homogeneous and self referenced assays, where no separation steps are required. Energy transfer (ET) is the result of long-range dipole-dipole interaction between donor and acceptor. The rate of energy transfer depends on the extent of overlap of the emission spectrum of the donor with the absorption spectrum of the acceptor, the relative orientation of the donor and acceptor transition dipoles,

and their distance. The energy received by the acceptor is less than that given by the donor. The remaining energy is consumed by radiationless transition to the ground state (fig. 2.5.).
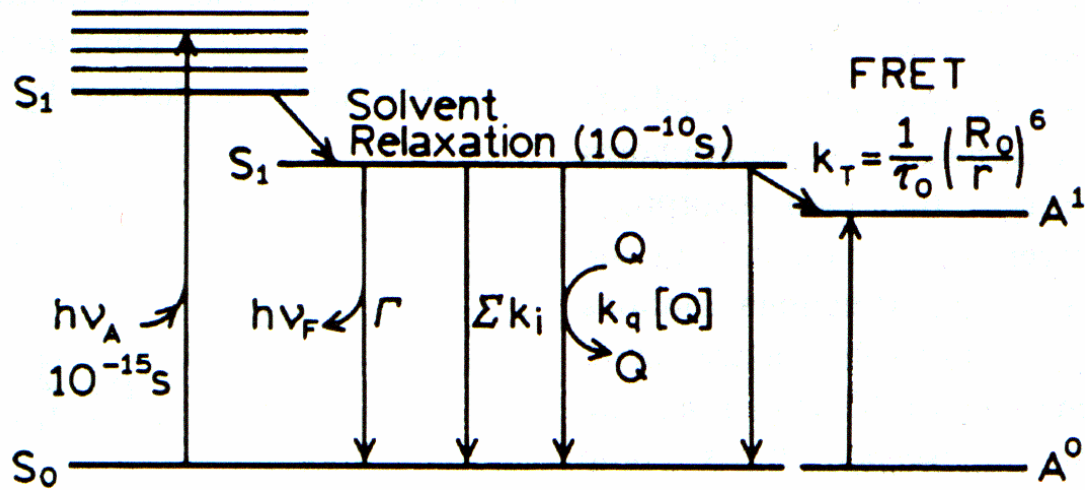
Fig. 2.5.   Jablonski diagram with collisional quenching and FRET: singlet energy transfer from donor to acceptor. $\sum k_i$ is used to represent nonradiative paths to the ground state besides quenching and FRET [31].

The rate of energy transfer (k_{ET}) form a specific donor to a specific acceptor is given by

$$k_{ET} = \frac{1}{\tau_D} \cdot \left(\frac{R_0}{r} \right)^6 \qquad (1)$$

where

      τ_D: lifetime of the unquenched donor in absence of acceptor

      r: the distance between donor and acceptor

      R_0:   Förster distance (where the efficiency of energy transfer is 50%)

At R_0, one half of the donor molecules decay by energy transfer and the other half due to usual radiative and nonradiative transition. Equation (1) shows that k_{ET} is dependent on the inverse sixth power of the intermolecular distance. Thus, FRET can be used for monitoring distances between donor and acceptor labeled targets. The conditions for FRET to occur are a) donor and acceptor molecules have to be in close proximity (typically 10-100 Å), b) the absorbance spectrum of the acceptor has to overlap the fluorescence emission spectrum of the donor and c) donor and acceptor transition dipole orientations have to be approximately parallel, and must not be oriented perpendicularly to each other, respectively [31, 32].

A FRET assay can be performed in a competitive format, which means that the analyte competes with a labeled compound for a binding place on a second also labeled compound. This means for example the antigen is labeled with a fluorescence donor dye and the

corresponding antibody is labeled with an acceptor dye. If non-labeled antigen is added, the donor labeled antigen is displaced and energy transfer efficiency is reduced. The acceptor dye can either be a quencher or, preferably, a fluorescent dye. If both donor and acceptor are fluorescent, ratiometric (2-wavelength) data evaluation is possible [31].

2.2.3. Immunoassays Based on Fluorescence Decay Time

A different approach is the investigation of the temporal properties of the fluorophores [33]. The fluorescence decay time τ is one of the most important characteristics of a fluorescent molecule, because it defines the time window for observation of dynamic phenomena.
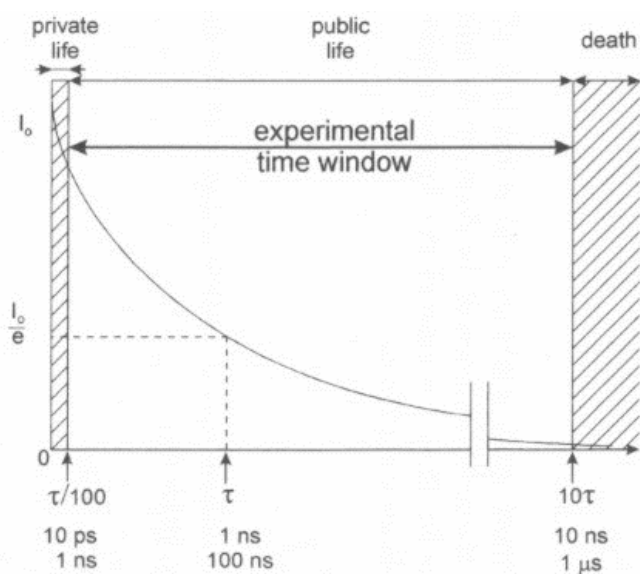
Fig. 2.6.   Decay of fluorescence intensity [34].

The lifetime τ is the time needed for the concentration of molecular entities to decrease to 1/e of its original value [34].

2.2.3.1. Time Gated Fluorescence Measurements

Gated fluorometry is a method for measuring fluorescence intensity as a function of analyte concentration. The measurement is started after the background fluorescence (lifetime < 20 ns) has ceased, while the fluorescence decay of the probe (lifetime > 1 µs) is still going on. It has the specific feature of enabling the suppression of potentially interfering background fluorescence. The scheme in figure 2.7. shows the principle of time-gated fluorescence experiments.
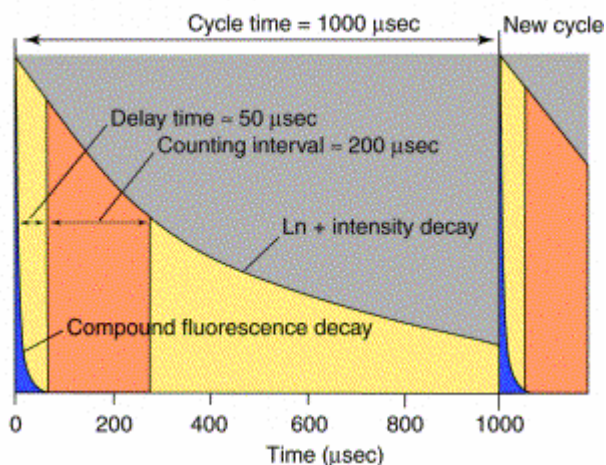
Fig. 2.7.   Principle of time-gated fluorescence lifetime experiments with an extremely long-lived emission (example of lanthanide complex).

This technique makes use of lanthanide complexes, which exhibit extremely long lived emission resulting from forbidden transitions between 5d and 7f orbitals. Europium and terbium labels have attracted particular interest because of their very long decay times (which can be in the ms range) and their line-like and longwave emissions. Various methods and applications, such as DELFIA, FIAgen and TRET, were established [35-40]. However, these labels require UV excitation, whereby absorbance owing to test compound and biological matrices reduces signal level due to the inner filter effect, and assay protocols are complicated needing enhancer reagents. The actual measured parameter is the fluorescence intensity within the pre-determined time-window, rather than the more reliable lifetime change. Thus, the measurements are not self-referenced, but employ internal correction schemes [41]. However, time gated fluorescence lifetime measurement still depends on the amount of fluorophores presented, on photobleaching and on the fluctuation of the light source.

2.2.3.2. Fluorescence Decay Time Measurements in Immunoassays

Fluorescence decay time is (in contrast to gated fluorometry) representing a self-referenced parameter which is not intensity based. In this scheme, the decay profile (or phase shift) of the emission is related to the respective excitation signal. Decay times can be determined in various ways, but preferably in either the frequency domain or the time domain [32].
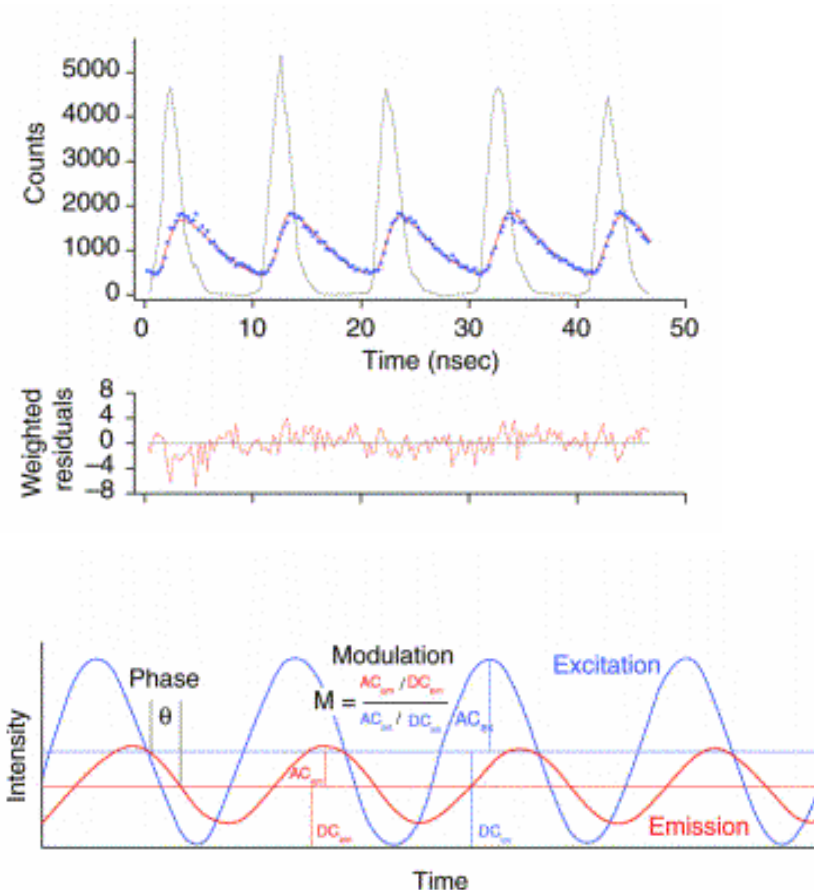
Fig. 2.8.   Top: The principle of the single photon counting technique. The graph shows experimental data (blue) and fit (red) against the pulse-train profile. Middle: The graph is a plot of weighted residuals (deviation of the data from the theoretically fitted function) used for the fit quality control. Bottom: The principle of the frequency-modulated method for measurement of fluorescence lifetime.

Time Domain Measurement. In the domain or pulse method, the sample is excited with short pulses of light and the time-dependent decay of luminescence intensity is measured (fig. 2.8.). The photon counting method measures the decay of the luminescence by recording the first photon after very weak pulses, whereas the pulse sampling method measures different periods after each pulse to obtain the whole time-resolved decay. The pulse method has the

advantages that disturbing fluorophores with lifetimes shorter than the incident light pulse are not measured. Short-lived background fluorescence can thus be easily separated. The disadvantage of the pulse method is the use of very sophisticated instrumentation. A detector with very short response time and a high bandwidth is needed not to distort the signals by time. Another problem is the light sources available, which can yield picosecond pulses with constant intensity. The observed luminescence decay has to be corrected for the width of lamp pulses, which is the so called deconvolution [41].

Frequency domain measurement. In the frequency domain or phase modulation method the sample is excited by sinusoidally modulated light. The lifetime of the fluorophore causes a time lag between absorbance and emission, expressed by the phase shift θ and a decreased emission intensity relative to the incident light, called modulation M (fig. 2.8. bottom). This phase and modulation change is directly related to the lifetime and is used to calculate the lifetime with the help of equ. (2):

$$\omega \cdot \tau = \tan \theta = \left(\frac{1}{M^2} - 1 \right)^{1/2} \qquad (2)$$

where   ω: angular modulation frequency (2π times modulation frequency)

τ: lifetime

θ: phase

M: modulation

Fluorescence decay time represents an intrinsic molecular property that is independent of the setup or adjustment of the instrument. The major advantages of these techniques are speed and ease of detection and analysis [42, 43]. Several lifetime immunoassays and gene assays have been reported based on labels with long (i. e. µs and ms) decay times. Ruthenium labels have been used in FPIA and FRET lifetime immunoassays [44, 45], but not in non-FRET type assays.

Recent advances in lifetime based sensing have led to the design of instrumentation for measurement of decay times in the ns time domain. These instrumentations for fluorescence lifetime were substantially simplified and reduced in size in recent years [46]. Figure 2.9. shows the instrument setup of LF 401 NanoScan used for the lifetime experiments described in chapter 4. The light source is a nitrogen laser with a dye laser filter module, which can easily be changed. The optical detection head is arranged above the microplate and the detector is a photomultiplier tube. Data acquisition of every single fluorescence pulse is performed using a fast transient recorder with a 5 GigaSample acquisition rate. In order to

improve signal-to-noise ratio an average of a number of single laser pulse events may be calculated.

Data analysis is done by fitting the fluorescence decay curves with a suitable exponential decay law. For the fitting process reduction of the chisquare value is achieved using the algorithm of Marquardt and Levenberg. Usually, a single-exponential decay law is de-convoluted with the "instrument response function" in order to obtain a good approximation of the measured decay curves.
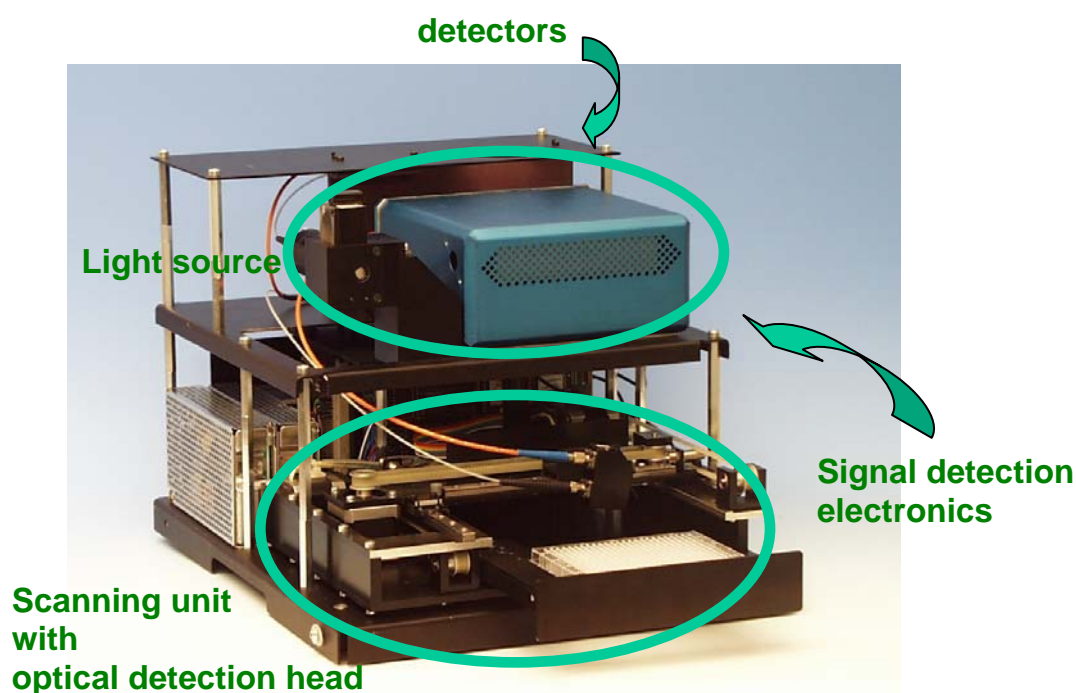
Fig. 2.9. Instrument setup (IOM, Berlin), main components for fluorescence lifetime measurements in the ns range.

Most protein labels used nowadays have decay times in the order of 0.5 – 5 ns. When using such labels the excitation light source can be pulsed at high rates, enabling a large number of measurements to be performed in short time. Therefore decay times can be determined with high precision and a high signal-to-noise ratio.

However, while almost any pair of labels can be used for FRET, if they match the fundamental conditions of the Förster relation, the choice of label is much more critical in case of fluorescence lifetime affinity assay (FLAA). This results from the need for a large relative change in the decay time of the label (bound to a protein) upon binding to its counterpart. Unfortunately, the change in decay time upon binding is virtually unpredictable.

2.3. Methods of Optical Hybridization Assay

Detection of DNA hybridization is often required in molecular biology, genetics, and forensics. A variety of methods has been used to detect DNA hybridization by fluorescence.

One can differentiate between fluorogenic intercalators and fluorescently labeled oligonucleotides. Intercalators (and related probes such as groove binders) associate with single- or double stranded DNA (or RNA) to undergo a significant change in their (fluorescence) optical properties, in most cases an increase in fluorescence intensity (quantum yield) or a spectral shift. Intercalators interact non-convalently [47]. Fluorescent labels, in contrast, are covalently attached to oligonucleotides, most often to the desoxyribose unit via phosphoramidite chemistry, or to an aminohexyl side group that has been introduced by chemical means into a single oligonucleotide. One or more labels may be used.

Most of the optical hybridization assays rely on energy transfer between donor and acceptor labeled DNA. The basic principles for optical assays based on FRET are described already in chapter 2.2.2., using immunoassays as example, and are in most instances similar to hybridization assays. The presence of complementary DNA sequences can be detected by increased energy transfer, when these sequences are brought into proximity by hybridization. Competitive hybridization (fig. 2.10.), in which increased amounts of non-labeled target DNA competes with the formation of donor-acceptor pairs, can also be performed [31, 48].
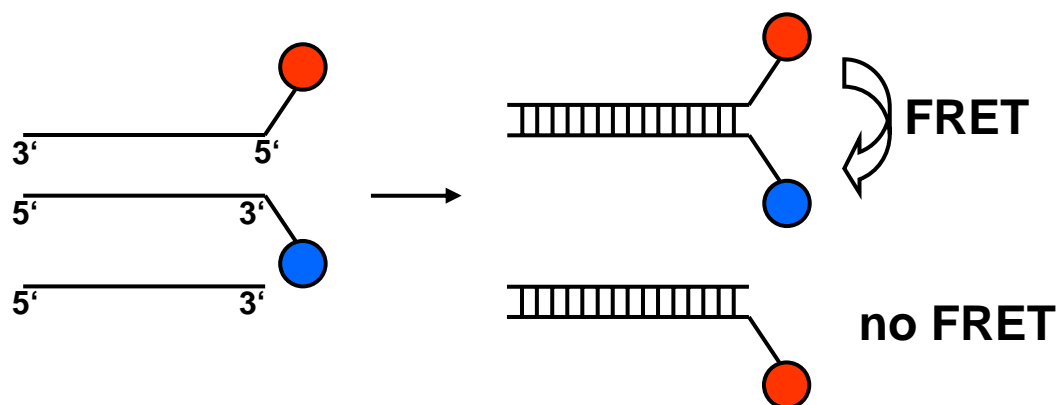
Fig. 2.10.   Scheme of a competitive hybridization assay.

Tyagi and Kramer have utilized a novel design of fluorescence energy transfer and developed a new class of oligonucleotide DNA probes, the molecular beacons (MB) [49]. MBs are single stranded DNA molecules that possess a stem- and loop structure. The loop portion of the molecule can form a double-stranded DNA in the presence of a complementary strand of nucleic acid (fig. 2.11.). They can recognize and report the presence of specific nucleic acids in homogeneous solution with high sensitivity.
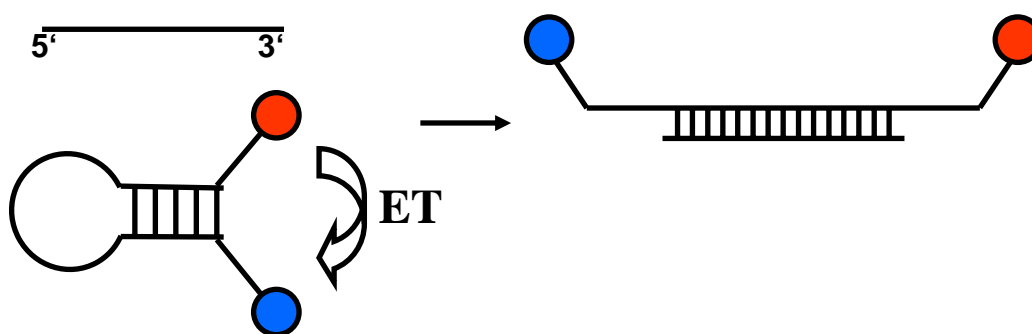
Fig. 2.11.   Scheme of an ET based hybridization assay with a molecular beacon.

A MB is labeled with a fluorophore and quencher or two FRET compatible fluorophores on each end of the stem. There are five to eight bases at each side of the two ends of the beacon which are complementary to each other. When the two ends hybridize, the beacon builds a loop and the fluorophores come in close proximity. So, the fluorescence of the donor fluorophore is quenched and the fluorescence of the acceptor is increased by energy transfer (fig. 2.11., left side). The beacon undergos a spontaneous fluorogenic conformational change, when it hybridizes to its target (fig. 2.11., right side).

Molecular beacons are useful in situations, where it is either not possible or not desirable to isolate the probe-target hybrids from an excess of the hybridization probes, such as real-time monitoring of DNA/RNA amplification reactions and the detection of RNA within living cells. Molecular beacons have been used for protein-DNA interaction studies, enzymatic cleavage measurements, for real-time monitoring of polymerase chain reactions, and even in the investigation of the progression of HIV-1 related disease [50].

So far, molecular beacons have been mainly applied in homogeneous liquid solution [50]. Self-quenching or energy-transfer molecular beacons suffer from their complexity of synthesis which makes cost prohibitive for many routine applications [51]. Specific labeling of both termini of molecular beacons with different fluorophores needs two different reaction steps with two different reactive dyes, two cleaning steps from side products and usually gives small yields only [52]. Another problem with double-labeled MBs can result from photo-destruction of the acceptor chromophore and the increase of donor fluorescence intensity which renders an unequivocal identification of hybridization events more difficult.

It is well known that the hybridization of a fluorescently labeled single strand oligonucleotide with a complementary sequence can substantially modify the fluorescence properties (intensity I and lifetime τ) of the fluorophore. Fluorescence decay time represents an intrinsic molecular property that is independent of the setup or adjustment of the

instrument. It has been recognized quite some time ago that the lifetime of a label changes on hybridization, but the practical implementation of respective assays was limited to long (i.e. >1µs) decaying emissions of suitable labels which have their merits because long lifetime can be determined more easily with adequate instrumental effort.

New fluorescent dyes that interact with DNA double helix and significantly change their fluorescence intensity and lifetime in the ns range are of considerable interest, because adequate lifetime readers are available. Only one marker is needed in an assay using this detection method [47, 53].

2.4. References

[1] M.P. Washburn, D. Wolters, J.R. Yates, Large-scale Analysis of the Yeast Proteome by Multidimensional Protein Identification Technology, Nat. Biotechnol. **2001**, 19, 242-247.

[2] J. Reidl, J. Hacker, Mol. Infection Biol. **2002**, 187-193.

[3] www.probes.com, handbook, figures, figure 9.1

[4] C. D. O´Connor, K. Rickard, Microarrays & Microplates **2003**, 61-68.

[5] P. Cutler, Protein Arrays: The Current State-of-the-Art, Proteomics **2003**, 1, 3-18.

[6] R.P. Haugland, Molecular Probes, Handbook of Fluorescent Probes and Research Products, 9th edition **2001**.

[7] T.H. Steinberg, L.J. Jones, R.P. Haugland, V.L. Singer, SYPRO Orange and SYPRO Red Protein Gel Stains: One-Step Fluorescent Staining of Denaturing Gels for Detection of Nanogram Levels of Protein, Anal. Biochem. **1996**, 239, 223-237.

[8] R.L. Dryer, G.F. Lata, Experimental Biochemistry, Oxford University Press, New York **1989**.

[9] P.J. Wirth, A. Romano, Staining Methods in Gel Electrophoresis, Including the Use of Multiple Detection Methods, J. Chromatogr. A **1995**, 698, 123-143.

[10] J.P. Goldring, L. Ravaioli, Solubilization of Protein-Dye Complexes on Nitrocellulose to Quantify Proteins Spectrophotometrically, Anal. Biochem. **1996**, 242, 197-201.

[11] W.F. Patton, Detection Technologies in Proteome Analysis, J. Chromatogr. B **2002**, 771, 3-31.

[12] M.F. Lopez, K. Berggren, E. Chernokalskaya, A. Lazarev, M. Robinson, W.F. Patton, A Comparison of Silver Stain and SYPRO Ruby Protein Gel Stain with Respect to Protein Detection in Two-dimensional Gels and Identification by Peptide Mass Profiling, Electrophoresis **2000**, 21, 3673-3683.

[13] I. Syrový, Z. Hodný, Staining and Quantification of Proteins Separated by Polyacrylamide Gel Electrophoresis, J. Chromat. B **1991**, 569, 175-196.

[14] W.F. Patton, A Thousands Points of Light: The Application of Fluorescence Detection Technologies to Two-dimensional Gel Electrophoresis and Proteomics, Electrophoresis **2000**, 21, 1123-1144.

[15] M.F. Lopez, Proteome Analysis: I. Gene Products are where the Biological Action is, J. Chromat. B, **1999**, 722, 191-202

[16] J.C. Nishihara, K.M. Champion, Quantitative Evaluation of Proteins in One- and Two-dimensional Polyacrylamide Gels using a Fluorescent Stain, Electrophoresis **2002**, 23, 2203-2215.

[17] R.M. Leimgruber, J.P. Malone, M.F. Radabaugh, M.L. LaPorte, B.N. Violand, J.B. Monahan, Development of Improved Cell Lysis, Solubilization and Imaging Approaches for Proteomic Analyses, Proteomics **2002**, 2, 135-144

[18] J. Bergquist, S.D. Gilman, A.G. Ewig, R. Ekman, Anal. Chem. **1994**, 66, 3512-3518;

[19] K.E. Asermely, C.A. Broomfield, J. Nowakowski, B.C. Courtney, M. Adler, Identification of a Recombinant Synaptobrevin-Thioredoxin Fusion Protein by Capillary Zone Electrophoresis Using Laser-Induced Fluorescence Detection, J. Chromatogr. B **1997**, 695, 67-75.

[20] M. Holtzhauer, Biochem. Labormethoden, 2. Auflage, Springer-Verlag, Berlin **1995**.

[21] B.K. Wetzl, S.M. Yarmoluk, D.B. Craig and O.S. Wolfbeis, Chameleon Labels for Staining and Quantifying of Proteins, Angew. Chem. Int. Ed. **2004**, 43, 5400-5402.

[22] W.W. You, R.P. Haugland, D.K. Ryan, R.P. Haugland, 3-(4-Carboxybenzoyl)quinoline-2-carboxyaldehyde, a Reagent with Broad Dynamic Range of the Assay of Proteins and Lipoproteins in Solution, Anal. Biochem. **1997**, 244, 277-282.

[23] C.M. Stoscheck, General Methods for Handling Proteins and Enzymes: Quantitation of Protein, in M.P. Deutscher (Ed.), Methods in Enzymology, Academic Press, New York, **1990**.

[24] O.H. Lowry, N.J. Rosebrough, A.L. Farr, R.J. Randall, Protein Measurement with the Folin Phenol Reagent, J. Biol. Chem. **1951**, 193, 265-275.

[25] P.K. Schmith, R.I. Krohn, G.T. Hermanson, Measurement of Protein using Bicinchoninic Acid, Anal. Biochem. **1985**, 150, 76-85.

[26] M.M. Bradford, A Rapid and Sensitive Method for the Quantitation of Microgram Quantities of Protein Utilizing the Principle of Protein-Dye Binding, Anal. Biochem. **1976**, 72, 248-254.

[27] A. Lorenzen, S.W. Kennedy, A Fluorescence-Based Assay for Use with a Microplate Reader, Anal. Biochem. **1993**, 214, 346-348.

[28] S. Udenfriend, S. Stein, P. Böhlen, W. Dairman, W. Leimgruber, M. Weigele, Fluorescamine. Reagent for Assay of Amino Acids, Peptides, Proteins, and Primary Amines in the Picomole Range, Science **1972**, 178, 871-872.

[29] P. Böhlen, S. Stein, W. Dairman, S. Udenfriend, Fluorometric Assay of Proteins in the Nanogram Range, Biochem. Biophys. **1973**, 155, 213-220.

[30] J.R. Crowther, Enzyme Linked Immunosorbent Assay (ELISA), from Molecular Biomethods Handbook, Humana Press Inc., Totowa NJ **1998**.

[31] J.R. Lakowicz, Principles of Fluorescence Spectroscopy (2nd edition), Kluwer Academic/Plenum Publishers, New York **1999**.

[32] O.J. Rolinski, D.J.S. Birch, Determination of Acceptor Distribution from Fluorescence Resonance Energy Transfer: Theory and Simulation, J. Chem. Physics. **2000**, 112 (20), 8923-8933.

[33] Z. Gryczynski, I. Gryczynski, J.R. Lakowicz, Methods in Enzymology **2003**, 360 (Biophotonics, Part A), 44-75.

[34] B. Valeur, Molecular Fluorescence, Principles and Applications, Wiley-VCH, Weilheim, **2002**.

[35] I. Hemmilä, S. Webb, Time-Resolved Fluorometry: An Overview of the Labels and Core Technologies for Drug Screening Applications, DDT **1997**, 2, 373-381.

[36] V.–M. Mukkala, M. Helenius, I. Hemmilä, J. Kankare, H. Takalo, Development of Luminescent Europium(III) and Terbium(III)chelates of 2,2:6,2-terpyridine Derivatives for Protein Labelling, Helv. Chim. Acta **1993**, 76, 1361.

[37] V.–M. Mukkala, M. Mikola, I. Hemmilä, The Synthesis and Use of Activated *N*-Benzyl Derivatives of Diethylenetriaminetetraacetic acids: Alternative reagents for Labeling of Antibodies with Metal Ions, Anal. Biochem. **1989**, 176, 319-325.

[38] G. Mathis, Rare Earth Cryptates and Homogeneous Fluoroimmunoassays with Human Sera, Clin. Chem. **1993**, 39, 1953-1959.

[39] E.P. Diamandis, R.C. Morton, E. Reichstein, M.J. Khosravi, Multiple Fluorescence Labeling with Europium Chelators. Application to Time-Resolved Fluoroimmunoassays, Anal. Chem. **1989**, 61, 48-53.

[40] T.K. Christopoulos, E.P. Diamandis, Enzymatically Amplified Time-Resolved Fluorescence Immunoassay with Terbium Chelates, Anal. Chem. **1992**, 64, 342-346.

[41] S. Turconi, R.P. Bingham, U. Haupts, A.J. Pope, Developments in Fluorescence Lifetime-Based Analysis for Ultra-HTS, DDT **2001**, 6, 12, S27-S39.

[42] S. Jäger, L. Brand, C. Eggeling, New Fluorescence Techniques for High-Throughput Drug Discovery, Curr. Pharm. Biotechnol. **2003**, 4, 463-476.

[43] Ch. Eggeling, L. Brand, D. Ullmann, S. Jäger, Highly Sensitive Fluorescence Detection Technology Currently Available for HTS, DDT **2003**, 8(14), 632-641.

[44] A. Duerkop, F. Lehmann, O.S. Wolfbeis, Polarization Immunoassays using Reactive Ruthenium Metal-Ligand Complexes as Luminescent Labels, Anal. Bioanal. Chem. **2002**, 372(5-6), 688-694.

[45] Ch.M. Augustin, B. Oswald, O.S. Wolfbeis, Time-Resolved Luminescence Energy Transfer Immunobinding Study Using a Ruthenium-Ligand Complex as a Donor Label, Anal. Biochem. **2002**, 305(2), 166-172.

[46] T.E. French, B. Bailey, D.P. Stumbo, D.N. Modlin, SPIE **1999**, 3603, 272-280.

[47] H.S. Rye, J.M. Dabora, M.A. Quesada, R.A. Mathies, Fluorometric Assay using Dimeric Dyes for Double- and Single-Stranded DNA and RNA with Picogram Sensitivity, Anal. Biochem. **1993**, 208, 144-150.

[48] O.S. Wolfbeis, M. Böhmer, A. Dürkop, J. Enderlein, M. Gruber, I. Klimant, C. Krause, J. Kürner, G. Liebsch, Z. Lin, B. Oswald, M. Wu, Advanced Luminescent Labels, Probes, and Beads, and Their Application to Luminescence Bioassay, and Imaging, *in* Springer Series in Fluorescence (R. Kraayenhof, Ed.), Springer Verlag, Berlin-Heidelberg **2002**.

[49] S. Tyagi, F.R. Kramer, Molecular Beacons: Probes that Fluoresce upon Hybridisation, Nat. Biotechnol. **1996**, 14, 303-308.

[50] X. Liu, W. Farmerie, S. Schuster, W. Tan, Molecular Beacons for DNA Biosensors with Micrometer to Submicrometer Dimension, Anal. Biochem. **2000**, 283, 56-63.

[51] K.D. Kourentzi, G.E. Fox, R.C. Willson, Hybridization-Responsive Fluorescent DNA Probes Containing the Adenine Analog 2-Aminopurine, Anal. Biochem. **2003**, 322, 124-126.

[52] J.-P. Knemeyer, N. Marmé, M. Sauer, Probes for Detection of Specific DNA Sequences at the Single-Molecule Level, Anal. Chem. **2000**, 72(16), 3717-3724.

[53] S.P. Lee, D. Porter, J.G. Chirikjian, J.R. Knutson, M.K. Han, A Fluorometric Assay for DNA Cleavage Reactions Characterized with BamHI Restriction Endonuclease, Anal. Biochem. **1994**, 220, 377-388.

3.   Representatives of the New Dye Class Containing a Pyrylium Group and their Conjugates

Representatives of the new pyrylium dyes and their conjugates are presented. The pyrylium dyes shown here belong to the class of cyanine dyes, except for one. The pyrylium dyes are separated into two groups: one group with an amine reactive pyrylium moiety which reacts under mild conditions in water, and the second one with a non-reactive pyrylium moiety because of sterically hindrance. The synthesis, reactivity and spectral properties of the dyes and their conjugates are described in the following.

3.1. A New Class of Reactive Pyrylium Labels: The Py Labels

Pyrylium salts with a metal organic residue in para position to the pyrylium oxygen were investigated by several authors [1] in the 80s. Their ability of reaction with primary amines even in proteins, leading to pyridinium salts, was described in the early 1970ies. The reaction of pyrylium salts with primary amines enabled the introduction of new functionalities under mild conditions or labeling to biomolecules. Organometallic labels with a pyrylium moiety were developed as sensitive analytic probes in IR spectroscopy or to aid in the solution of three-dimensional X-ray crystal structures of proteins [1]. Fluorescent labels based on the structure of cyanine dyes were investigated first by Yarmoluk in 1999 [2].

3.1.1.   Survey of the New Compounds and their Spectral Properties

All dyes synthesized in this work contain only one reactive group, which avoids crosslinking. A dye containing a pyrylium moiety has already one reactive group and needs no further activation by another reaction step. This is a major advantage compared to labels employing a carboxy group to amine labeling which has to be converted into a reactive oxysuccinimide ester (OSI ester). The general synthesis of a pyrylium reactive dye is shown in figure 3.1.
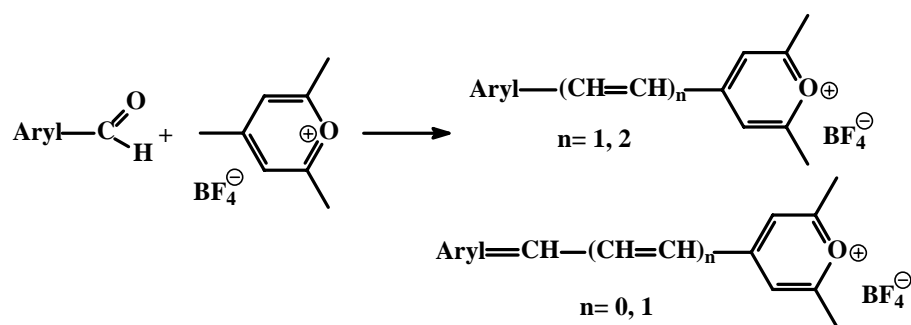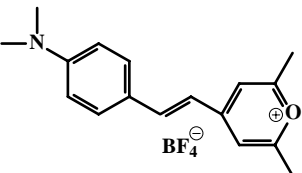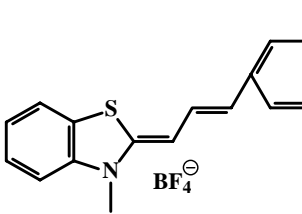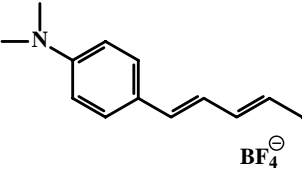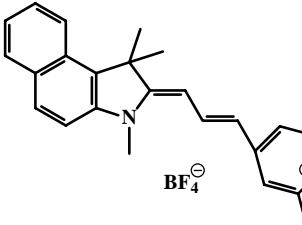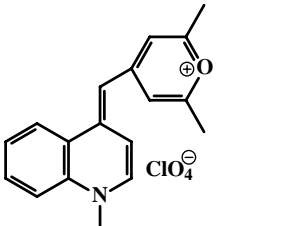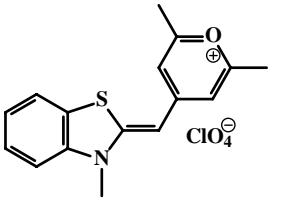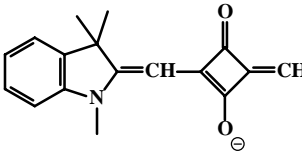
Fig 3.1.   General synthetic strategy for a pyrylium reactive dyes.

The spectral and chemical properties of the chromophores are influenced by the selection of the aryl system, which contains either a heterocycle or an amine in para position to the aldehyde group. This aldehyde forms a covalent bond in a one step reaction with the para-methyl group of 2,4,6-trimethyl pyrylium salt. The product can be either recrystallized from ethanol or purified via column chromatography. Various combinations gave a list of pyrylium reactive dyes (table 3.1). All labels have a quantum yield lower than 1% in aqueous and organic solutions.

Table 3.1. Names, chemical structures and spectral properties of the new Py labels and their conjugates to HSA.

name	structure of the label	$\lambda_{abs}^{max} / \lambda_{em}^{max}$ ε (molar absorbance) *in methanol #in aqueous solution	$\lambda_{abs}^{max} / \lambda_{em}^{max}$ QY conjugated to HSA in aqueous solution
Py-1		611 / 665 nm* # 70 000 L/(cm·mol)* 63 000 L/(cm·mol)#	503 / 602 nm ≤ 60% d. DPR
Py-2		574 / 593 nm* 90 000 L/(cm·mol)*	514 / 595 nm ≤ 20% d. DPR

Py-3		578 / 640 nm * 568 / 640 nm # 50 000 L/(cm·mol)*	465 / 580 nm ≤ 2% d. DPR
Py-4		573 / 586 nm* 570 / 589 nm# 90 000 L/(cm·mol)*	536 / 586 nm ≤ 24% d. DPR
Py-5		645 / 732 nm* 25 000 L/(cm·mol)*	465 / 630 nm ≤ 14% d. DPR
Py-6		598 / 627 nm * 568 / 627 nm # 35 000 L/(cm·mol)	540 / 593 nm ≤ 44% d. DPR
Py-7		507 / 540 nm* #	530 / 560 nm ≤ 1%
Py-8		457 / 525 nm* 457 / 519 nm#	445 / 535 nm ≤ 21% d. DPR
Py-20		670 / 695 nm* 100 000 L/(cm·mol)* 70 000 L/(cm·mol)#	583 / 644 nm ≤ 14% d. DPR

d. DPR means depending on the dye to protein ratio

Py-1 is a dimethine dye which can be synthesized via a two step reaction. The Vilsmeier formylation of the julolidine 2,3,6,7-tetrahydro-1H,5H-pyrido[3,2,1-ij]quinoline gives the benzaldehyde. Equimolar amounts of the benzaldehyde and 2,4,6-trimethyl pyrylium salt are

reacted in methanol. The product precipitates out of ether and can be recrystallized in ethanol or purified via column chromatography.

The dye contains one amine reactive pyrylium group. It gives a blue solution with an absorbance maximum of 611 nm in aqueous solution and organic solvents. The fluorescence is weak (QY less than 1%) with a maximum at 665 nm. Upon labeling to a protein the quantum yield rises up to 60% depending on the DPR.

Py-2 is a trimethine dye which can be synthesized via a three step reaction. The first step is to quaternize 2,3,3-trimethyl-3H-indole with methyl iodide to achieve the quaternized indole [3]. The Vilsmeier formylation of this indole gives the carbaldehyde. Equimolar amounts of the carbaldehyde and 2,4,6-trimethyl pyrylium salt are reacted in methanol. The product is purified via recrystallization from ethanol or column chromatography. The dye gives a pink solution in organic solvents with an absorbance maximum at 574 nm and a weak emission with a maximum at 593 nm. Upon reaction with amino functions of proteins, the absorbance maximum shifts to 514 nm and the conjugate gives a strong fluorescence at 595 nm.

Py-3 is a dimethine dye which can be easily synthesized via a one step reaction from equimolar amounts of 4-dimethylamino-benzaldehyde and 2,4,6-trimethyl pyrylium salt in methanol. The dye can be recrystallized from ethanol. It gives a violet solution in organic solvents with an absorbance maximum at 578 nm and very weak fluorescence with the maximum at 640 nm. The absorbance maximum of the dye in buffered solution shifts from 568 nm to 465 nm on reaction with a protein, and the emission maximum of the conjugate is at 580 nm with a weak intensity.

Py-4 is a trimethine dye and can be synthesized by analogy to Py-2: first, the quaternization of 2-methyl-2,3-dihydro-benzothioazole is performed with methyl iodide, followed by the formylation and finally the reaction with 2,4,6-trimethyl pyrylium salt to the dye. The dye gives a pink solution in methanol with an absorbance maximum at 573 nm and in aqueous solution with an absorbance maximum at 570 nm. The emission maxima are also very similar in both solvents lying at 586-589 nm. The emission intensity increases upon conjugation of the dye to a protein. The QY increases from <1% to about 24% depending on the DPR, and the absorption maximum shifts to 536 nm.

Py-5 is a quatromethine dye using a synthesis path, very similar to that of Py-3. The 4-(dimethylamino)-cinnamaldehyde (3-(4-dimethylamino-phenyl)-propenal) is reacted with 2,4,6-trimethyl pyrylium salt to give the amine reactive dye. Its absorbance maximum is at 645 nm and shifts to 465 nm upon reaction with a protein. The fluorescence intensity of the label is very weak with an emission maximum at 732 nm, but it increases with conjugation of the label to a protein (QY 14% depending on the DPR), with a maximum at 630 nm. The spectral shift of the absorbance maximum of the label when conjugated to a protein is 180 nm. The color changes from blue to yellow upon conjugation. The Stokes' shift of 165 nm is in the order of transition metal or lanthanide complexes and very large for an organic dye.

Py-6 is a trimethine dye and can be synthesized in analogy to Py-2. The quaternation of 1,1,2-trimethyl-1H-benzo[e]indole with methyl iodide is followed by the formylation. The reaction with 2,4,6-trimethyl pyrylium salt gives the label. The black crystals of the dye give a violet solution with an absorbance maximum at 598 nm in methanol and 568 nm in aqueous solution. The emission maximum is at 627 nm in both solvents. The emission intensity upon conjugation of the dye to a protein increases from < 1% to over 44% depending on the DPR. The absorption maximum shifts to 540 nm.

Py-7 is a monomethine dye, which can be synthesized via a two step reaction. Lepidine is quaternized with methyl iodide. Equimolar amounts of this product are reacted with 2,6-dimethyl-gamma-pyrone to form the dye. It is purified via column chromatography. The absorbance maximum both in aqueous and organic solvents is at 507 nm. The emission is very weak with a maximum at 540 nm. The fluorescence intensity does not increase when the label is conjugated to a protein. The absorbance of the conjugate is determined at 530 nm, which means in comparison to the other Py labels a widdershins effect. The quinolinium heterocycle of Py-7 has completely different effects compared to the indolium heterocycle of the other labels.

Py-8 is a monomethine dye, which can be synthesized in analogy to Py-7. The quaternized indole is reacted with 2,6-dimethyl-gamma-pyrone to form the dye. The absorbance maximum in aqueous and organic solvents is at 457 nm. The emission is very weak, with a maximum at 520 nm. The emission intensity increases upon conjugation of the label to a protein. The absorbance maximum shifts to 445 nm and the emission maximum to 535 nm. The QY increases from < 1% to about 21% depending on the DPR.

Py-20 is an exception to the other labels according to its structure. Py-20 is an unsymmetrical squarylium dye. It can be synthesized via a three step reaction. First, the 2,3,3-trimethyl-3*H*-indole is quaternized with methyl iodide. The indole derivate and 3,4-dibutoxy-3-cyclobutene-1,2-dione react in ethanol in presence of catalytic amounts of triethylamine. The semi-substituted squaric acid derivative reacts with 2,4,6-trimethyl pyrylium salt to give the label Py-20, which is purified by column chromatography. The dye has an absorbance maximum of 670 nm in methanol and an emission maximum at 695 nm. The spectral properties change upon binding to a protein. The emission maximum is at 644 nm and the absorbance maximum at 583 nm. The fluorescence intensity increases (QY up to 14%). The label and the dye conjugates have a low chemical stability in aqueous buffered solutions.

3.1.2. Stability and Reactivity of Py Labels

Pyrylium salts are very sensitive according to nucleophilic attacks (see fig. 1.6.) and react with primary amines to form pyridinium salts. Secondary and tertiary amines also react with pyrylium salts and cause a ring opening.

Stability of Py-1 in different solvents

Py-1 was dissolved in methanol, doubly distilled water pH 7.8, tap water pH 7.6, and tris buffer pH 7 ([Py-1] = 2 µmol/L). The absorbance of the solutions at 630 nm was measured after an incubation time of 0, 30, 60 and 90 minutes.
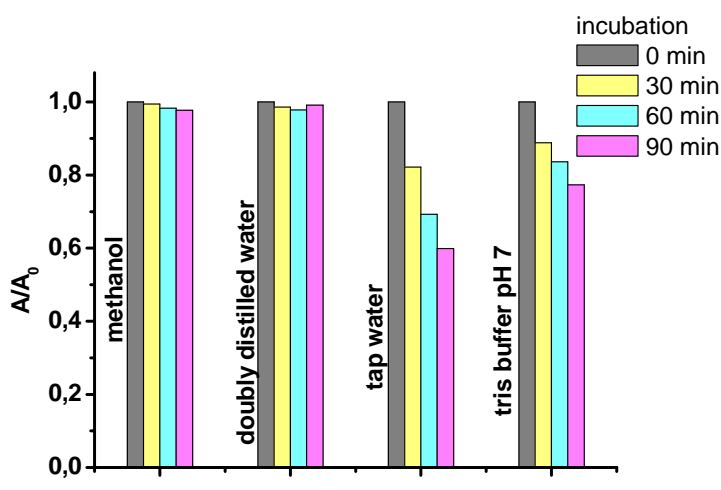
Fig 3.2.   Stability study of Py-1 in different solvents. The absorbance (A) of the solutions was measured after 0, 30, 60 and 90 min.

Label Py-1 forms a blue colored solution in organic and aqueous solvents, with an absorption maximum around 630 nm. It is stable for 90 min in methanol and in doubly distilled water as shown here in figure 3.2. The small decreases in absorbance intensity in both solutions can be explained by measurement or dilution inaccuracies. Experiments over a longer period (data not given here) showed that a solution of Py-1 in methanol, stored at 4 °C remains reactive according to reaction with primary amines and can therefore be used for several weeks. The absorbance of the dye in tap water and tris buffer at λ_{max} 630 nm decreases to 60 and 77%, respectively, within 90 min. Although the label containing a reactive pyrylium ring is not stable in tap water and tris buffer over a longer period, it is stable enough to react with primary amines in these solvents. The different stabilities of the dye in doubly distilled water, tap water and tris buffer suggest not only a dependency on the pH value, but also on the ions (species and ionic strength) in the aqueous solutions.

Stability of Py-1 in buffered solutions of different pH values

A stock solution of the label Py-1 in methanol ($1 \cdot 10^{-4}$ mol/L) was diluted 1:3 (v/v) with PB of different pHs in a micro plate. The concentration of label in each well was $2.5 \cdot 10^{-5}$ mol/L. The plate was incubated at RT and the absorbance measured after 2 and 5 h at 590 nm on a Tecan Sunrise absorbance reader.
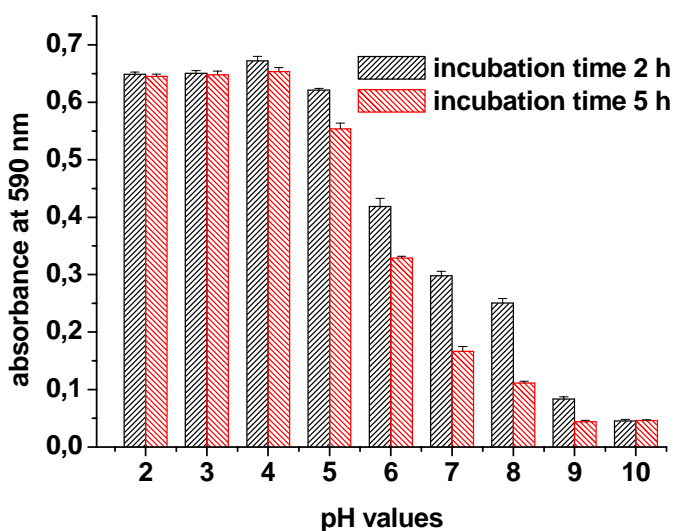
Fig. 3.3.   Effect of pH on the stability of the reactive label Py-1. Each point is the average of eight determinations with standard deviations as error bars.

After incubation of 2 h the concentration of reactive label Py-1, which can be detected by absorption measurements of the blue component, has decreased under 50% in all samples of a

pH higher than 7. This effect is even more visible upon incubation for 5 h (fig. 3.3.).

Pyrylium reactive dyes are very sensitive to basic pH solutions, which cause ring opening of the pyrylium and therefore the loss of the origin color of the reactive label. In the case of Py-1 the dye solution turns from deep blue to sallow. The disadvantage of instability can be used advantageously as a method to destroy excess of reactive label in a covalent labeling step. The labels react very fast with primary amines or fade to the non reactive and non fluorescent yellow form.

Changes of absorption spectra of Py-1 and Py-6 upon reaction with amines and thiol
1 mL of a solution of Py-1 and Py-6, respectively, in acetonitrile (concentration of $1 \cdot 10^{-3}$ mol/L) was added to 1 mL of a thiol or different aromatic and aliphatic amines dissolved in acetonitrile (concentration $2 \cdot 10^{-3}$ mol/L). The mixtures (dye and amines/thiol) were stirred at room temperature and the absorbance spectra were measured after 10 min, 120 min (only Py-1) and 2 days, respectively. The spectra are shown in figure 3.4. for Py-1 and 3.5. for Py-6.
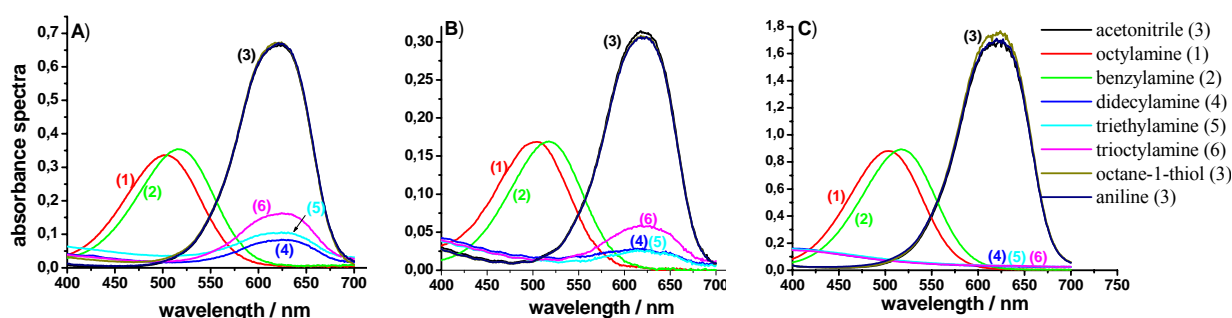
Fig. 3.4.   The influence of different amines and thiol on the absorbance spectra of Py-1 in acetonitrile. A) incubation of 10 min; B) incubation of 120 min; C) incubation of 2 days.

Py-1 reacts within 10 min with primary aliphatic amines like octylamine (1) (red line) and benzyl amine (2) (green line) to form a red conjugate. The absorption maximum shifts from 623 nm to 500-510 nm. The reaction with secondary and tertiary amines is different. These amines can also affect the pyrylium ring of the label and open it. But no recyclisation can take place. The origin color of the label disappears and the solution turns sallow.

After 10 min of reaction (figure 3.4. part A) it can be distinguished between trioctylamine (6) (magenta line), triethylamine (5) (cyan line) and didecylamine (4) (blue line). The absorbance peaks at 623 nm decrease to 24% of the initial value for the tertiary

long-chain amine trioctylamine, to 17% for the tertiary amine with ethyl chains, and to 12% for the secondary amine didecylamine, respectively. After an incubation of 120 min, there is no difference between the triethylamine and didecylamine. The attack of the different amines is dependent on their nucleophilicity and on the kind of amine. Primary amines attack very fast to form the pyridinium species, which can be detected via a decrease of the absorbance maximum of the label and an increase of the absorbance of the conjugate. Secondary amines also react very fast by a ring opening reaction of the pyrylium, but do not form a new peak in the absorbance spectra of this experiment. The reaction of tertiary amines is slower.

Py-6 is another reactive pyrylium dye, which changes obviously its color from violet to pink, and therefore its absorption maximum, on reacting with primary amines (spectral shift of over 60 nm). Secondary and tertiary amines cause a ring opening reaction of the pyrylium moiety and therefore a destruction of the chromophoric system of the dye, which can be followed by a decrease of the absorbance at 590 nm. Different primary, secondary and tertiary amines in acetonitrile were mixed with a Py-6 solution and their absorbance spectra were measured after 10 min and after 2 days.
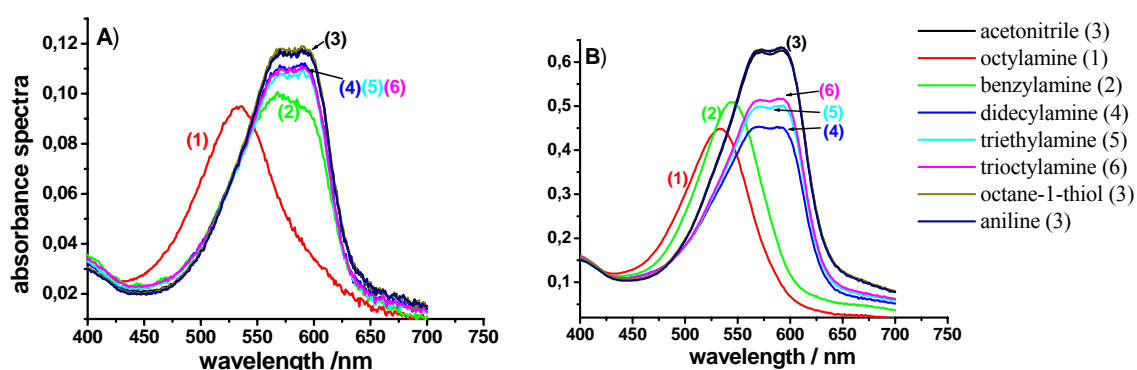
Fig. 3.5.   The influence of different amines and thiol on the absorbance spectra of Py-6 in acetonitrile. A) incubation time 10 min; B) incubation time 2 days.

In comparison to Py-1, the reaction rate of Py-6 with amines is slower. Py-6 is more resistant against attacks of nucleophilic amines. Octylamine (1) (red line) reacts with Py-6 within 10 min to form a stable pyrylium product with a new absorption maximum at 530 nm. The reaction with benzylamine is complete within 1 h (graph not shown) and results in a new maximum at 545 nm. Within two days of incubation of the amines with the label, the secondary amine (didecylamine (4), blue line) causes the largest decrease of the absorption maximum of the dye at 590 nm. Addition of didecylamine (4) decreases the absorption

maximum to 73% after 2 days incubation. The lipophilic tertiary amine trioctylamine (6) causes the least change in absorbance compared to all other amines.

In both figures (3.4. and 3.5.) octane-1-thiol (3) (dark yellow line) has no effect on the absorption maximum of the reactive dye. The labels are neither destroyed (which would be obvious from a loss of color) nor is there a new absorption peak, which would reveal a conjugate. Pyrylium reactive labels are therefore not thiol-reactive.

Effect of pH and buffer type on labeling

Py labels react easily with amino groups of proteins (but also with other amines). This reaction causes a significant spectral change. Upon reaction with the proteins, the label becomes highly fluorescent, which enables the detection of proteins. Py labels react with primary amino groups of proteins as shown in fig. 3.6., most probably with ε-amino groups of lysine.
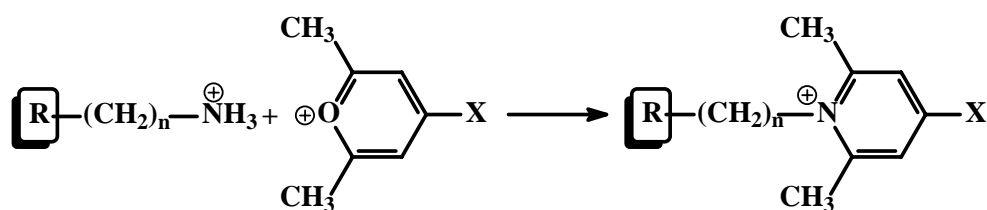
Fig. 3.6.   Scheme of the labeling reaction with Py labels. R stands for an organic substitutent or a protein, and X for the substituents on the pyrylium rings shown in table 3.1. Note that the positive charge is retained.

The reaction with amines and proteins proceeds quickly in aqueous solution of neutral or slightly alkaline pH and even in aqueous methanol and acetonitrile. The rate of the reaction can be followed easily by observing the color change.

We assume that when labeling proteins, the Py labels preferably bind to the terminal amino groups of lysine, but possibly also to other amino acids. Since the charge of amino groups is highly pH dependent, pH was expected to have a significant effect on the efficiency of labeling. In order to study this effect, an HSA solution (53 μg/mL) was reacted with a Py-1 stock solution at different pHs, and fluorescence intensity was measured after 60 min. The results are shown in figure 3.7. and, indeed, reveal a strong pH dependence. The plot has the shape of a pH titration plot which, however, does not reflect the pK_a of a primary amino group. The optimal pH for labeling HSA is higher than pH 7. However, even at pH 7 a high degree of labeling can be achieved. This is important in case of labeling pH-sensitive proteins such as certain antibodies. The optimal pH for labeling is likely to be slightly different for

each protein and probably also depends on its isoelectric-point.
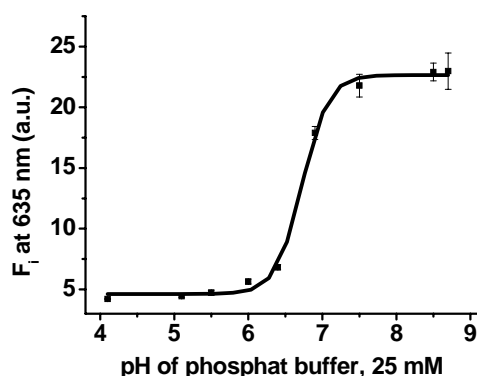
Fig. 3.7.   Fluorescence intensity (at 635 nm) of Py-1 HSA solution after 60 min of reaction at different pHs. Each point is the average of four determinations with standard deviations as error bars.

Fluorescence quantum yields and effect of dye-to-protein ratio (DPR)

The quantum yields (QY) of the dyes labeled to proteins are much higher than those of the unreacted Py dyes. The determination of the QYs of conjugates is complicated, unfortunately, because the effect of the so-called dye-to-protein ratio (DPR). In essence, the term refers to the frequent finding that the QY of a labeled protein depends on dye loading. The DPR is the average number of chromophores conjugated to a single protein molecule.

In our study, QYs of Py-1 and Py-6 conjugated to HSA, respectively, at varying DPR were determined (cresyl violet as a standard reference dye). The results are plotted in fig. 3.8. and show that the QY decreases with increasing DPR, which could be expected since self-quenching increasingly takes place with increasing DPR.
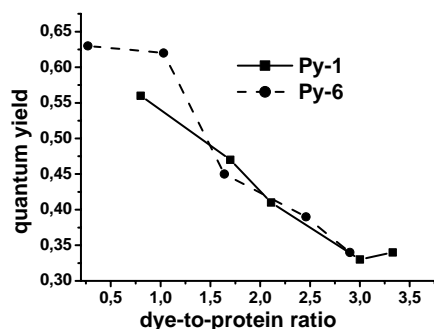
Fig. 3.8.   Effect of the dye-to-protein ration on the quantum yields of HSA labeled with Py-
             1 and Py-6, respectively.

3.1.3. Chemical Modifications of Py Labels

The amine reactive pyrylium group of the labels described in the previous chapter may not only be used for direct linkage to biomolecules, but also for reaction with aliphatic amines. These aliphatic amines can be used for example to introduce a spacer between the chromophore and a biomolecule, or a new reactivity. The reaction of a Py label with an amino alcohol leads to a chromophore, which can be used to form a phosphoramidite derivative of the dye. Phosphoramidite labels are very useful for labeling the terminal phosphate group of nucleotides and oligonucleotides. Amines with long aliphatic chains lead to lipophilic dyes.

The reaction of the labels with small aliphatic amines (propylamine) released the following problem: The Py label and its conjugate have very different spectral properties. Therefore also the molar extinction coefficient cannot be similar for the label and the conjugated dye. The solution was to react the label with an amine and use this conjugate for the determination of the molar extinction coefficient.
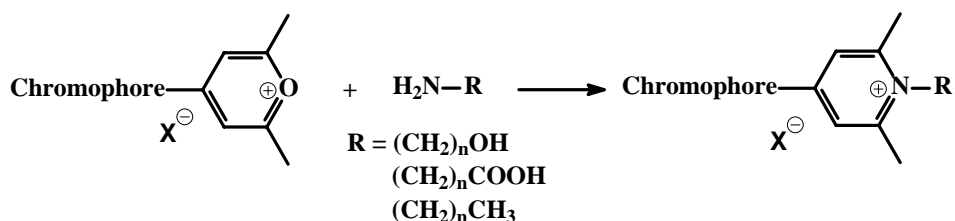
Fig. 3.9.   General reaction scheme of a reactive Py label with aliphatic amines.

The label was dissolved in methanol and added to a solution (methanol with a small amount of triethylamine) of the amine. The reaction was refluxed and the conjugate purified by column chromatography. Thereby a number of conjugates were synthesized and their spectral properties were examined.

Table 3.2. List of the labels reacted with different amines (modification) and their spectral
properties.

label_modification	H$_2$N-R	$\lambda_{abs}^{max}/\lambda_{abs}^{max}$	ε [L/(cm·mol)]
Py-1_propyl	R = (CH$_2$)$_2$CH$_3$	508 / 624 nm	25 000
Py-1_acid	R = (CH$_2$)$_5$COOH	507 / 611 nm	24 000
Py-2_propyl	R = (CH$_2$)$_2$CH$_3$	516 / 577 nm	42 000* 30 000
Py-2_acid	R = (CH$_2$)$_5$COOH	510 / 562 nm	
Py-3_propyl	R = (CH$_2$)$_2$CH$_3$	467 / 595 nm	25 000* 21 000
Py-3_acid	R = (CH$_2$)$_5$COOH	450 / 600 nm	
Py-4_acid	R = (CH$_2$)$_5$COOH	535 / 584 nm	14 000
Py-4_C18	R = (CH$_2$)$_{17}$CH$_3$	544 / 589 nm[#]	
Py-5_propyl	R = (CH$_2$)$_2$CH$_3$	484 / 671 nm*	30 000* 25 000
Py-5_acid	R = (CH$_2$)$_5$COOH	520 / 665 nm*	
Py-6_propyl	R = (CH$_2$)$_2$CH$_3$	535 / 600 nm	31 000* 25 000
Py-6_C18	R = (CH$_2$)$_{17}$CH$_3$	536 / 600 nm[#]	50 000* 71 000[#]
Py-8_propyl	R = (CH$_2$)$_2$CH$_3$	440 / 477 nm*	

determined in *methanol and [#]chloroform, others in aqueous solution

R contributes to the residue shown on fig. 3.9.

Variation of colors of Py labels and their conjugates

In figure 3.10. the absorbance and emission spectra of Py-1 and its conjugates are shown. The
absorbance maximum of the label shifts from 611 nm to 503 nm when reacted with a primary
amine, regardless if the amine is aliphatic or part of a protein. The emission maximum of the
label is at 665 nm has a very low QY of less then 1% (noisy black curve). The QY of the label
increases to 2% upon conjugation to aminocaproic acid and the emission maximum shifts to
627 nm. The conjugate of Py-1 attached directly to HSA and Py1-acid attached to HSA via
the OSI ester reaction (described in chapter 1.2.1) have the same absorption and emission
maxima and a almost similar curve shape.
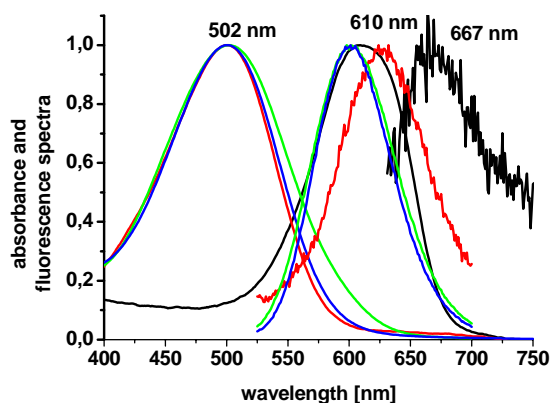
Fig. 3.10. Absorption and emission spectra of Py-1 (black curves), Py-1_acid (red curves), HSA labeled with Py-1 (green lines) and with Py-1_acid (blue lines). The label was dissolved in distilled water, the conjugates in PB. The spectra were normalized.

The variety of nice colors from yellow to blue of Py labels attached to HSA is shown in figure 3.11. HSA was labeled with the different Py labels listed under the photo and separated after 30 min from the excess of label via size exclusion chromatography. The second picture was taken with a digital camera in a black box with UV lamp excitation at 254 and 366 nm. Py-17 conjugates (λ_{abs} 615 nm, structure table 3.3.) can of course not be excited with this lamp, but the other conjugates showed a nice fluorescence.
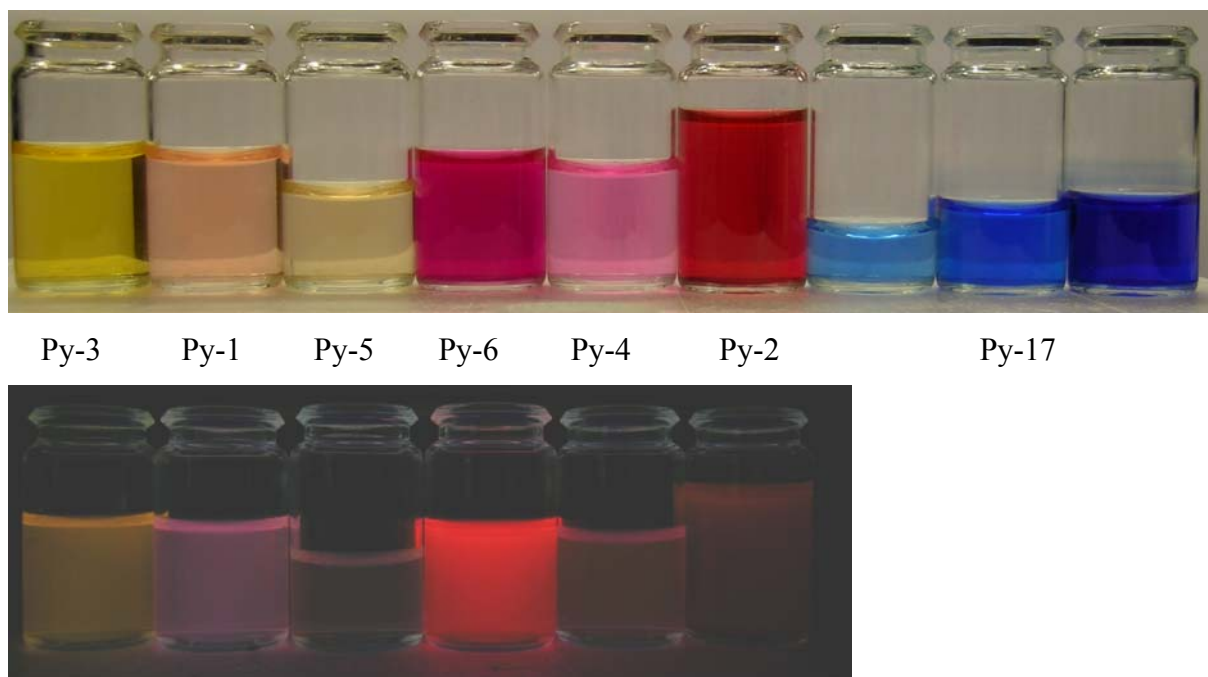
Fig. 3.11. Picture of HSA conjugates of Py labels in PB, pH 7.2. The pictures are taken with a commercially available digital camera in day light (top) and under the UV-lamp (bottom). It should be mentioned that the conjugates have neither the same DPR nor the same concentration.

Photostability study of Py labels compared with other fluorescent dyes

The photo stability of the pyrylium labels (aminopropyl conjugates) in membranes has been tested under continuous wave irradiation at the maximum of excitation for each dye in a flow through cell for one hour. The membrane with fluorescein was immersed into phosphate buffer pH 10.0 to ensure that only the deprotonated form of the indicator is present in the membrane.

dye	% photobleaching per h
Py-2_propyl (1)	0%
Py-6_propyl (2)	2%
fluorescein (3)	75%
sulforhodamin G (4)	4%
sulforhodamin B (5)	3%
ATTO 550 (6)	5%
Bodipy TRX (7)	6%
Py-1_propyl (8)	6%
Py-3_propyl (9)	4%
Py-5_propyl 10)	4%
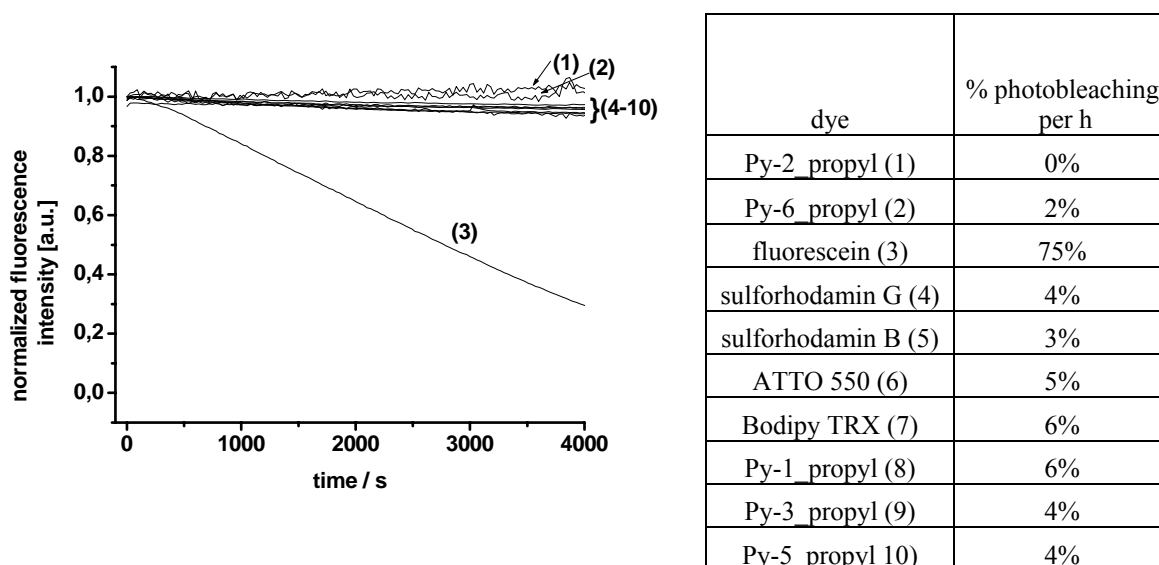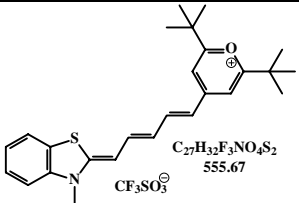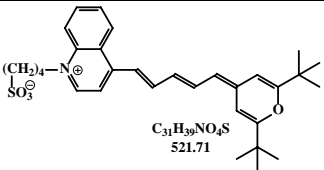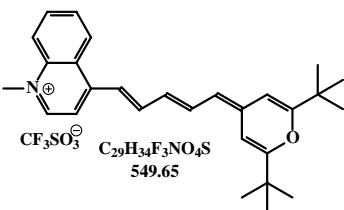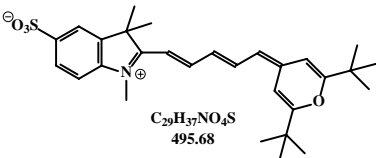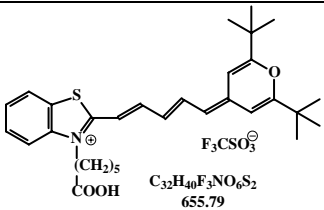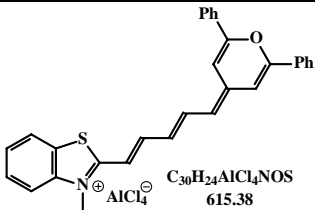
Fig. 3.12. Photobleaching of dye membranes followed via fluorescence intensity. Membranes: Hydrogel 8.3% (10 g of polymer Hydromed D4 from Cardiotech, 100 g ethanol, 10 g water), 2 mM dye per kg polymer.

The photostability of the Py_propyl dyes in membranes is excellent. After 1 h of continuous illumination in the fluorometer at their excitation maximum, with a bandpass setting of 4 nm (i.e. the bandpass under which most experiments were performed) using a 150 W xenon lamp, the fluorescence intensity decreases less than 6% for all membranes dyed with Py-dyes. A membrane containing 5-(octadecanoylamino) fluorescein was used as reference and showed a fluorescence signal of only 34% after 1 h (λ_{exc} = 500 nm, $\lambda_{em.}$ = 520 nm). The fluorescein chromophore has a limited photostability and suffers from irreversible photobleaching. Figure 3.12. shows the decomposition of the dyes followed via fluorescence intensity of the different membranes over time.

3.2. Dyes with a Sterically Hindered Pyrylium Moiety

Several derivatives of pyrylium salts are known. The stability of the pyrylium moiety against nucleophilic attack and the exchange of the oxygen by nitrogen is dependent on the substituents of the pyrylium salt. Several dyes with two tertiary butyl groups in ortho position to the oxygen and one with two phenyl groups were synthesized (table 3.3.), and their reaction with primary amino groups of proteins was tested. Labeling of proteins was tested in BCB at pH 9 at room temperature from 1 to 12 h. Under these mild labeling conditions the sterically hindered pyrylium dyes do not bind covalently to proteins.

Table 3.3. Structures of pyrylium dyes with a sterically hindered pyrylium group and their spectral properties.

name	structure	λ_{abs}^{max} / λ_{abs}^{max}	ε [L/(cm·mol)] QY	τ (distribution τ_1/τ_2)
Py-9	$C_{27}H_{32}F_3NO_4S_2$ 555.67 $CF_3SO_3^{\ominus}$	674 / 715 nm*	130 000* 86 000 10%	1.09 ns* 0.75 ns
Py-11	$C_{31}H_{39}NO_4S$ 521.71	647 / 765 nm* 623 / 765 nm		
Py-12	$CF_3SO_3^{\ominus}$ $C_{29}H_{34}F_3NO_4S$ 549.65	639 / 765 nm* 639 / 765 nm	43 000* 42 000 <1%	0.5/0.22 ns* (5% / 95%) 0.5 / 0.25 ns (2% / 98%)
Py-13	$C_{29}H_{37}NO_4S$ 495.68	677 / 701 nm* 672 / 693 nm	160 000* 168 000 3%	0.11 / 0.3 ns* (81% / 19%) 0.28 / 0.11 ns (25% / 75%)
Py-17	$F_3CSO_3^{\ominus}$ $C_{32}H_{40}F_3NO_6S_2$ 655.79	666 / 672 nm* 615 / 690 nm bound to HSA	91 000* 66 000	0.14 / 1,5 ns* (81% / 19%)
Py-18	$C_{30}H_{24}AlCl_4NOS$ 615.38 $AlCl_4^{\ominus}$	645 / 664 nm* 567 / 644 nm	26 000* 22 000	

*methanol as solvent; others: aqueous solution

i) Pyrylium dyes with a 2,6-di-tert-butyl-pyrylium group

Py-9, Py-11, Py-12 and Py-13 were synthesized via a three step reaction. The quaternized indoles or lepidines were reacted with malonaldehyde bis(phenylimine)monohydrochloride in acetic acid anhydride to yield an intermediate, which formed, in the next step, the corresponding dye with equimolar amounts of 2,6-di-tertbutyl-4-methylpyranylium trifluoro-methanesulfonate. The dyes were separated from impurities by column chromatography.

The dyes showed no large spectral shift of the absorption maximum when they were added to a protein (HSA) solution (in BCB pH 9). Protein solutions containing Py-9 and Py-12, respectively, showed a characteristic protein band upon separation on a Sephadex G25 column, which normally implies that labeling has occurred. These bands were comparatively broad. A second separation on the column led to a decomposition of the dye-protein conjugate. From this observation it was concluded that the dyes were linked only non-covalently to the protein. The QY of Py-9 does not increase upon non-covalent labeling to HSA, the quantum yield of Py-12 increased to 7% upon noncovalent binding to protein.

ii) Pyrylium dye with a 2,6-di-phenyl-pyrylium group

Py-18 was synthesized in analogy to Py-9 to -13. Instead of the di-tertbutyl-pyrylium, 4-methyl-2,6-diphenyl-pyrylium aluminium tetrachloride was used. The dye was purified by column chromatography. The dye has an absorbance in methanol at 645 nm and in water at 567 nm, the emission is very weak with a maximum of 664 nm in methanol and 644 nm in water. Upon noncovalent interaction with HSA the absorbance maximum shifts to 580 nm and the emission maximum to 627 nm.

iii) Pyrylium dye with a carbonyl acid group for activation to an reactive OSI ester

Py-17 belongs to the series of pyrylium dyes with tertiary butyl substituents next to the pyrylium oxygen atom. As the pyrylium moiety of the dye is non reactive to amines under mild conditions, a carboxylic acid group was introduced for covalent labeling via the NHS/DCC method. The synthesis is equivalent to that described in i). The indole was alkylated with 6-bromohexanoic acid to introduce a carboxylic acid as the reactive center [4]. The reactive dye is prepared by reacting the acid with NHS and DCC in dry acetonitrile [5]. The mild reaction conditions do not lead to decomposition of the dye and a high yield can be achieved. The absorbance maximum of Py-17 bound to HSA is at 615 nm, the emission intensity at 690 nm.

Non-covalent Staining of Proteins

As an additional experiment the effect of non-covalent staining of proteins with non-reactive dyes was tested. A solution of non-reactive Py-9 and Py-12 ([Py] = $1 \cdot 10^{-6}$ mol/L), respectively, was titrated with various amounts of HSA (0-500 mg/L) in order to find out whether non-covalent conjugation of HSA affects the fluorescence of Py-9 and Py-12.
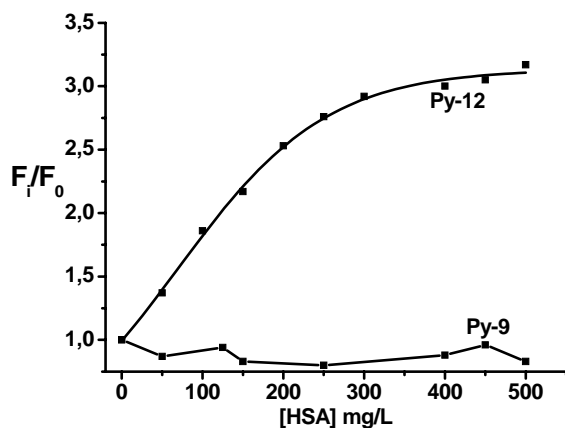
Fig. 3.12. Plot of the fluorescence intensity of Py-9 and Py-12 at the emission maximum versus the concentration of the added HSA. [dye] = $1 \cdot 10^{-6}$ mol/L. λ_{exc} = 640 nm.

Addition of HSA increases the fluorescence intensity of Py-12 about three-fold (fig. 3.12.). The fluorescence intensity of Py-9 does not increase upon addition of HSA. The position of the fluorescence maximum is shifted by 3 nm to longer wavelength in case of Py-9 and by 20 nm in the case of Py-12. The enhancement of the fluorescence intensity allows the speculation that Py-12 may interact with HSA and move into the hydrophobic domains of the protein. There the chromophore is rigidized and shielded from the solvent molecules, which otherwise might act as quenchers.

3.3. Conclusion

The pyrylium salt was chosen as an amine-reactive group to be a part of the structure of new covalent fluorescent labels. Cyanines and squaraines are well known fluorescent markers and therefore gave the basis for a new class of dyes. All dyes contain only one reactive group which avoids crosslinking.

Py labels can be linked covalently to primary amines of proteins, but also to other molecules containing a primary amino group. This reaction causes a change in the structure of the chromophore and therefore in the spectral behavior of the label. The absorption maximum

shifts to shorter wavelength (except Py-7) and the emission intensity increases. The molar extinction coefficient of the label is higher (between 35 000 and 100 000 L/(cm·mol)) and decreases upon conjugation (determined by reaction with propylamine between 14 000 and 70 000 L/(cm·mol)).

Py labels are not stable in buffered solution with a pH higher than 7. They react very fast with primary amines both in buffered solution and in organic solvents to form stable pyridinium analogues. With secondary and tertiary amines the pyrylium ring is nucleophilically attacked and opened. This effect can be detected by the loose of the original color of the label.

The significant spectral change upon covalent binding of the label to a primary amino-group can be easily used for several applications. The changes of the absorption maximum and the increase of fluorescence intensity upon conjugation are particularly characteristic for the labels Py-1 and Py-6. So both can be used in absorptiometric and in fluorometric assays for instance for detection and quantization of proteins. The decrease in the absorption maxima (at 611 and 568 nm, respectively) or the increase in the absorption maxima of the conjugates (at 503 and 540 nm, respectively; see chapter 4.1.) may be measured. Both Py-1 and Py-6 have their specific merits. Py-6 is more stable in aqueous solution than Py-1, while Py-1 is more easily prepared and is obtained in higher yield. Py-1 also is prefered, because it reacts more rapidly, gives larger spectral effects upon reaction with primary amines and has a higher QY upon conjugation. The use of the Py-1 label for detection and determination of proteins in solution and in a gel matrix is shown in chapter 4.

Other Py labels from the series shown here and their conjugates were used for lifetime affinity assays, in hybridization assays based on lifetime detection in the nanosecond range, and as new fluorescent markers for cytometric analysis (see chapter 4).

Sterically hindered pyrylium salts (here with the example of 2,6-di-tertiary butyl and 2,6-di-phenyl pyrylium) do not react with amino groups of proteins under mild labeling conditions, but as it is shown with the example of Py-9 and Py-12, form non-covalent protein-dye conjugates. Amine reactive derivates may be formed by introduction of carboxy groups.

3.4. References

[1] a) A.T. Balaban, G.W. Fischer, A. Dinulescu, A.V. Koblik, , G.N. Dorofeenko, V.V. Mezheritski, W. Schroth, Pyrylium salts: Synthesis, reaction and physical properties, Advanced in heterocyclic chemistry, Suppl. II (A.R. Katritzky, Ed.) Academic Press, New York **1982**, b) M. Salmain, K.L. Malisza, S. Top, G. Jaouen, M. Sénéchal-Tocquer, D. Sénéchal, B. Caro, [η^5-Cyclopentadienyl]metal Tricarbonyl pyrylium salts: Novel Reagents for the Specific Conjugation of Proteins with Transition Organometallic Labels; Bioconjug. Chem. **1994**, 5, 655-659; c) A.R. Katritzky, J.L. Mokrosz, M.L. Lopez-Rodriguez, Pyrylium-mediated transformation of natural products. Part 5. Reactions of gelatin and chymotrypsin with 4-(4-methoxy-3-sulfophenyl)-2,6-bis-(4-sulfophenyl)pyrylium perchlorate, J. Chem. Society, Perkin Transactions 2: Physical Organic Chemistry (1972-1999) **1984**, 5, 875-878; d) B. Caro, F. Le Guen-Robin, M. Salmain, G. Jaouen, 4-Bechrotrenyl Pyrylium Salts as Protein Organometallic Labelling Reagents, Tetrahedron **2000**, 56, 257-263; e) K. Dill, S. Hu, A.R. Katritzky, M. Sutharchanadevi, New method of blocking lysyl residues of proteins using 4-(4-methoxy-3-sulfophenyl)-2,6-bis-(4-sulfophenyl)pyrylium   perchlorate.   J.   Biochem. Biophys. Methods **1988**, 17(1), 75-8.

[2] S.M. Yarmoluk, A.M. Kostenko, I.Y. Dubey, Abstract of papers, The 8th European Conference on Spectroscopy of Biological Molecules, The Netherlands **1999**.

[3] M. Gruber, FRET Compatible Long-Wavelength Labels and their Application in Immunoassays and Hybridization Assays, Dissertation, University of Regensburg **2002**.

[4] R.B. Mujumdar, L.A. Ernst, S.R. Mujumdar, C.J. Lewis, A.S. Waggoner, Cyanine Dye Labeling Reagents: Sulfoindocyanine Succinimidyl Esters, Bioconjugate Chem. **1993**, 4, 105-111.

[5] B. Oswald, L. Patsenker, J. Duschl, H. Szmacinski, O.S. Wolfbeis, and E. Terpetschnig, Synthesis, Spectral Properties, and Detection Limits of Reactive Squaraine Dyes, a New Class of Diode Laser Compatible Fluorescent Protein Labels, Bioconjugate Chem. **1999**, 10, 925-931.

4. Bioanalytical Applications

4.1. Protein Determination Using Py Dyes

Pyrylium dyes were tested as a new class of labels for gel electrophoresis and also for general protein quantitation in solution. The pyrylium groups react with primary amines of proteins to form the respective pyridinium analogs. These conjugates can be used for determination and quantification of proteins.

4.1.1. Protein Detection in a Gel Matrix

Analysis of the human genome is completed. The focus is now on the proteome analysis to deliver an accurate picture of cellular metabolism. A very common working tool is the SDS gel electrophoresis. There is a great demand for new and sensitive detection systems for proteins on SDS gels.

4.1.1.1. Protein Staining after Electrophoresis

Label Py-1 was tested with respect due to its suitability in electrophoresis on SDS-PAGE gels. Py-1 has a blue color and is virtually nonfluorescent. It reacts with primary amino groups of proteins separated via gel electrophoreses in aqueous solution of pH 8 - 9 at room temperature to give a covalently stained red conjugate in the gel matrix. Simultaneously, the fluorescence quantum yield increases (up to 50%) depending on the protein to be labeled and on the dye-to-protein ratio (DPR). Figure 4.1. shows the result of an electrophoretic separation of a variety of proteins on a standard gel with 10 different proteins. The gel was analyzed using a standard laser-based scanner and the results (table 4.1.) show that even in these initial experiments the limits of detection for most proteins are as good as with the (highly sensitive but tedious) silver staining method, and often better than those obtained with Coomassie Brilliant Blue (CBB) and the SYPRO stains [1-3].

Table 4.1.   Detection limits for proteins (ng/band) in SDS-PAGE as determined by
                staining with silver, Coomassie Brilliant Blue (CBB), and Py-1, respectively.

protein	silver staining[a]	CBB [a]	Py-1
myosin	1	8-16	1
β-galactosidase	3	8-16	0.8
glycogen-phosphorylase	1	16-30	3
bovin serum albumin	3	16-30	< 2.5
glutamate dehydrogenase	3	16	< 0.8
lactate dehydrogenase	n. d.	n. d.	4
carbonic anhydrase	6	16-30	4
trypsin inhibitor	3	16-30	12
lysozyme	4	16-30	14
aprotinin	6	16-30	4

[a] data from ref. [1]
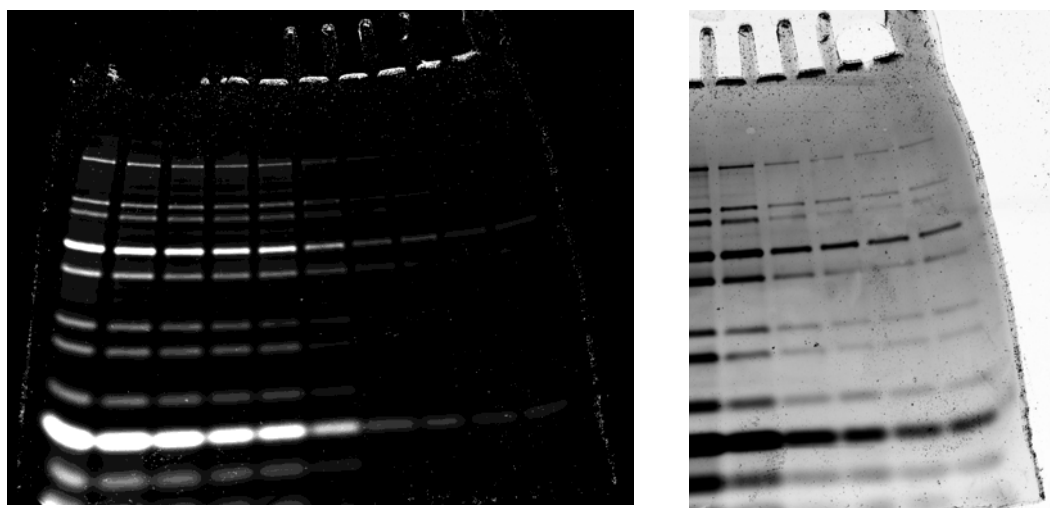
Fig. 4.1.   *Left:* standard SDS polyacrylamide gel with ten lines of a serial dilution of the
             mass-standard. (see Experimental Part, chapter 5.4.). *Right*: Right side of the gel
             (lines 5 to 10). Right gel displayed in inverted intensity.

The fluorescence of the red conjugate formed between Py-1 and proteins can be excited
between 470 and 530 nm and therefore matches several standard laser lines, whilst the free
(blue) label is not excited at all at this wavelength. Thus, the fluorescence of the stained

protein is measured against an almost dark background even if residual free (blue) label is still present.

In addition to the fact that the Py labels undergo a large color change on conjugation and a transition from a nonfluorescent to a strongly fluorescent state, they have two additional attractive features: The first is that labeling causes a relatively small increase in the mass of the protein ($\Delta m = 288$ g/mol in case of mono-labeling with Py-1). Secondly (and possibly even more importantly), the electrical charge of a protein does not change on conjugation (since a positively charged amino group is replaced by a positively charged pyridinium group). The second feature is particularly significant, since it has been reported that (multiple) labeling of proteins with dyes that have no (or even a negative) charge results in differently charged labeled proteins. As a result, a certain protein can display different migration rates in (capillary) electrophoresis and consequently give rise to more than one peak or substantial band broadening [4].

On the other hand, it must be kept in mind that most covalently binding stains interfere with mass spectrometry as a detection method for proteins after gel electrophoresis. Although the stain Py-1 is rather "small", it cannot be excluded that more than one Py-1 is linked to a protein, thus complicating MS analysis.

4.1.1.2. Pre-Staining before Electrophoresis

In an additional experiment, pyrylium labels were tested and compared with other amine-reactive dyes as labels for staining proteins <u>before</u> electrophoretic separation of a protein standard mixture. This is a so called pre-staining experiment. A protein standard (low range standard from Sigma) was dissolved in bicarbonate buffer (BCB) of pH 9 and labeled with two different concentrations of seven amimo-reactive dyes for 30 min (see experimental part, chapter 5.4.). Figure 4.2. shows the pockets of a gel electrophoresis device, loaded with the pre-stained protein samples. The first, the medium (9th) and the last pocket were filled with the protein standard (S) without pre-staining reagent. The other numbers in the figure refer to the respective dye, where Py-2 is 1, Py-4 is 2, Py-6 is 3, Py-1 is 4, ATTO 550 is 5, Bodipy TR-X is 6, and C546 is 7. The left pockets numbered from 1 to 7 are filled with the protein standard stained with 1 µL of the seven concentrated dye solutions ([dye] = 2 g/L), the protein standard in the right pockets was stained with 1 µL of the seven diluted dye solutions ([dye] = 0.2 g/L).
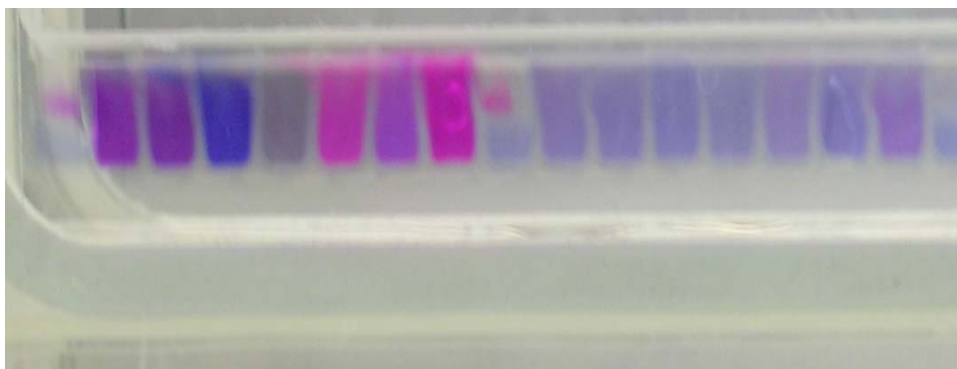
S 1 2   3   4 5   6   7 S 1   2   3 4 5   6   7   S

Fig. 4.2.   Picture of the gel pockets of an electrophoresis device. For the assignment of
numbers to dyes see the text above.

The gel was run and afterwards the fluorescent bands of the pre-stained and separated proteins
on the gel were detected on a UV screen with a camera (fig. 4.3.).
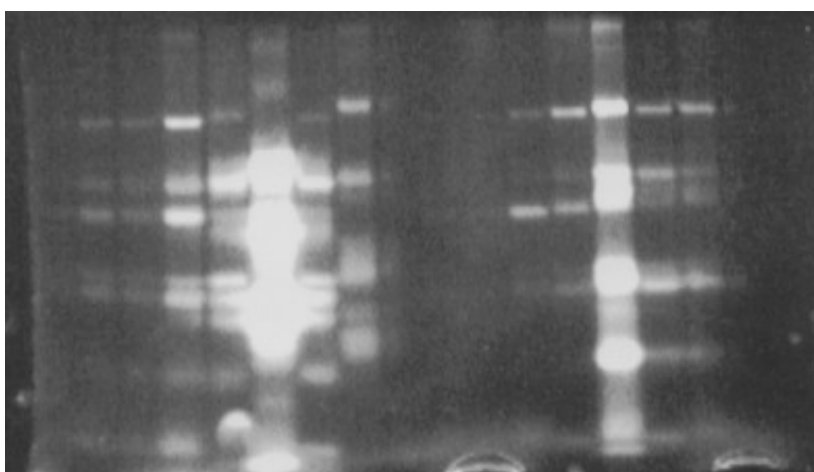
S 1 2 3 4 5 6 7 S 1 2 3 4 5 6 7 S

Fig. 4.3.   Picture of the SDS gel after electrophoresis on a UV screen.

The brightness of the bands is influenced by the efficiency of the pre-staining and binding of
the labels to the different proteins, the effect of self-quenching, the possibility of exciting the
label with UV light, and the detection of the fluorescent bands with a normal camera. ATTO
550 (5) gives the brightest bands on the gel due to this detection method. Its fluorescence
outshined nearly the other bands. But all dyes are sufficiently bright for detection of the bands
of the protein standard even on a normal UV screen. In the right part of the gel, proteins in
line 1 and 2 (Py-2 and Py-4) are not detectable any longer. This can be explained with a low
label concentration, a low labeling rate and the fact that Py-2 and Py-4 have excitation
maxima at 514 and 540 nm, not fitting the UV-excitation, and a QY of about 20% conjugated
to a protein.

All of the labels used in this experiment have survived the denaturizing step of the proteins before SDS PAGE separation. In a last step the gel was stained with Coomassie Brilliant Blue (CBB) using a standard procedure in order to ease the comparison between the different protein lines [5]. At the end the gel was dried because of easier handling and better durability.

Figure 4.4. is a picture of the dried gel taken with a scanner (HP ScanJet 5370 C). All bands are now visible and can be examined according to their migration rate and broadness.

S 1 2 3 4 5 6 7 S 1 2 3 4 5 6 7 S
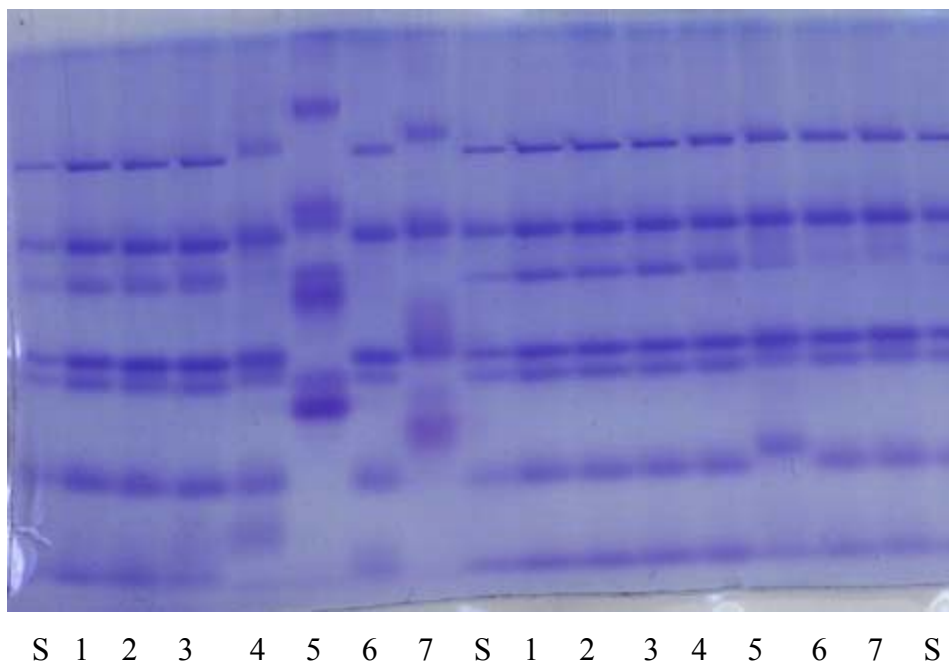
Fig. 4.4.   Scan of the gel after staining with CBB and drying.

The proteins are separated on the SDS gel according to their molecular mass. Since proteins are charged at any pH other than their isoelectrical points, they migrate in an electric field at a rate dependent on their charge density. Charge density is the ratio of charge to mass. In this experiment reduced and denaturized samples, which means the proteins were boiled in the presence of an ionic detergent (SDS) and a reducing agent (β-mercaptoethanol), were separated. Under these conditions there is a linear relationship between the log of molecular mass and migration distance in the gel.

Before the denaturizing step, the protein mixtures were covalently stained with different labels in two different concentrations. One protein can bind several dye molecules, which means several species of this protein can exist. The label can cause different effects on the SDS coat and therefore on the charge density of the denaturized protein. SDS is negatively charged, so when the label also has a negative charge, the SDS coat of the protein can be thinner in the proximity of the stain, and the migration of the protein can decrease. The dye-

to-protein rate of each sort of protein is only a statistical number, so band broading can also appear.

A strong effect on the migration rate can be seen in the row (5) and (7), where ATTO 550 and C546 were used in high concentration for pre-staining (left part of the gel shown in fig. 4.3.). But also in row (4) where Py-1 is used for labeling, the migration of the smallest protein is somewhat slower compared to the band of the same protein without fluorophore (S). In the right part of the gel shown in figure 4.4., the proteins were pre-stained with the tenth part of label and an effect on the migration can be seen only on the row labeled with ATTO 550 (5). ATTO 550 is a dye with a high molare absorbance (120 000 $M^{-1}L^{-1}$) and a QY of 80% when conjugated. Its precise structure is not available but is based on a rhodamine structure. C546 is a cyanine dye with only one reactive OSI ester group and an additional negative charge (SO_3^-).

A variation in migration and the effect of band broadening for pre-stained proteins can be explained by variations in the homogeneous SDS coat. The label influences the coating of the protein with SDS by repulsion. This effect can be increased by higher DPRs and is influenced by the charge of the label.

A better method for examination of these effects is capillary electrophoresis. It is more sensitive to migration rates and peak broadening. Capillary electrophoresis experiments with Py-1 and Py-6 as covalent dyes for protein detection were done in cooperation with D. Craig and published [6]. Py-1 and Py-6 were used to label a test protein (HSA), and the sample was analyzed using capillary electrophoresis and laser-induced fluorescence detection. Detection limits after a 60 min labeling reaction at 22 ^{o}C (Py-1) and 50 ^{o}C (Py-6) were 6.5 ng/ml (98 pM) of HSA for Py-1 and 1.2 ng/ml (18 pM) of HSA for Py-6.

4.1.2. General Protein Assay Using Py-1 as a Chromogenic and Fluorogenic Amine-Reactive Probe

A new protein assay, that makes use of easily accessible new class of reagents, works at neutral and slightly alkaline pH, can be adapted to both photometry and fluorometry, and has very low limits of detection, is described here. It is based on the use of Py-1. This dye reacts easily with amino groups of proteins, and this reaction causes a significant spectral change to occur (color change from blue to red). Upon reaction with the proteins, the label becomes highly fluorescent, and this enables the quantitation of proteins with limits of detection that are comparable to the best methods known, however without the need for additional oxidative

or toxic reagents.

The reaction with primary amino groups of proteins as shown in chapter 3.1.2., fig. 3.6., occurs in most cases with the ε-amino group of lysines. Experiments (in chapter 3.1.2.) revealed that the Py-1 reacts with primary amines, but not with secondary amines or with thiols, to form a new fluorescent species. Thus Py-1 may also be used for labeling and photometric determination of synthetic alkylamines and of biogenic amines such as phenethylamine. The reaction with amines and proteins proceeds quickly in aqueous solution of neutral or slightly alkaline pH and even in aqueous methanol and acetonitrile. The rate of the reaction can be followed easily by observing the color change of the solution (see chapter 3.1.2.).

The visually observable color change from blue to red is paralleled by a shortwave shift of 108 nm of the absorption maximum. The shift in emission, in contrast, is much smaller (-63 nm). Unlike cyanine-labeled proteins, the Py-labeled proteins display fluorescences with rather large Stokes' shifts (40 – 100 nm), and this strongly facilitates the separation of scattered excitation light from fluorescence.
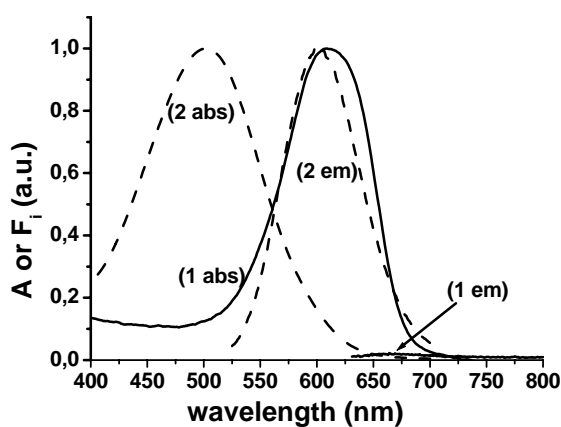
Fig. 4.5.   Normalized absorption spectra and emission spectra of free Py-1 (1 abs and 1 em, continous lines) and of Py-1 conjugated to HSA (2 abs und 2 em, dotted lines) in phosphate buffer of pH 7.2. The DPR of the conjugate was 1.7.

The large differences of the absorption maxima of the unconjugated dye Py-1 and its HSA conjugate, and the strong increase in fluorescence intensity on labeling a protein are also evident from fig. 4.5. The approximately 50-fold enhancement of fluorescence intensity on conjugation is particularly significant. Moreover, the excitation/emission peaks of the free dye (611/665 nm) are spectrally very different from those of the conjugate (503/602 nm). By

exciting the conjugate at around 500 nm, the unreacted dye is not excited at all and thus causes no undesired background. The large spectral shift that occurs on labeling is not unusual since pyridinium chromophores in organic solvents have much shorter absorption maxima than the respective pyrylium chromophores [7]. The fluorescence enhancement is due to the exchange of the pyrylium oxygen atom by the nitrogen atom from the amine moiety [8, 9].

The spectra do not notably vary from protein to protein. The decay times of the fluorescence of the conjugates are slightly different and are in the order of 2 ns, while those of the free Py labels are <0.1 ns. Importantly, the absorption and emission spectra of the conjugates are not affected by pH in the range between pH 5 and 10.

Unlike practically all other protein labels, the Py dyes do not yield conjugates with side bands. The widely used Alexa dyes, for example, give shortwave sidebands, while the bodipy dyes give longwave sidebands in the emission spectra (www.probes.com). Sidebands are highly undesirable since they broaden the emission band, compromise the quality of multicolor assays, and give rise to non-monoexponential fluorescence decay profiles.

Py-1 has its specific merits. It reacts rapidly and gives larger spectral effects on reaction with proteins than the other Py labels (see fig. 3.4. and 3.5.). The label can be used both in photometric and in fluorometric protein assays. In photometric assays, the decrease in the absorption maxima (at 611 nm) of the free dye or the increase in the absorption maxima of the conjugates (at 503 nm, see fig. 4.5.) may be measured. Photometry with standard photometers enables proteins to be quantified in the concentration range from several μg to several mg per mL.

The assay can be made more sensitive by exploiting the increase in fluorescence intensity that occurs on labeling. The fluorescence of the conjugates may be measured at the respective peaks of excitation or emission, but also by using the standard filter combinations of microplate fluorescence readers. The 485/635-nm combination of one of the readers used in these experiments turned out to be best for proteins labeled with Py-1.

Photometric protein assay

The findings mentioned above can be applied in a straightforward photometric or fluorometric general protein assay, provided the examined protein is known. The assay was worked out for HSA, BSA, apoferritin, lysozyme, pepsin, and γ-globulin. A typical absorptiometric calibration plot is shown in fig. 4.6. (for HSA). The limit of detection (LOD) is found to be 1.2 μg/mL. This is significantly lower than the detection limit for protein determination based on the absorbance at 280 nm, which is 17.9 μg/mL and which is strongly interfered by

biological material absorbing in the ultraviolet [10]. The assay may even be applied to HSA in urine since its concentration in urine is usually $2 - 4$ mg L^{-1}, which increases to $5 - 10$ mg L^{-1} in case of borderline microalbuminurea [11] but can be much higher in case of albuminuria. Commercially available immuno tests for detection of albuminuria have LODs of 10 µgL^{-1}.
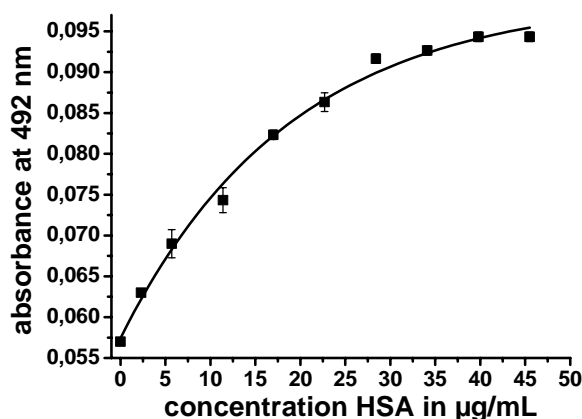
Fig. 4.6.   Calibration plot for the HSA assay with Py-1 based on absorptiometry, and error bars for n = 3.

Fluorimetric protein assay

Effect of the Dye-to-Protein Ratio

Solutions of apoferritin (4 µg/mL) and lysozyme (10 µg/mL) were prepared in BCB of pH 9.0. Various volumes of the respective solutions (10, 25, 37, 50 and 100 µL for apoferritin; 5, 10, 25, 37, 50, 75, 100 µL for lysozyme) were added to the wells of a microplate and made up to 100 µL with BCB. The aqueous Py-1 reagent solution (described in chapter 5.5.) was diluted to concentrations of 5, 3.2, and 2.5 µmol/L and then was added in amounts of 100 µL to the different protein solutions in the wells. In order to test different instruments, the resulting fluorescence intensities were measured on the Ascent reader (in case of apoferritin) and on the Tecan reader (lysozyme) at excitation/emission wavelengths of 485/650 nm (Ascent) and 485/635 nm (Tecan), respectively. A kinetic study over 120 min showed that the lowest limits of detection are obtained after an incubation time of 90 min (also see fig. 4.7.).

It has been shown before that the fluorescence intensity (and quantum yields) of a labeled protein depends on the DPR which contrasts the situation in absorbance which virtually goes linear with the DPR. This can be clearly demonstrated in case of the fluorescence assays for apoferritin and lysozyme. Respective calibration plots are shown in fig. 4.7. They show that different DPRs cause quite different slopes and shapes even over identical concentration ranges of the same protein. On the other hand, high reproducibility is

obtained (see the data in the validation part) if the same protocol is used for the sample runs and the calibration runs.
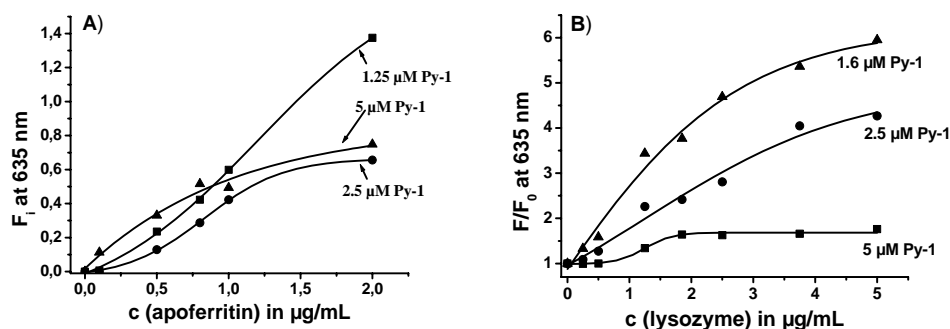
Fig 4.7.   Calibration plots for apoferritin (A) and lysozyme (B) at different dye-to-protein ratios (DPRs). The plots in A were obtained with data of the Tecan Genios plus reader, those in B on the Fluoroskan Ascent reader. Each data point is the average of eight readings.

Variation of the protein

Lysozyme, globulin and pepsin were dissolved in BCB of pH 9.0 in a concentration of 10 µg mL^{-1}, and diluted with BCB in the wells of a microplate to the corresponding concentrations (10, 9, 7.5, 5, 2.5, 2, 1, 0.5 µg/mL in a final volume of 100 µL). 100 µL of the reagent solution (described in chapter 5.5.) were added to these solutions. Fluorescence was measured at room temperature after shaking the solutions for 60 min.

The shapes of the calibration plots for various proteins are different and this probably reflects the number (and proximity) of amino groups that can be labeled. The results obtained with lysozyme, pepsin, and γ-globulin (using Py-1 as the label) are given in fig. 4.8.
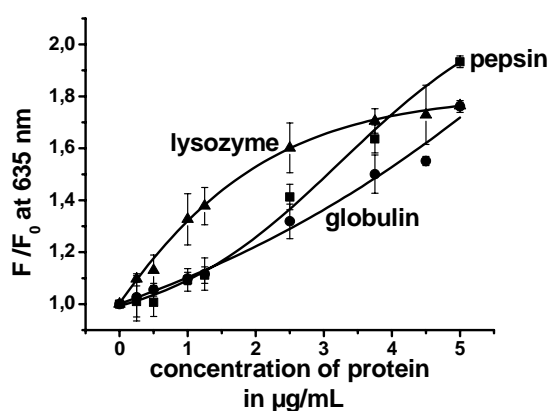
Fig. 4.8.   Fluorometric calibration plot for three proteins of different molecular weight.

The findings can be interpreted by (a) self-quenching of fluorescence, and (b) the large

differences in the molecular weight of the proteins studied. All proteins were applied in the same mass concentrations. Small proteins like lysozyme (14.4 kDa) therefore will be present in higher molar concentration than proteins of higher M_r. When applying the same labeling protocols, this will result in a lower DPR compared to pepsin (36 kDa) and globulin (160 kDa), and thus in reduced self-quenching. Indeed, the lysozyme calibration plot is the steepest (fig. 4.8.), while the slopes are very similar for pepsin and globulin, at least in the lower concentration range.

Serum albumins are probably the proteins that are to be determined most often in practice. A calibration plot for the optimized fluorescence assay for BSA (using Py-1 as a reagent) is presented in fig. 4.9. BSA can be determined best over the concentration range from about 0.1 to 5 µg/mL. The LOD (3σ/slope) is 60 ng/mL. As can be seen in the inset of fig. 4.9., there is a linear relationship between fluorescence and BSA concentration in the range between 0 and 0.45 µg/mL. At concentrations higher than 1 µg/mL the plots get nonlinear.
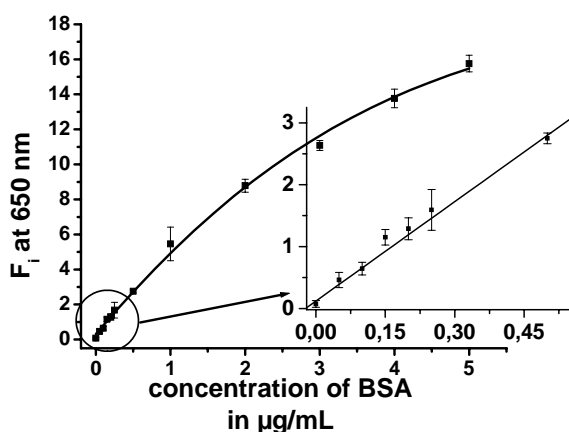
Fig. 4.9.   Calibration plot (and standard deviations for n = 5) for the fluorometric BSA assay. The inset shows the plot for the low concentration range.

Validation of the BSA Assay

So far, the new assay format was demonstrated for purified proteins only. In the next step, unknown protein samples were analyzed and the results were validated. The determination of total protein in serum or plasma served as an example.

As a preliminary experiment plasma (unspecified) was diluted 1:100 v/v (plasma/BCB of pH 9.0). Different quantities (10, 20, 30, 40, 50, 60, 70 µL) of this pre-diluted plasma were re-filled with BCB in the wells of a microplate to a total volume of 100 µL and 20 µL of aqueous Py-1 solution ($6 \cdot 10^{-5}$ mol/L) were added. The plasma dilution factor in plot 4.10.

gives the percentage of the pre-diluted plasma in each well (a plasma dilution factor of 0.1 is equal to 10 µL of pre-diluted plasma in a total volume of 100 µL) before addition of the dye solution. The results showed that there is a linear increase in fluorescence intensity (fig. 4.10.) with this plasma between dilution factor 0.1 and 0.25, which means a dilution of the unspecific bovine plasma from 1:1000 to 1:400 (v/v, plasma/BCB). Therefore a pre-dilution of the origin plasma sample of 1:1000 and 1:500 in the following experiments was chosen.
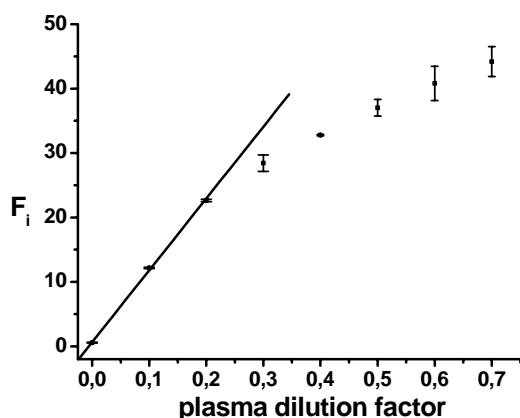
Fig. 4.10.   Plot of the fluorescence intensity of Py-1 (10 µM) titration with different concentrations of plasma in BCB pH 9. A linear increase in fluorescence intensity is shown with a linear fit.

A calibration plot was established by first preparing a stock solution of bovine serum albumin (BSA) in BCB (120 µg/mL). Volumes of 5, 10, 25, 30, 40 and 50 µL, respectively, of this solution were placed in the wells of a 96-well microplate and made up with BCB to a volume of 108 µL. Thereafter, 12 µL of the Py-1 methanol stock (see chapter 5.5.) solution were added. After 1-h incubation at 25 °C fluorescence intensity was read and used to establish a calibration plot. Spiking experiments were performed with unspecified bovine blood plasma. It was diluted by 1:1000 (v/v) with BCB, and 50 µL of this solution were spiked with 5, 10, 25, 30, 40 and 50 µL of a BSA stock solution (120 µg mL^{-1}), made up with BCB to 108 µL, reacted with Py-1, and fluorescence intensity read as described above.

The data resulting from this type of spiking and recovery experiments are shown in figure 4.11. Plot A in fig. 4.11 is the calibration plot of BSA and plot B shows the results of bovine plasma (dilution of the origin plasma 1:1000 v/v in BCB) spiked with known BSA concentration. The fluorescence intensity in both plots was measured under the same conditions.
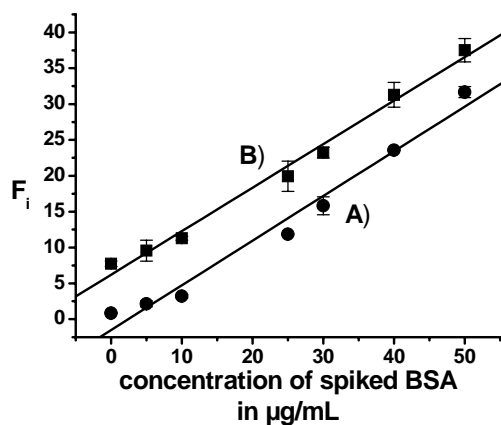
Fig. 4.11.   Validation of the BSA assay. Calibration plot for BSA obtained by spiking bovine
plasma with increasing concentrations of BSA. (A), calibration plot for pure BSA;
(B), plasma spiked with BSA. Error bars represent the standard deviation
(for n = 3).

Plot A can be described by the linear fit y = -1.5 + 0.62x. Data analysis (for n = 7) gave r = 0.9885. Plot B has virtually the same slope as plot A. The difference in the intercept between plot A and B was determined to be 7.7. This intercept and a slope of 0.62 form the basis for the calculation of recovery data. Recoveries between 91 and 103% (average 97%; see table 4.2.) were obtained and demonstrate the robustness of the assay even in diluted blood plasma.

Table 4.2. Recovery data for the determination of BSA in spiked plasma samples.

BSA added to the plasma sample (μg mL^{-1})	F_i measured	F_i calculated	SD of F_i measured (n = 3)	Recovery (%)
5	9.560	9.313	1.462	103
10	11.291	12.427	0.264	91
25	19.931	21.769	2.106	92
30	23.227	24.883	0.751	93
40	31.285	31.111	1.728	101
50	37.512	37.339	1.631	100

The total protein content of the serum and plasma samples was determined by a standard addition experiment. Defined quantities of specified adult bovine serum (ABS; total protein concentration 68 mg mL^{-1}) were used to determine the concentration of total protein of the unspecified bovine serum and bovine plasma in a second spiking experiment. Both, unspecified serum and plasma samples were diluted with BCB by 1:500 (v/v) and spiked with 20, 30, 40, and 50 μL, respectively, of adult bovine serum (ABS) diluted by 1:100 (v/v) with BCB. The samples in the wells were made up to a total volume of 108 μL, labeled with 12 μL of methanol stock solution (see chapter 5.5.), and fluorescence was measured at exc/em wavelengths of 485/635 nm after an incubation time of 1 h. The resulting data and the respective linear regression functions are shown in fig. 4.12.
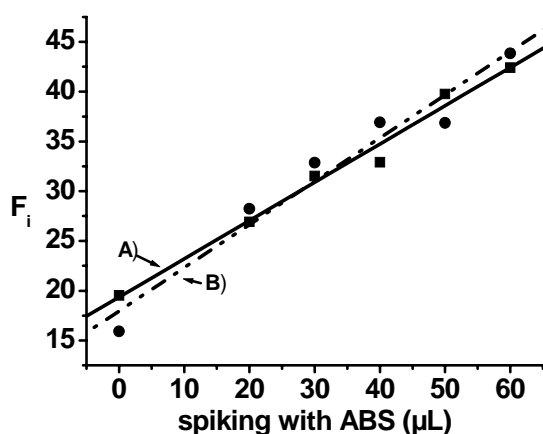
Fig. 4.12. Results of the total protein assay in plasma. The data for unspecified serum and for plasma were obtained by spiking the solutions with increasing quantities of adult bovine serum (ABS). (A), plot for serum spiked with ABS; (B), plot for plasma spiked with ABS.

Linear extrapolation to y = 0 gives an intercept of 50.5 µL on the x-axis for plot (A), and of 41.4 µL for plot (B). By using the known protein concentration of ABS, a concentration of 77 g/L of protein can be calculated for the unspecified serum, and of 64 g/L for the plasma.

The spiking experiments also demonstrate that protein concentrations in bovine serum and bovine plasma can be determined by applying the standard addition method and using specified ABS. The variation of the concentration of total protein is around 10% only. In fact, this method (like any standard addition method) does not require a calibration plot to be established with pure proteins but only the serum (or plasma) to be spiked with a reference serum of known total protein concentration

4.1.3. Conclusion

The assays presented here make use of a new type of staining reagents for proteins and are well suited for rapid quantitation of proteins, and probably also of other analytes containing primary amino groups. Py-1 is an exciting new protein label that can be applied in proteomics, e.g. in SDS electrophoresis, but also for general protein assays.

Fluorescence detection of proteins in SDS gels was done by staining the gel after the electrophoresis, which resulted in very low detection limits. Several Py labels were also tested for pre-staining proteins before gel separation. The conjugates were stable under the denaturising conditions and cause only minor effects on the migration rate of the proteins. This effect was also tested with Py-1 and Py-6 pre-stained proteins on capillary electrophoresis.

While the method for protein quantification in solution presented here is not specific for a particular protein (since it is a general protein assay), it can be performed in both photometry and fluorometry, the respective LODs and dynamic ranges being different. Since staining results in large changes of spectral maxima and quantum yields, excess (unconjugated) dyes do not measurably affect the assay. Therefore, neither separation steps nor washing steps are required. The assay is based on a single and affordable reagent and can be performed at room temperature. Toxic reagents are avoided. Comparative data are given in table 2.1. Additional features include very low limits of detection, full compatibility with microplate formats (shown for two different kinds of readers), and high robustness as shown by very good recovery data for BSA in spiked serum samples.

The features of the labels include (a) ease of preparation (b) a chameleon type of labeling (c) a transition from a nonfluorescent state to a strongly fluorescent state upon

conjugation (d) very low limits of detection for both gel assays and solution assays and (e) the fact that the charge of a protein is not changed on labeling.

4.2.   Hybridization Studies based on FRET Measurements

This chapter deals with the applicability of the new labels in homogeneous hybridization studies. The Py labels are used, respectively, as donor (red circle, fig. 4.13.) and acceptor dyes (blue circle, fig. 4.13.) in FRET studies.
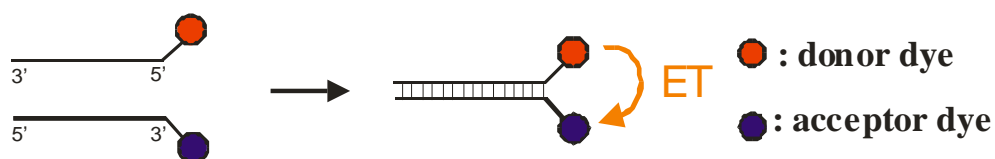
Fig. 4.13. Energy transfer (ET) between a donor labeled oligonucleotide and its acceptor labeled counterstrand upon hybridization.

Hybridization assays based on the scheme in figure 4.13. are shown in the following. In these cases amino-modified 15-mer oligonucleotides were labeled with OSI esters or pyrylium reactive dyes, respectively. The sequences of the oligonucleotides are shown in chapter 5.1., table 5.1.

Py-4 as acceptor label

A representative hybridization study based on energy transfer measurements is shown in figure 4.14. C482, an OSI ester reactive benzindolone label (prepared by Dr. A. Karasyov, University of Regensburg; structure see fig. 5.1., chapter 5.1.1.), was linked to the 5'-end of an amino-modified 15-mer oligonucleotide (oligo-1). Py-4 was labeled to the 3'-end of a complementary amino-modified 15-mer oligonucleotide (oligo-3). The donor C482_oligo-1 of constant concentration ([C482_oligo-1] = $1 \cdot 10^{-6}$ mol/L) was titrated with various amounts of acceptor Py-4_oligo-3. Molar ratios are 1:0, 1:0.125, 1:0.25, 1:0.5, 1:1, 1:2, 1:3 and 1:4. The fluorescence intensity of donor decreases and the acceptor fluorescence increases with increasing amounts of acceptor labeled counterstrand due to energy transfer.
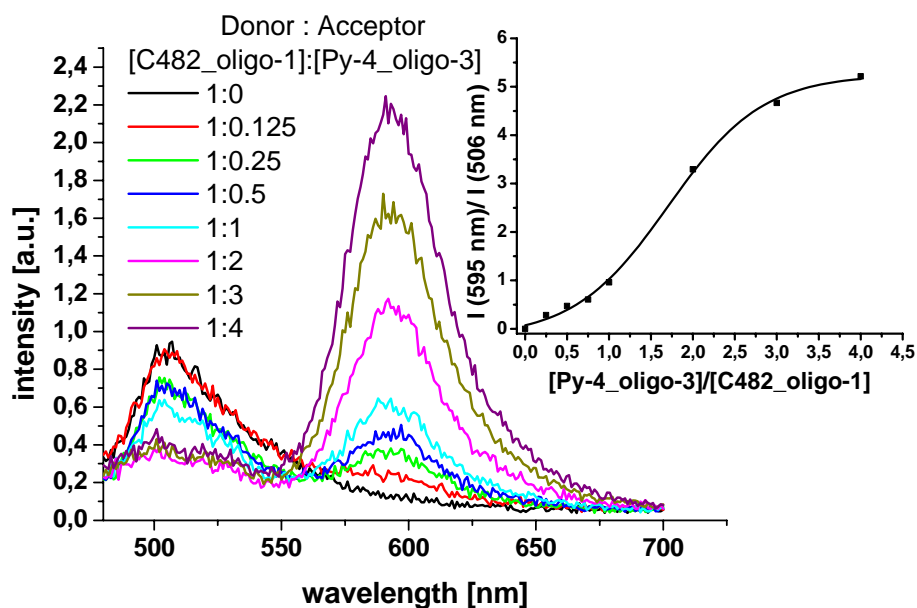
Fig. 4.14. Energy transfer study in which C482_oligo-1 of constant concentration ([C482_oligo-1] = 1·10^{-6} mol/L) was titrated with Py-4_oligo-3 (λ_{exc} = 480 nm).

The inset in figure 4.14. shows the plot of the ratio of the fluorescence intensity at 595 nm and 506 nm versus the ratio of the concentrations of C482_oligo-1 and of Py-4_oligo-3. It shows a sigmoidal binding curve, which goes into saturation at a 3 fold extent of counter strand.

Py-1 as donor label

Another hybridization study based on energy transfer measurements is shown in figure 4.15. Here the pyrylium label Py-1 is used as the donor dye. Py-1 was linked to the 3'-end of an amino-modified 15-mer oligonucleotide (oligo-3). C642 (λ_{max}^{abs}/λ_{max}^{em} 642/660 nm) was labeled to the 5'-end of a complementary amino-modified 15-mer oligonucleotide (oligo-1). The donor Py-1_oligo-3 of constant concentration ([Py-1_oligo-3] = 2·10^{-7} mol/L) was titrated with various amounts of acceptor C642_oligo-1. Molar ratios are 1:0, 1:0.25, 1:0.5, 1:0.75, 1:1, 1:2, 1:3, 1:4 and 0:4. The fluorescence intensity of donor decreases with increaseing amounts of acceptor due to energy transfer. The increase of the fluorescence intensity of the acceptor can not be detected clearly, because of the spectral overlap of the two emission spectra.
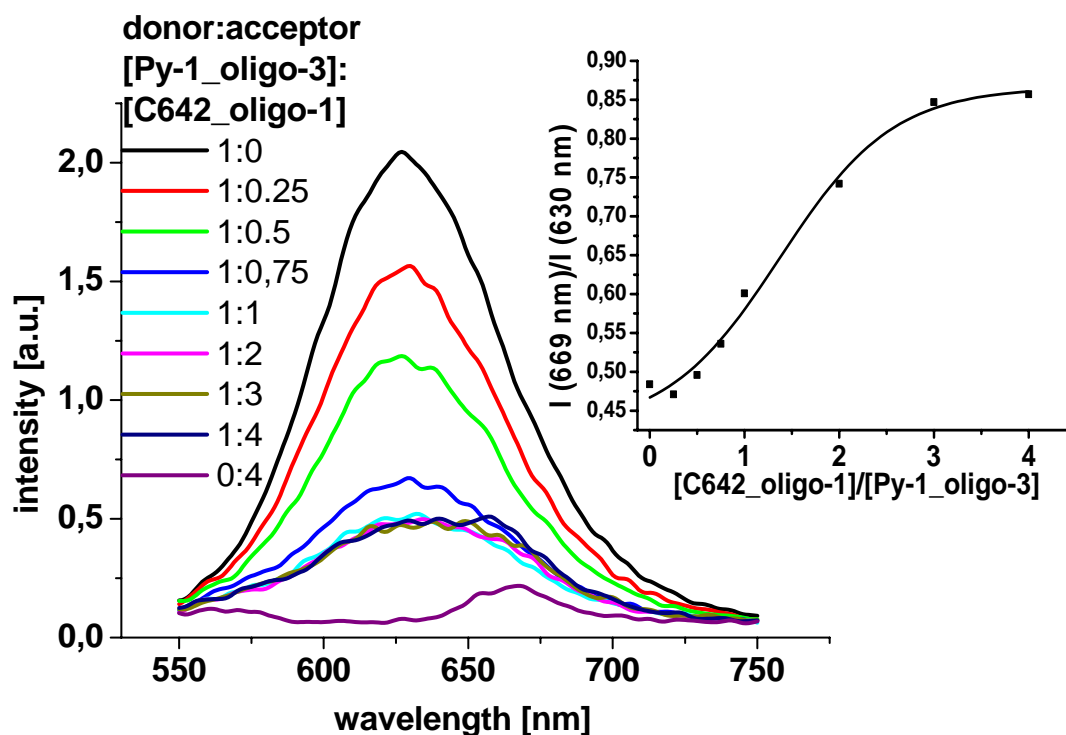
Fig. 4.15. Energy transfer study in which Py-1_oligo-3 of constant concentration ([Py-1_oligo-3] = $2 \cdot 10^{-7}$ mol/L) was titrated with C642_oligo-1 (λ_{exc} = 490 nm).

The fluorescence intensity of the donor decreases by 75% upon addition of an equimolar amount of C642_oligo-1 (fig. 4.14., 1:1) compared to the intensity without acceptor (fig. 4.14., 1:0). The inset in figure 4.15. shows the plot of the ratio of the fluorescence intensities at 669 nm and 630 nm versus the ratio of the concentrations of Py-1_oligo-3 and the concentration of C642_oligo-1. The ratiometric plot shows the sigmoidal binding curve of this system.

Energy transfer study in microplate format

In this hybridization study based on energy transfer measurements both donor and acceptor dyes are pyrylium dyes. Py-1 was linked to the 5'-end of an amino-modified 15-mer oligonucleotide (oligo-1). Py-17 was labeled to the 3'-end of a complementary amino-modified 15-mer oligonucleotide (oligo-3) via a OSI reactive ester. The donor Py-1_oligo-1 of constant concentration ([Py-1_oligo-1] = $1 \cdot 10^{-6}$ mol/L) was titrated with various amounts of acceptor Py-17_oligo-3. Molar ratios are 1:0, 1:0.125, 1:0.25, 1:0.5, 1:0.75, 1:1, 1:1.5, 1:2 and 1:3. The energy transfer study was detected in a microplate format, with three replications

of each concentration. The fluorescence intensity of donor decreases to 40% of the intensity measured without acceptor.
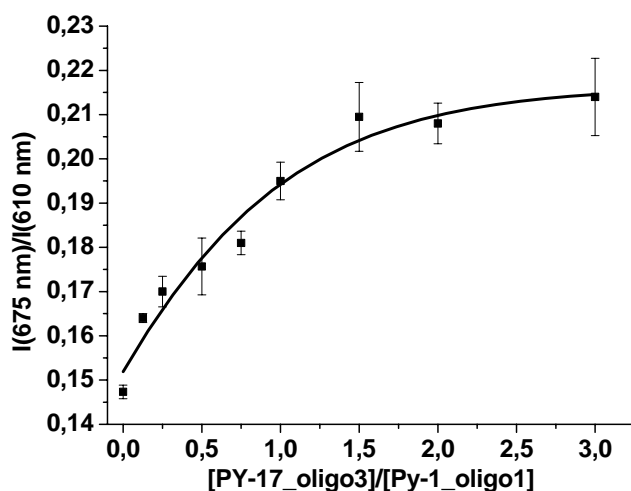
Fig. 4.16. Plot of the ratio of the fluorescence intensities at 675 nm and 610 nm versus the ratio of the concentration of Py-1_oligo-1 ([Py-1_oligo-1] = $1 \cdot 10^{-6}$ mol/L) and the concentration of Py-17_oligo-3.

The data were collected on a microplate reader with the filter combination for exc/em of 485/610 nm and 485/675 nm. Figure 4.16. shows the plot of the ratio of the fluorescence intensities at 675 nm and 610 nm versus the ratio of the concentrations of Py-1_oligo-1 and the concentration of Py-17_oligo-3. The plot reaches saturation at a ratio of 1.5 of donor to acceptor. Although the filter combination is not optimal for this label pair, an effective energy transfer was shown with the help of the combination of these labels and filters.

These three energy transfer systems show the efficiency of pyrylium labels as donor and acceptor dyes in FRET studies. The absorbance and emission spectra of pyrylium labels are broad, which is on the one hand a disadvantage, for example for multicolor detection. On the other hand, broad absorbance spectrum is preferable because several excitation sources can be used. The broad emission spectrum of a donor dye can overlap more easily with the acceptor absorbance. In microplate readers with filters for wavelength selection for excitation and emission wavelength, labels with a broad band are favorable to match the adequate filter pair.

4.3. Application of Py Dyes in Lifetime Measurements

4.3.1. Screening Scheme Based on Measurement of Fluorescence Lifetime in the Nanosecond Domain (FLAA)

Affinity assays play a major role in diagnostic testing, in particular in immunoassays, and in high throughput screening (HTS). Numerous methods are known but the most sensitive ones include radioimmunoassay (RIA) [12-14], chemiluminescence immunoassay (CLIA) [15-17], and fluorescence immunoassay (FIA) [18-21]. Electrochemical affinity assays also can be quite sensitive but are less often used in practice [22-25].

This chapter deals with an affinity assay scheme that is based on the measurement of fluorescence decay times in the ns time domain. This has become possible after having discovered several fluorophores, which – after conjugation to a protein – undergo a substantial change in decay time following affinity binding. These findings have enabled the straightforward affinity assay described here.

Choice of the affinity system

The streptavidin-biotin (SA-Bt) affinity system was chosen since it is most established as a model system, because the resulting assay is simple and popular. Both species involved can be labeled easily with fluorophores by applying standard protocols. Streptavidin (SA) binds biotin (Bt) with extremely high affinity, with a K_A in solution around 10^{15} M^{-1}. This strong and specific binding has resulted in many powerful bioanalytical applications but also is often used as a model in studying receptor-ligand interactions [26].
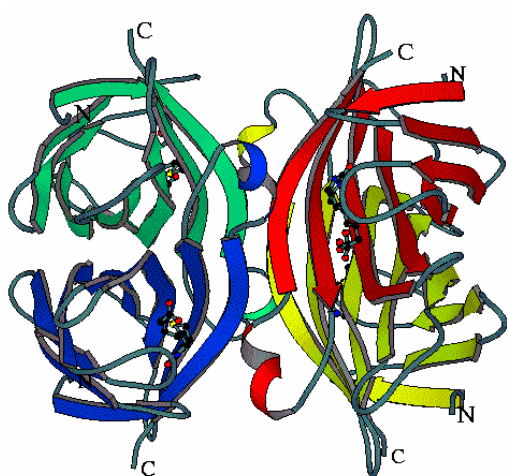
Fig. 4.17. Streptavidin is a tetrameric protein. Each monomer binds one biotin molecule.

Moreover, the system offers additional advantages since it represents an almost universal system and antibodies can be easily biotinylated without loss of biological activity. Finally SA is a very stable protein that usually is not deactivated upon labeling [27].

Choice of labels

Numerous fluorophores are known for labeling proteins. However, good labels are insensitive to their micro-environment and do not undergo a change in their absorption and emission maxima on conjugation and, subsequently, on affinity binding. One needs to discern between (a) changes in decay time that occur on conjugation of the label to a protein, and (b) changes that occur on affinity binding. The second important aspect is the exponentiality of the decay of the emission. Many labels, after having been conjugated to proteins, display multi-exponential rather than mono-exponential decay times (τ). Multi-exponential decays are usually characterized by the decay times and the respective weighing factors, i.e. the contribution of a single exponential to the total decay profile. The fraction (weighing factor) of each component (each τ) may change on affinity binding, a situation that is highly undesirable in practice.

Numerous labels out of a series of commercially available pyrylium, cyanine and cumarin dyes were screened but only a few showed (a) significant $\Delta\tau$ when linked to Bt and then bound to SA (or vice versa), and (b) a > 90% mono-exponential decay (a criterion set by ourself). Four labels were finally chosen, Py-1, Py-4, Py-6 and C546 for testing in lifetime assays. Label C546 has a high quantum yield (QY) in both the reactive (label) form and in the protein-conjugated form. The Py labels are different in being virtually nonfluorescent but being strongly fluorescent after conjugation to a protein. The decay times of the labels are sometimes smaller than 0.1 ns but increase to 2.5 ns if conjugated a protein (or after affinity binding). Py-1, Py-4 and Py-6 are exceptional (and therefore termed chameleon-) labels since they undergo a significant change in color following conjugation to a protein (e.g. color change from blue to red). This is due to the fact that labeling causes a major change in the electronic structure of the fluorophore as shown in chapter 3.1.2, figure 3.6. Finally, the fluorescence of Py-labeled proteins has an unusually large Stokes' shift, a fact that facilitates the separation of fluorescence from interfering residual light. Table 3.1. in chapter 3.1.1. summarizes the photophysical data of suitable labels.

Fluorescence lifetime affinity assays (FLAA) using labeled biotin and streptavidin

Biotin ethylenediamine was labeled either with Py-1, Py-4 or Py-6. The resulting conjugates were titrated with SA by adding varying quantities of SA into the wells of a black 96-well microplate to the stock solutions of the labeled biotin (Bt*). The total volume was 250 µL. The concentration of Bt* was $8 \cdot 10^{-7}$ mol L^{-1} in all experiments. The decay times of the three systems were determined after 30 min. Binding curves were established from the lifetime data and are shown in fig. 4.18. The shapes of the three plots in fig. 4.18. are largely different. Bt* labeled with Py-4 gives the largest increase in decay time ($\Delta\tau$ >0.6 ns), while Bt* labeled with Py-6 gives a steeper slope and the lowest limit of detection (which was determined graphically and is defined as $3\sigma/slope$, where σ is the S.D. for n = 3).
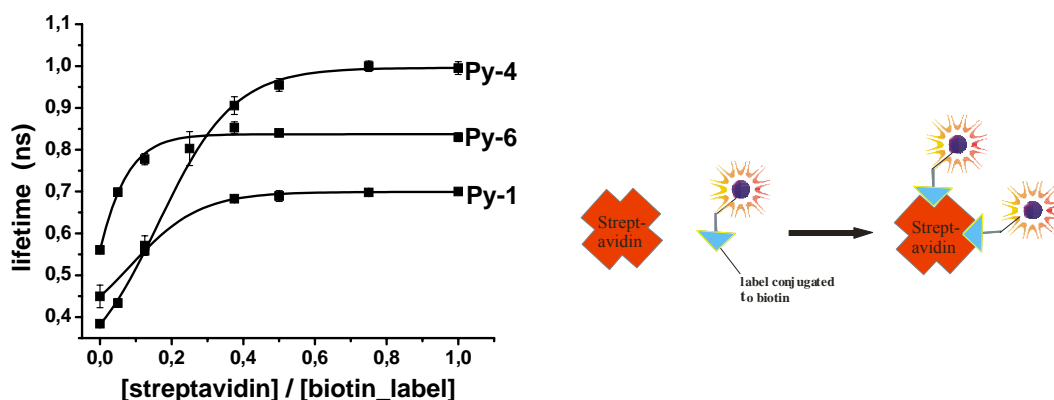
Fig. 4.18.   Fluorescence lifetime study on the binding of Bt* (labeled with Py-1, Py-4 and Py-6, respectively) to unlabeled streptavidin (SA).

The binding curves of the titration of Bt* labeled with Py-6 reaches saturation at a Bt*/SA ratio of 0.25, obviously because SA can bind four Bt. However, the respective plot for Bt* labeled with Py-4 and titrated with SA displays saturation only when (statistically) two Bt* are attached to one SA. Finally, the system Bt* labeled with Py-1 and titrated with SA reaches saturation at a Bt*/SA ratio of 0.4. This cannot be explained at present.

   In order to assess the quality of these results, the parameter Z' was determined for each system. The meaning and calculation of Z' is described in chapter 5.9. A Z' value of bigger than 0.5 is considered to be indication for a reliable assay [28, 29]. The results are given in table 4.3. They show that Z' for each binding curve in fig. 4.18. is larger than 0.8, thus indicating a robust assay. The $\Delta\tau$ in the binding curves of Bt*(Py-1) and Bt*(Py-6) is comparatively small (only 250 and 270 ps, respectively). However, due to the good resolution of the instrument used and due to averaging the error bars remain small (fig. 4.18.).

Table 4.3. Experimental data on changes in lifetime ($\Delta\tau$), the limits of detection (LODs), and Z' values for the FLAA using labeled biotin (Bt) that binds to unlabeled streptavidin (see fig. 4.17.).

label on Bt	$\Delta\tau$ (ns)	LOD / nmol L^{-1}	Z'
Py-1	0.25*	50	0.8
Py-4	0.61	17	0.92
Py-6	0.27*	10	0.95

* the resolution of the reader is 80 ps at 0.2 ns (see 5.1.4.)

It should be noted that the labels used in the lifetime experiments also undergo changes in intensity and the results go in parallel to those of the lifetime. However, these results are not as distinct, and the errors are larger. Moreover, fluorescence intensity is much more affected by inner filter effects and thus is a parameter that is clearly inferior to lifetime. It is also worth noting that in mixtures between free and bound species intensity-weighted lifetimes are measured. The labeled Bt* in solution gives a lower fluorescence intensity than the Bt* coupled to SA. Under these circumstances, there will be a nonlinear relationship between the fraction of the label in the bound form and in the uncomplexed form. This is valid for both ligand-receptor and protein-protein interactions. Similar situations arise in fluorescence polarization assays.

Py-6 seems to be the best label in this experiment with respect to the limit of detection (LOD) and Z', but the change in lifetime ($\Delta\tau$) is rather small (270 ps). As can be seen from table 4.3., the change in lifetime ($\Delta\tau$) is 0.61 ns in case of Py-4, which is distinctly more than with the other labels. This results in a better resolution (given the fact that the instrument can resolve 80 ps). It should be noted that in the FLAA the relative change in lifetime is an adequate information and that precise data on lifetimes do not need to be known [30]. Py-1 gives comparable poor LODs and therefore is considered to be inferior to Py-4.

FLAA for the system Bt-BSA and labeled SA
The affinity system studied before (see fig. 4.17.) reflects the situation of a label attached to a small organic molecule. In the second example a large molecule (BSA) was biotinylated and its binding to a large labeled receptor (SA*) was investigated. SA was labeled with Py-1, Py-4, and C546, respectively, and titrated with different quantities of Bt conjugated to BSA (Bt-BSA). The DPR of the conjugates with SA were determined to be 3.6 for Py-1, 5.3 for Py-4, and 2.5 for C546. A plot of decay times versus the ratio of SA* and Bt-BSA is shown in fig.

4.19. The concentration of SA* was kept constant at 33.3 nmol L^{-1}.
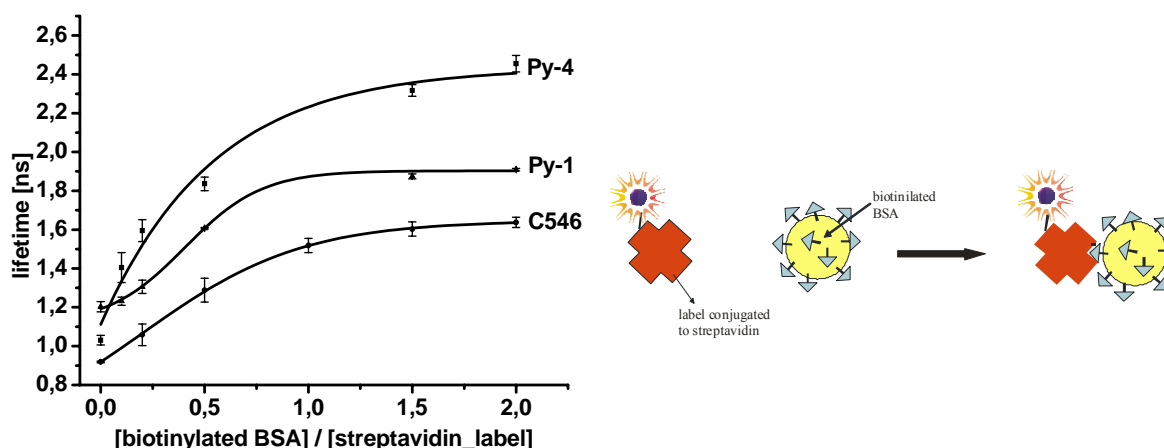
Fig. 4.19.   Fluorescence lifetime study on the binding of streptavidin (labeled with labels Py-
1, Py-4 and C546, respectively) to biotinylated BSA.

The resulting graphs reveal saturation at an equimolar ratio between Bt-BSA to SA*. However, SA is known to bind four biotins, and its binding capacity is not expected to be affected by labeling. It appears that the first binding step (first Bt-BSA to SA*) has the most distinct effect on the decay time of SA*, while binding of additional Bt-BSA has only a marginal effect. This result may be explained by assuming that the label is located next to the first binding site of SA* for Bt and that the label is affected most strongly already by the first binding event. Another explanation for this finding results from the fact that – according to the manufacturer's specification – twelve biotins are statistically attached to one BSA. Therefore, more than one streptavidin may be bound to one BSA. Sterically hindrance and the kinetic of the binding may also slower the second Bt-BSA to SA* binding. By assuming an equimolar ratio of SA* to BSA, a cluster composed of several SA* and Bt-BSA molecules may form. We did not observe precipitation, though.

Limits of detection (LOD) and Z' values (definition see chapter 5.9.) are summarized in table 4.4. SA*(Py-4) gives an unexpectedly large increase in decay time (from 1.0 ns to 2.4 ns), while SA*(Py-1) gives the best results with respect to LOD and Z', and an increase in τ of more than 0.7 ns, which is more than adequate for this application.

Table 4.4. Experimental data on changes in lifetime ($\Delta\tau$), the limits of detection (LODs), and
Z' values for the FLAA using labeled streptavidin (SA) that binds to biotinylated
bovine serum albumin.

label on BSA	$\Delta\tau$ ns	LOD / nmol L^{-1}	Z'
C546	0.72	5.6	0.97
Py-1	0.71	2.1	0.98
Py-4	1.43	3.0	0.88

As can be seen from tables 4.3. and 4.4., the LODs are in the range from 2.1 to 50 nM, which
is suitable for a variety of studies. In order to improve the LODs, which is needed for example
in competitive-inhibition assays, the concentration of the label may be reduced.

4.3.2. Homogeneous Hybridization Assay in Solution Based on Measurement of Fluorescence Intensity and on Fluorescence Decay Time in the Nanosecond Time Domain

The intention of this chapter was to examine the potential of lifetime-based homogeneous
hybridization assays using a single label only. It is well known that the hybridization of a
fluorescently labeled single strand oligonucleotide with a complementary sequence can
substantially modify the fluorescence properties of the fluorophore [31]. Py-1 was attached to
the end of an amino modified 15-mer oligonucleotide, which can be used as a probe for
detection of hybridization events in solution. The method was used to distinguish between
fully complementary and mismatch oligonucleotides. The synthesis of a molecular beacon
with a single label, in contrast to FRET MBs, is very simple. The measurement of
fluorescence decay times in the ns range gives fast results and referenced data. The
fluorescence decay profile has to remain monoexponential (a criterion set by ourself is a
> 90% mono-exponential decay).

Hybridization assay in solution

In a typical experiment, amino-modified ss-oligonucleotide oligo-1 was labeled with Py-1.
fig. 4.20. shows the results of the titration of labeled oligo-1 (oligo-1*), which is present in
constant concentration ($3.3 \cdot 10^{-8}$ mol/L), with its nonlabeled counterstrand oligo-3.
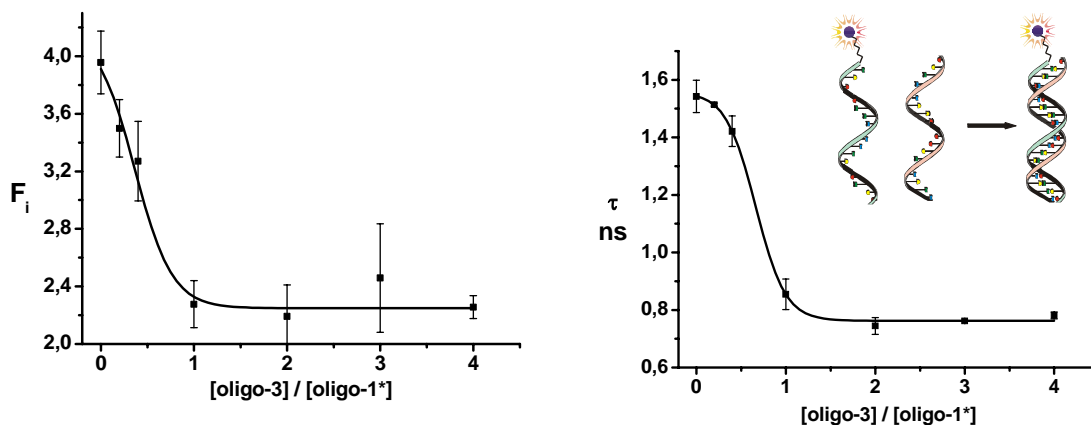
Fig. 4.20.   *Left*: Plot of the fluorescence intensities at 630 nm versus the ratio of the concentrations of oligo-3 and its counterstrand oligo-1 labeled with Py-1 (oligo-1*). *Right*: Plot of the fluorescence decay time of Py-1 labeled to oligo-1 versus the concentration of oligo-3 and oligo-1*. Plots are data from the same experiment (performed in triplicate).

Increasing fractions of the complementary oligonucleotide (oligo-3) cause the fluorescence intensity (left panel) and the fluorescence decay time (right panel) to decrease by 50%. Both plots display a distinct endpoint at a molar ratio of 1:1. The detection limit was graphically determined to be 12 nmol/L (which is equiv. to 1.9 pmol per well) for the fluorescence intensity plot, and 8 nmol/L (equiv. to 1.2 pmol per well or 36.4 ng/mL) for the lifetime plot. These LODs and the plots in figure 4.20. show that in this experiment the lifetime data and therefore the determination of the concentration of complementary oligonucleotide are more sensitive. In order to improve the LODs (which is needed for example in competitive-inhibition assays), the concentration of the label may be reduced. Moreover the error bars for the decay time based assay are much smaller than for the intensity based assay. Fluorescence intensity is much more strongly affected by several parameters, e.g. by inner filter effects, and thus is a parameter that is clearly inferior to lifetime.

Detection of Mismatches with a Homogeneous Hybridization Assay

The effect of two mismatches in the sequence of the complementary oligonucleotide was examined by titrating oligo-1* (in a constant concentration of $2.5 \cdot 10^{-7}$ mol/L) with oligo-3 (no mismatch), oligo-5 (two mismatches), oligo-6 (two mismatches with a matching base in between) and oligo-4 (negative control), respectively. The resulting plots are shown in fig.

4.21. Oligo-3 (which is exactly complementary to oligo-1*) causes the most distinct effect on fluorescence lifetime (a drop from 2.2 ns to 1.3 ns, $\Delta\tau$ = 0.9 ns). In oligo-5 two mismatches are placed at the end of the sequence and a smaller decrease in lifetime (from 2.2 ns to 1.86 ns, $\Delta\tau$ = 0.34 ns) is observed (fig. 4.21), not the least because the mismatch is close to the site of labeling.

If a matching base is introduced between the two mismatches (oligo-6), the fluorophore at the complementary oligonucleotide is even less strongly influenced by hybridization, and the effect on the decay time within the experimental error of +/- 60 ps (a decrease from 2.2 ns to 2.13 ns, $\Delta\tau$ = 0.07 ns). As expected, oligo-4 has virtually no effect on the fluorescence decay time of the label. Emission intensity plots of the same experiments resulted in very similar shaps (data not shown here), but display more scattered data and, therefore, larger error bars. This lifetime assays can not only be used for determination of a complementary oligonucloetide strands, but also for mismatch detection in homogeneous assay formats.
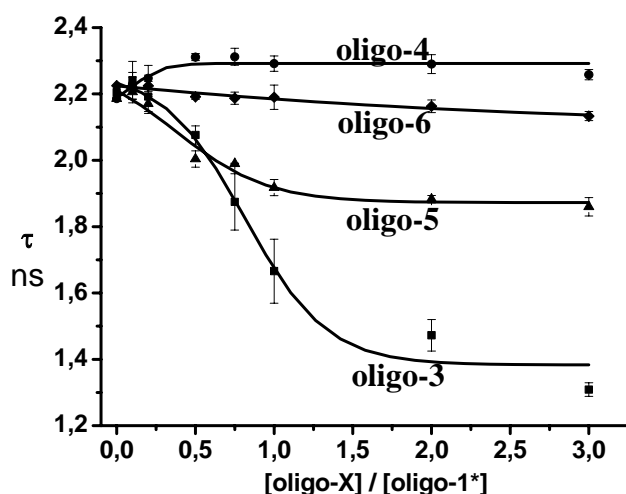
Fig. 4.21.   Plot of changes in the lifetime τ of labeled oligo-1* on titration with complementary and non-complementary oligonucleotides. Oligo-1* in constant concentration (2.5 10^{-7} mol/L) was mixed with oligo-3 (no mismatch), oligo-5 (double mismatch), oligo-6 (two mismatches with a matching base in between) and oligo-4 (non-complementary oligo).

Molecular Beacon with a Single Label for homogeneous hybridization assays

It is known that the fluorescence intensities of coumarins, rhodamines and oxazins are affected by DNA bases. In particular guanosine can act as a more or less strong quencher for certain dyes. Covalent linkage of such dyes to oligonucleotides containing guanosine results in a reduced fluorescence quantum yield and decay time dependent on the distance between the guanosine moiety and the fluorophore. This has been observed by several groups [32-34], and was used to study conformational fluctuations in DNA oligonucleotides at the single-molecule level by FRET and time-resolved fluorescence. The difference in behavior of neighboring dG compared to dA, dT, or dC bases can be attributed to the lower oxidation potential of dG [32].

In addition to previous experiments a molecular beacon (MB) has been designed, consisting of 25 bases and a C_6-amino residue at the 5' end. The sequence is shown in fig. 4.22. The MB possesses a stem-loop structure with (a) a loop consisting of 13 nucleotides that is complementary to the sequence in the target, and (b) a stem that is formed by annealing of two complementary arm sequences, one a 5-nucleotide and the other a 7-nuclotide arm, which are unrelated to the target sequence. The dye was conjugated to the MB via a method described in chapter 5.6.2. It should be noted that the label in the beacon is located in proximity to a run of deoxyguanosines presented in the complementary stem part.
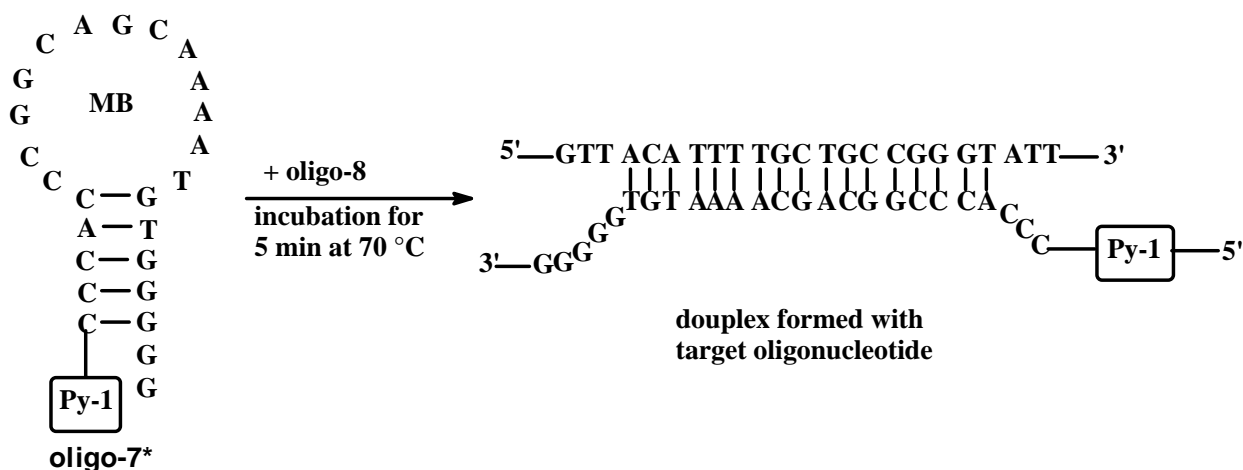
Fig. 4.22.   Sequence of the MB (oligo-7*) used in this study, and of the product of hybridization with a complementary target oligonucleotide (oligo-8).

As long as label Py-1 is in close contact with the 3' end of the MB, which is rich in G, its fluorescence intensity will be strongly quenched. When the hairpin probe encounters its target (oligo-8), it will form a longer and more stable hybrid (fig. 4.22.). The dye will be more distant now from the guanosine residues, thereby increasing the fluorescence intensity and

decreasing the decay time of Py-1. The fluorescence decay profile remains monoexponential, however. These findings have been used to establish the binding curve shown in fig. 4.23. As can be seen, the spontaneous formation of the (more stable) probe-target duplex can be used to detect the presence of the specific target sequence. The LOD was graphically determined to be $1.1 \cdot 10^{-7}$ mol/L of oligo-8. In order to lower the LODs, the concentration of the beacon may be further reduced.
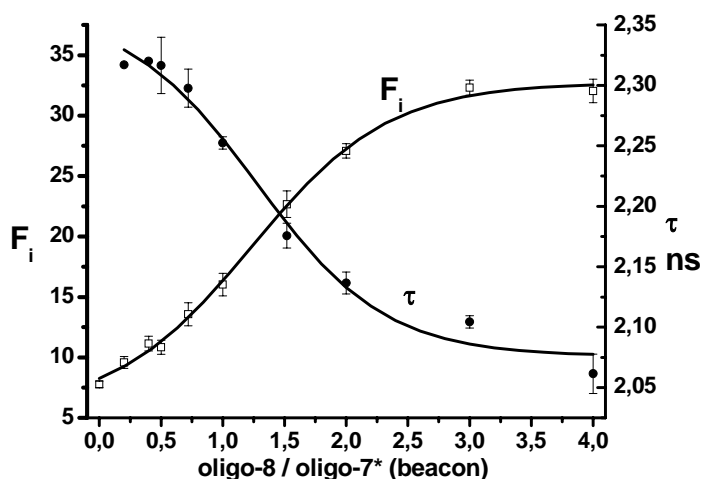
Fig 4.23.   Relative fluorescence intensity plot (F_i, open squares) and fluorescence decay time plot (τ, solid circles) for the titration of a $3.3 \cdot 10^{-7}$ molar pH 7.5 solution of a MB (oligo-7*) with increasing concentrations of complementary target (oligo-8).

Contrary to all expectations and to the results obtained with non beacon single strand probes, the fluorescence lifetime of the label attached to the molecular beacon decreases upon opening of the stem-loop structure by the complementary target. The emission intensity is 4-fold enhanced upon the hybridization experiment, while the fluorescence lifetime undergoes a rather small decrease (from 2.32 to 2.06 ns).

Lifetime measurements can be used for distinguishing static and dynamic quenching. Formation of static ground-state complexes does not decrease the decay time of the uncomplexed fluorophores because only the unquenched fluorophores are observed in a fluorescence experiment. Dynamic quenching is a rate process acting on the entire excited-state population and thus decreases the mean decay time of the excited-state population. Additional can be added, that in the closed hairpin the energy of the excited label can be transferred to the proximate guanosines, so fluorescence intensity of the label is decreased. In the closed hairpin structure of the MB the energy transfer from the fluorophore to guanosine,

and the dynamic and static quenching cause a lifetime of 2.3 ns, but very weak fluorescence intensity. By adding the complementary strand oligo-8, the energy transfer is reduced which means an increase in fluorescence intensity of the label, statistic quenching is reduced and dynamic quenching enhanced. Fluorescence decay time is decreasing. Three different effects cause the unusual results. Two parameters can be determined within one experiment and one measurement cycle.

4.3.3. Fluorescence Decay Measurements of Affinity Binding and Hybridization Assays on Solid Phase

The experiments described so far relate to solution assays. However, screening – like immunoassay - often is performed with colored or turbid solutions, and this may compromise the significance of the result due to either inner filter effects, to straylight, or due to the intrinsic fluorescence of the sample or support. In such situations, it is desirable to have the receptor bound on the surface of a microtiterplate (MTP), whose fluorescence can be more readily interrogated. This parallels the approach made in immuno sorbent assays.

FLAA using biotinylated BSA on solid-phase SA
We have made use of commercially available streptavidin (SA) coated MTPs, which were first labeled with Py-6 in different dye-to-protein ratios (DPRs) by adding different quantities of label solution to give "lifetime plates" (LPs), where the SA on the surface of the MTP was present in differently intensely labeled form; see the Exptl. Part (chapter 5.6.1.). Varying quantities of Bt-BSA were then placed in the wells, and after incubation of 30 min and without washing the decay time was determined as a function of the quantity of Bt-BSA added. The results are plotted in fig. 4.24.

The curve obtained for the highest DPR is less steep than the others. The increase in lifetime is comparably small but larger at low DPR. However, the quality of an assay is not only dependent on the $\Delta\tau$, but also on the signal-to-noise ratio of the analytical data (not evident from fig. 4.24.) which of course is better at high DPR. Consequently, a high DPR is more desirable but unfortunately large DPRs may cause self-quenching of the label, thereby reducing the signal. Obviously, each system has its own optimal DPR. In essence, the results show that the DPR has a critical effect on the quality of the assay, which parallels the situation found in immunoassay.
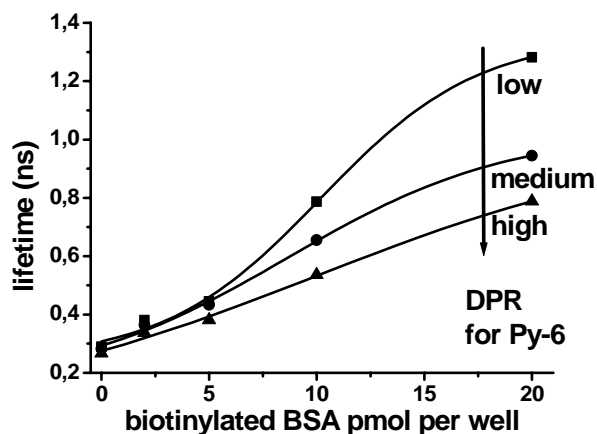
Fig. 4.24. Plots of fluorescence lifetime of streptavidin (SA) labeled with Py-6 and coated onto the surface of the wells of a micro titer plate on addition of biotinylated bovine serum albumin. SA was labeled at different dye-to-protein (DPR) ratios (high, middle, low; see chapter 5.6.1.) in order to study the effect of DPR.

The use of lifetime plates (LPs) results in several attractive features: (a) the receptor (the capture molecule) bound to the surface of the microtiterplate also acts as the detection molecule (if fluorescently labeled); (b) unspecific binding of the analyte to the uncovered surface of the MTP does not result in false positive signal (which is a major limitation in SPR and radioassay technologies); (c) the LPs may also be used in FRET-type of immunoassays and even extended to sandwich types of assays; (d) the LPs may be prepared well before use in coated and labeled form; (e) the binding assay then requires addition of the potential ligand only ("mix and measure"). Like SPR, the LP method may be considered as a biosensor (biochip) method. This together in our opinion makes the approach presented here quite attractive.

FLAA using biotinylated anti mouse IgG on solid-phase SA

The streptavidin coated microplate was covered with biotinylated goat-anti-mouse IgG, and after washing labeled with Py-1 (Bt-anti-IgG). Varying quantities of mouse IgG were then placed in the wells, and after incubation of 30 min and without washing the decay time was determined as a function of the quantity of mouse IgG added. The results are plotted in fig. 4.25.
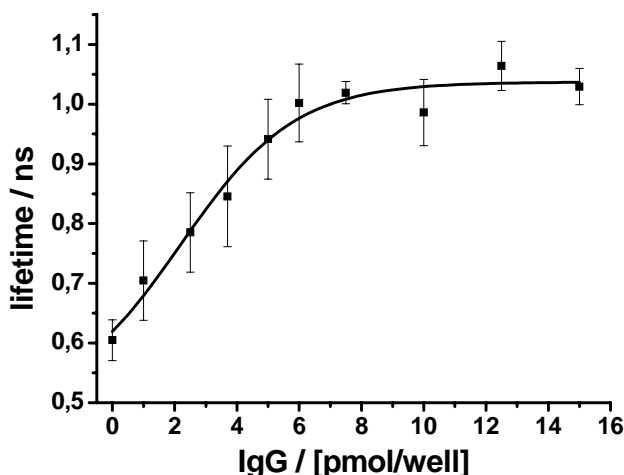
Fig. 4.25.   Plot of the fluorescence lifetime of Bt-anti-IgG labeled with Py-1 and coated onto the surface of the wells of a micro titer plate on addition of IgG (see chapter 5.6.1.).

The binding curve of anti IgG labeled with Py-1 reaches saturation at an IgG concentration of 6 pmol per well, which means a ratio of IgG/anti IgG of 1.2 (the theoretical binding capacity of the plates is 5 nmol biotin per well). The $\Delta\tau$ of the assay is very small (400 ps). The Z' value of this experiment was determined to be 0.78. The LOD was graphically determined to be $2\cdot10^{-12}$ mol/well or $1\cdot10^{-8}$ mol/L. The signal-to-noise ratio is small. Due to fact that several washing steps were needed during the experiments, the distinctive error bars in this binding curve can be explained.

Hybridization assay on solid phase

Oligo-2 is amino-modified on its 5'-end and biotinylated on the 3'-end. In a typical experiment, oligo-2 is labeled with Py-1 and attached via its biotin residue to the surface of a streptavidin coated microplate. Different amounts of the complementary oligonucleotide oligo-3 are added and the lifetime is measured after a washing step.
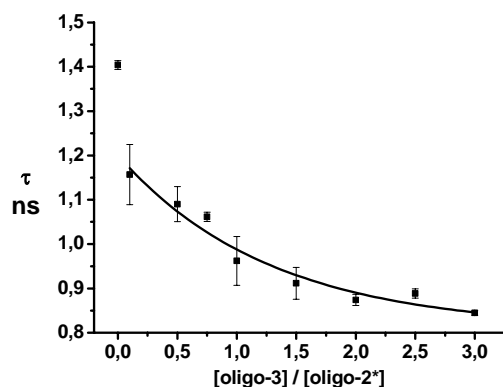
Fig. 4.26.   Plot of the lifetime (τ) vs. the ratio of complementary oligo-3 to oligo-2*, which is immobilized via biotin-streptavidin binding) to the surface of a microtiter plate.

According to the manufacturer's specification, each well contains enough streptavidin to bind 5 pmol of biotin (Bt). This number may however be smaller since not each binding site at the streptavidin molecule will be accessible to Bt because of steric hindrance on the surface of the micro plate. Figure 4.26. shows a plot of the fluorescence lifetime of oligo-2* versus the ratio of oligo-3 and oligo-2*. The first data point (x = 0) in figure 4.26. is the fluorescence lifetime of the single strand (ss) labeled oligo-2, bound to the surface. This first point is omitted from the fit for the further titration which can be described by an exponential decay curve. The change of lifetime due to hybridization events is from 1.40 to 0.84 ns ($\Delta\tau$ = 0.56 ns). The titration with oligo-1, a non-complementary strand, showed no characteristic change in lifetime (plot not shown). An amount of 0.5 pmol complementary oligonucleotide can be determined in this experiment, which in our experiment corresponds to 11.5 ng/mL.

One has to differentiate between two effects on lifetime. The first is caused by immobilization of the oligo* on the solid support, the second by hybridization. The decay times of labeled ss-oligonucleotides are different in solutions and when bound to a solid phase (compare with data and fig. 4.20). Py-1 labeled ss-oligo-1 has a lifetime of 1.54 ns free in solution. Py-1 labeled ss-oligo-2 has the same sequence, but is bound to the surface of a microplate via a Bt-SA interaction. Its lifetime is 1.40 ns. The decrease in decay time is therefore larger if hybridization is performed in solution.

4.3.4. Conclusion

The new detection scheme introduced here (and refered to as fluorescence lifetime affinity assay; FLAA) for use in affinity assays is based on the determination of fluorescence decay time (rather than fluorescence intensity, polarization, or the efficiency of energy transfer) in the nanosecond time domain. Fluorescence lifetime measurement in the ns domain is found to represent a fast and self-referenced detection scheme. The method requires labeling of one of the two binding partners only, and several labels (Py-1, Py-4, Py-6 and C546) were identified that undergo significant changes in their decay time following affinity binding. FLAA has the advantages of being (a) straightforward; (b) compatible with existing microplate technology and methods for decay time analysis; (c) applicable to both small and large binding partners (a fact that contrasts many polarization assays); (d) fast (in that hundreds of samples can be analyzed within minutes); and (d) requiring minute sample volumes only. These features meet many of the needs in present day high-throughput screening.

The label Py-1 is a viable probe for detecting specific recognition of complementary target DNA in homogenous assay formats via measurement of its fluorescence intensity and decay time. Unlike in certain other methods, single-labeling is adequate. Mismatches in the sequence of the complementary oligonucleotide can be detected, which means that within this method it can be distinguished between fully complementary and mismatch oligonucleotides. Molecular beacons are useful single oligonucleotides for reporting the presence of specific DNA strands. In contrast to double-labeled molecular beacons (FRET pair with donor and acceptor or donor and quencher label), the synthesis of the mono-labeled MB is easier, faster, and gives higher yields. Binding a MB to its counter-strand showed an affect on both, fluorescence intensity and fluorescence lifetime.

The examples studied here show that the FLAA is applicable to both solutions and solid phase assays (LPs). Solid phase assays are necessary in applications with turbid samples, when washing steps are necessary. The capture molecule bound to the surface of the microtiterplate can also act as the detection molecule (if fluorescently labeled) and the LPs may be prepared well before use and stored.

4.4. New Fluorophores for Cytometric Analysis

Cytometry refers to the measurement of physical and/or chemical characteristics of cells or other biological particles. Flow cytometry is a process, in which such measurements are made while the cells or particles pass through the instrument in a fluid stream. The modern flow cytometers consists of a light source (laser), collection optics, electronics and a computer to translate signals to data. Scattered and emitted fluorescent light is collected by two lenses (one set in front of the light source and one set at a right angle) and by a series of optics, beam splitters and filters, specific wavelength intervals of fluorescence can be measured. Forward (FSC) and side scatter (SSC) are used for preliminary identification of cells. FSC is detected along the axis of the incident light and related to the relative size of the cell. SSC is detected at a 90° angle and related to the cell granularity and complexity. Fluorescence labeling is used to investigate cell structure and function. The labels can be excited by two lasers (488 nm and 635 nm) and the fluorescence intensity can be detected by four photomultipliers with different detection wavelengths (PMT1: 515-545 nm, PMT2: 564-606 nm, PMT3: above 670 nm and PMT4: 653-669 nm).

Cytometric techniques as e. g. flow cytometry, microscopy, array technologies and others require fluorochromes with unique (bio-)physical properties: excitation and emission wavelength compatible with the lasers and filters of the instruments, high affinity (covalent or noncovalent) to the particles or cells, without washing out effects, high quantum yield bound to the cell or particle, to name a few. The development or derivatization of fluorophores with specific chemical and (bio-)physical properties is of particular interest for the optimization of research and diagnostic applications. Here, we introduce two fluorophores characterized by individual qualities - Py-4_acid and Py-4_C18.

The applicability in flow cytometry was tested on a FACS-Calibur instrument equipped with standard optics (fig. 4.27.). J82 stained cells (tumor cell line) were excited with 488 nm and a 630 nm laser line, respectively.
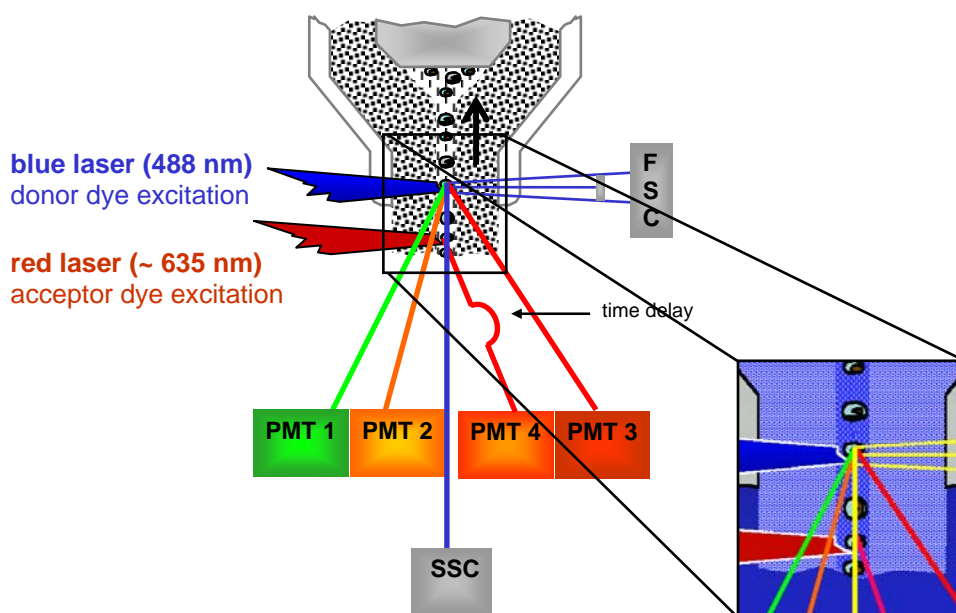
Fig. 4.27. Dual laser excitation in a flow cytometer – FACS-Calibur (Becton Dickinson Biosciences). PMT1 (515-545 nm), PMT2 (564-606 nm) and PMT3 (above 670 nm) are the detectors for the blue laser excitation, PMT4 (653-669 nm) for the red laser excitation.

Potential toxicity, i. e. number of dead cells induced by a 24 h period of dye incubation, was tested using a flow cytometric BCECF cell function assay [35, 36]. Adherent cells in a culture bottle with culture medium were incubated for 24 h with 10 µM of Py-4_C18, Py-4_acid and 100 nM staurosporine, respectively (staurosporine is used as an inducer of apoptosis in many cell types). The dyes and staurosporine were removed, the cells striped with trypsin, washed with PB and incubated with BCECF AM (2.3 µg/mL in PB) for 1 h. Protocol analog to [37]. Cytotoxicity assays using BCECF AM are based on the generation of fluorescence by intracellular esterase action and its retention correlated with membrane integrity as indicators of cell viability. The cells were centrifuged, washed with PB and measured in the FACS. Vital cells are detected by a strong fluorescence signal of BCECF in FL-1 (exc 488 nm).
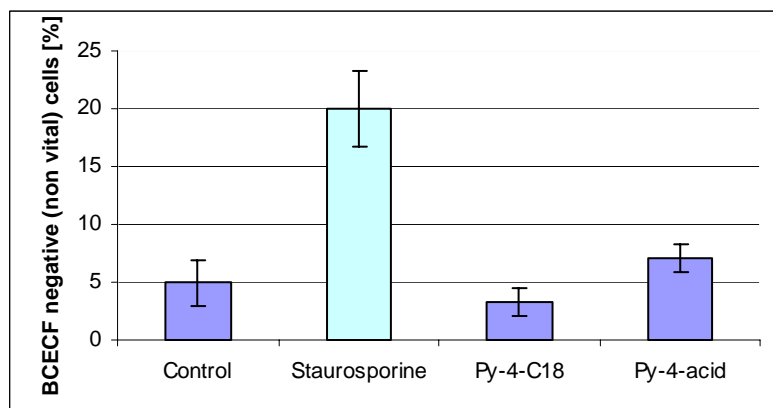
Fig. 4.28. Fraction of dead J82 tumor cells determined via the flow cytometric BCECF assay.

Staurosporine treatment results in 20% dead cells. In contrast 24 h incubation with the fluorophores does not induce cell death compared to the control.

Cellular staining localization was microscopically determined. J82 tumor cells were grown on slides in cell medium. After washing with PB, the slides were incubated 15 min with the dyes in cell medium (10 µM). After another washing step, the cells were covered and microscopically analyzed with a Zeiss Axiovert S100 inverted microscope. Images were generated with a CCD camera (Princeton Instruments). Cellular staining revealed that Py-4_acid can be exclusively found in the cell nucleus (fig 4.29., left picture). Py-4_C18 is found to a higher degree in the cytoplasm of the cells (fig 4.29., right picture). The toxicity tests and the cell staining experiments were done at the Institute of Pathology, University Hospital of Regensburg (Gero Brockhoff, gero.brockhoff@klinik.uni-regensburg.de).
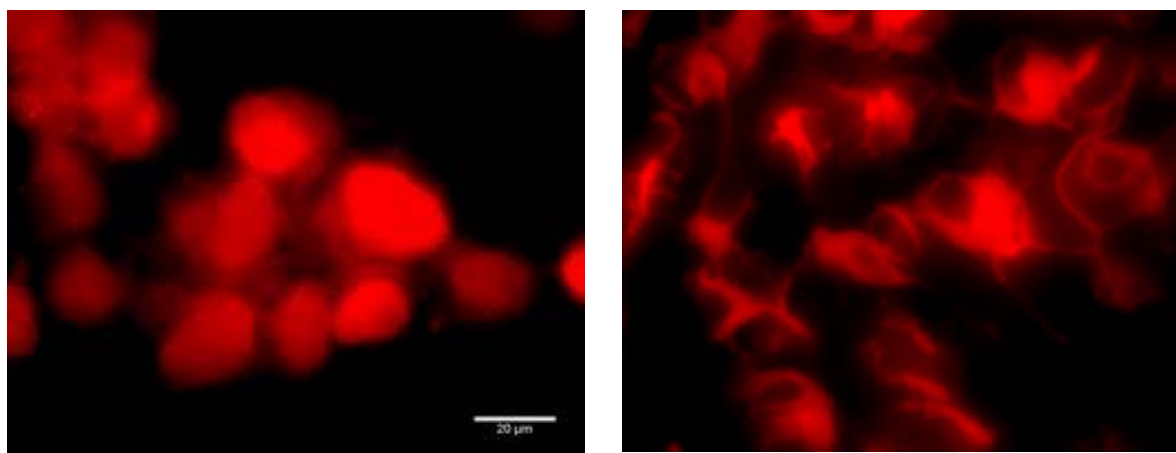
Fig. 4.29. Py-4_acid is exclusively located in the cell nucleus (left picture), while Py-4_C18 is found in the cytoplasm (right picture).

The microscope tests showed that Py-4_acid is located in the cell nucleus, thus the spectral behavior of the dye in the presence of dsDNA was examined. The dye was dissolved in doubly distilled water (1 µM), and titrated with fish sperm DNA. The fluorescence intensity was measured after 10 min incubation in cuvettes (fig. 4.30.). The experiment was performed in order to find out whether non-covalent conjugation or intercalation to a dsDNA affects the fluorescence of Py-4_acid.
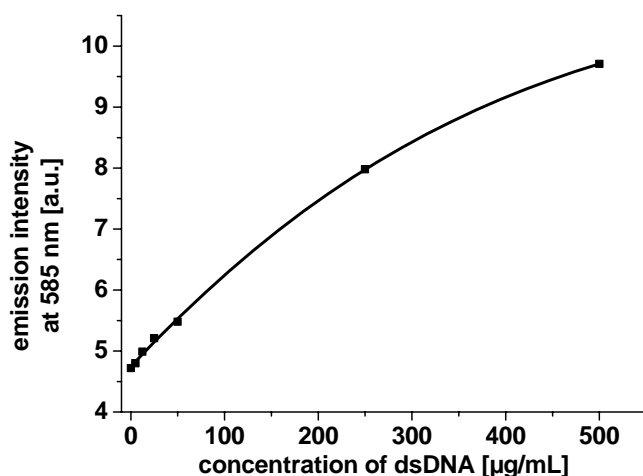
Fig. 4.30. Fluorescence intensity of Py-4_acid in the presence of increasing amounts of dsDNA (λ_{exc} 530 nm).

The fluorescence intensity increases with increasing quantities of DNA, which indicates that the fluorescent dye Py-4_acid interacts with the double helix. Addition of 500 µg/mL dsDNA causes a ~2-fold enhancement of the fluorescence intensity (fig. 4.30.). This effect is probably due to the fact that the dye interacts with the DNA. The dye can bind into the grooves of the double helix or intercalate between the bases of the DNA. The example of the widely used and commercially available intercalators TOTO and YOYO shows that positively charged fluorescent dyes intercalate into the double helix. These probes can detect very low quantities of DNA [38].

The influence of temperature on the formation of the dye-dsDNA complex was also investigated. When a solution containing Py-4_acid (c = 1 µmol/L) and dsDNA complex (c = 250 µg/mL) in doubly distilled water is heated to 80 °C the fluorescence intensity decreases. Py-4_acid (c = 1 µmol/L) in water was also heated to 80 °C to compare the effect of temperature on the free dye with the effect on dye-dsDNA complex. It is known that fluorescence intensity is affected by temperature [39].
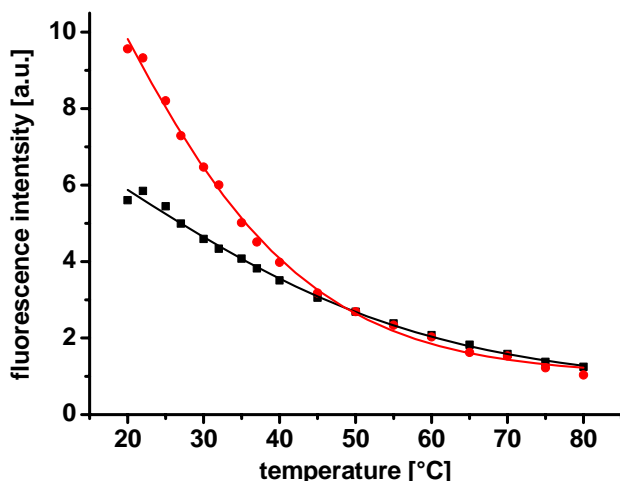
Fig. 4.31.   Temperature dependency of the fluorescence intensity of the free dye (Py-4_acid,
             black curve) and a dye-DNA-complex (red curve).

Py-4_acid incubated with dsDNA at 20 °C displays a 41% higher fluorescence intensity than the dye without DNA (first data points of the plots in fig. 4.31.). The fluorescence intensity of both samples decreases with increase of the temperature due to collisional quenching. At temperature higher than 50-60 °C both samples show the same fluorescence intensities. The hydrogen bonds between the nucleic bases weaken and the double strands of DNA begin to melt at this temperature. The dye, which is intercalated or groove bound to the DNA, no longer has the rigidity and the protecting environment from solvent by the double helix. This explains the same behavior of the two dye samples at temperatures higher than 50 °C, where quenching effects of the solvent and radiationless deactivation of the excited state of the molecules are the same in the dye solution with and without DNA.

Compared to widely used intercalators (for example TOTO and YOYO) the Py-4_acid is less suitable for detection of small quantities of dsDNA, because it is fluorescent in the unbound sate, and it coincides spectrally with the fluorescence of the dye-nucleic acid complex. This decreases the signal to background ratio and prevents to detect very small amounts of nucleic acids.

The new chromophores presented here are characterized by unique biophysical properties. They show specific excitation and emission maxima and are suitable for flow cytometric and/or microscopic cell analysis. Since the dyes are non-toxic they can be applied for cellular assays. Either the cell nucleus or the cytoplasm of the cells can be stained. Py-4_acid is exclusively introduced in the nucleus of a cell. Fluorescence microscopy of the

nucleus made it possible to study the 3 D arrangement of chromosomes, active and inactive genes, DNA replication and transcription processes.

4.5. References

[1]   T.H. Steinberg, L.J. Jones, R.P. Haugland, V.L. Singer, SYPRO Orange and SYPRO Red Protein Gel Stains: One-Step Fluorescent Staining of Denaturing Gels for Detection of Nanogram Levels of Protein, Anal. Biochem. **1996**, 239, 223-237.

[2]   M.F. Lopez, K. Berggren, E. Chernokalskaya, A. Lazarev, M. Robinson, W.F. Patton, A Comparison of Silver Stain and SYPRO Ruby Protein Gel Stain with Respect to Protein Detection in Two-dimensional Gels and Identification by Peptide Mass Profiling, Electrophoresis **2000**, 21, 3673-3683.

[3]   W.F. Patton, A Thousands Points of Light: The Application of Fluorescence Detection Technologies to Two-dimensional Gel Electrophoresis and Proteomics, Electrophoresis **2000**, 21, 1123-1144.

[4]   D.B. Craig, N.J. Dovichi, Multiple Labeling of Proteins, Anal. Chem. **1998**, 70, 2493-2494.

[5]   M. Holtzhauer, Biochemische Labormethoden, 2. Auflage, Springer Labor Manual, Heidelberg **1995**.

[6]   D.B. Craig, B.K. Wetzl, A. Duerkop and O.S. Wolfbeis, Determination of Picomolar Concentrations of Proteins Using Novel Amino Reactive Chameleon Labels and Capillary Electrophoresis Laser-Induced Fluorescence Detection, Electrophoresis **2005**, accepted.

[7]   H. Zollinger, Color Chemistry, Wiley-VCH Publ., Weinheim, Germany **2003**.

[8]   O.M. Kostenko, S.Y. Dmitrieva, O.I. Tolmachev, S.M. Yarmoluk, New Approach for Fluorescent Peptide Labeling with Pyrylium Cyanine Dyes, J. Fluoresc. **2002**, 12, 173-175.

[9]   S.M. Yarmoluk, A.M. Kostenko, I.Y. Dubey, Interaction of Cyanine Dyes with Nucleic Acids. Part 19: New Method for the Covalent Labeling of Oligonucleotides with Pyrylium Cyanine Dyes, Bioorg. Med. Chem. Letters **2000**, 10, 2201-2204.

[10]   C.M. Stoscheck, General Methods for Handling Proteins and Enzymes: Quantitation of Protein, in M.P. Deutscher (Ed.), Methods in Enzimology: Guide to Protein Purification, Academic Press, New York **1990**.

[11] M.K. Kessler, A. Meinitzer, W. Petek, O.S. Wolfbeis, Microalbuminuria and Borderline-Increased Albumin Excretion Determined with a Centrifugal Analyzer and the Albumin Blue 580 Fluorescence Assay, Clin. Chem. **1997**, 43, 996-1002.

[12] M. Senholdt, M. Siemann, K. Mosbach, L.I. Andersson, Determination of Cyclosporin A and Metabolites Total Concentration using a Molecularly Imprinted Polymer Based Radioligand Linding Assay, Analytical Letters **1997**, 30(10), 1809-1821.

[13] V. Boonkitticharoen, K. Laohathai, Variables Influencing Cell Binding Assays for Antibody Binding Kinetics, Nucl. Med. Comm. **1993**, 14(1), 70-75.

[14] K. Schilling, M.C. Aletsee-Ufrecht, An Immunoblot Assay for the Simultaneous Quantification of Several Antigens, Anal. Biochem. **1989**, 177, 203-206.

[15] K. Demuth, V. Ducros, S. Michelsohn, J.-L. Paul, Evaluation of Advia Centaur Automated Chemiluminescence Immunoassay for Determining Total Homocysteine in Plasma, Clinica Chimica Acta **2004**, 349(1-2), 113-120.

[16] S. Ambretti, M. Mirasoli, S. Venturoli, M. Zerbini, M. Baraldini, M. Musiani, A. Roda, High-Throughput Polymerase Chain Reaction Chemiluminescent Enzyme Immunoassay for Typing and Quantifying Human Papillomavirus DNAs, Anal. Biochem. **2004**, 332(2), 349-357.

[17] J. Wang, W. Huang, Y. Liu, J. Cheng, J. Yang, Capillary Electrophoresis Immunoassay Chemiluminescence Detection of Zeptomoles of Bone Morphogenic Protein-2 Rat Vascular Smooth Muscle Cells, Anal. Chem. **2004**, 76(18), 5393-5398.

[18] A. Zeytun, A. Jeromin, B.A. Scalettar, G.S. Waldo, A.R.M. Bradbury, Fluorobodies Combine GFP Fluorescence with the Binding Characteristics of Antibodies, Nature Biotech. **2003**, 21(12), 1473-1479.

[19] J. Henry, A. Anand, M. Chowdhury, G. Cote, R. Moreira, T. Good, Development of a Nanoparticle–Based Surface-Modified Fluorescence Assay for the Detection of Prion Proteins, Anal. Biochem. **2004**, 334(1), 1-8.

[20] S. D'Auria, N. DiCesare, M. Staiano, Z. Gryczynski, M. Rossi, J.R. Lakowicz, A Novel Fluorescence Competitive Assay for Glucose Determinations by using a Thermostable Glucokinase from the Thermophilic Microorganism Bacillus Stearothermophilus, Anal. Biochem. **2002**, 303(2), 138-144.

[21] A.-M. Steff, M. Fortin, C. Arguin, P. Hugo, Detection of a Decrease in Green Fluorescent Protein Fluorescence for the Monitoring of Cell Death: An Assay Amenable to High-Throughput Screening Technologies, Cytometry **2001**, 45(4), 237-243.

[22] S. Grant, F. Davis, J.A. Pritchard, K.A. Law, S.P.J. Higson, T.D. Gibson, Labeless and Reversible Immunosensor Assay based upon an Electrochemical Current-Transient Protocol, Anal. Chim. Acta **2003**, 495, 21-32.

[23] C.A. Wijayawardhana, H.B. Halsall, W.R. Heineman, Editor(s): A.J. Bard, M. Stratmann, in Encyclopedia of Electrochemistry, 145, 147-174, Wiley-VCH Verlag Weinheim, Germany **2002**.

[24] F.W. Scheller, C.G. Bauer, A. Makower, U. Wollenberger, A. Warsinke, F.F. Bier, Coupling of Immunoassays with Enzymatic Recycling Electrodes, Analytical Letters **2001**, 34(8), 1233-1245.

[25] P. Treloar, J. Kane, P. Vadgama, Editor(s): C.P. Price, D.J. Newman, Principles and Practice of Immunoassay (2nd Edition), 481, 483-509; Publisher: Macmillan Reference, London **1997**.

[26] S. Huang, M.D. Stump, R. Weiss, K.D. Caldwell, Binding of Biotinylated DNA to Streptavidin-Coated Polystyrene Latex: Effects of Chain Length and Particle Size, Anal. Biochem. **1996**, 237,115-122.

[27] E.P. Diamandis, T.K. Christopoulos, Europium Chelate Labels in Time-Resolved Immunoassays and DNA Hybridization Assays, Anal. Chem. **1990**, 62, 1149A-1157A.

[28] J.H. Zhang, T.D. Chung, K.R. Oldanburg, A Simple Statistical Parameter for use in Evaluation and Validation of High-Throughput Screening Assays, J. Biomol. Screen. **1999**, 4, 67-73.

[29] www.qiagen.com; Qiagen News, Issue No. 4, **2002**.

[30] U. Kosch, I. Klimant, O.S. Wolfbeis, Long-Lifetime Based pH Micro-Optodes without Oxygen Interference, Fresenius J. Anal. Chem. **1999**, 364, 48-53.

[31] S.P. Lee, D. Porter, J.G. Chirikjian, J.R. Knutson, M.K. Han, A Fluorometric Assay for DNA Cleavage Reactions Characterized with BamHJ Restriction Endonuclease, Anal. Biochem. **1994**, 220, 377-383.

[32] J.-P. Knemeyer, N. Marmé, M. Sauer, Probes for Detection of Specific DNA Sequences at the Single-Molecule Level, Anal. Chem. **2000**, 72, 3717-3724.

[33] A.O. Crockett, C.T. Wittwer, Fluorescein-Labeled Oligonucleotides for Real-Time PCR: Using the Inherent Quenching of Deoxyguanosine Nucleotides, Anal. Biochem. **2001**, 290, 89-97.

[34] S.A.E. Marras, F.R. Kramer, S. Tyagi, Efficiency of Fluorescence Resonance Energy Transfer and Contact-Mediate Quenching in Oligonucleotide Probes, Nucleic Acid Res. **2002**, 30 (21), e122.

[35] C. Dive, J.V. Watson, P. Workman, Multiparametric Analysis of all Membrane Permeability by Two Colour Flow Cytometry with Complementary Fluorescent Probes, Cytometry **1990**, 11(2), 244-252.

[36] J.R. Sellers, S. Cook, V.S. Goldmacher, A Cytotoxicity Assay Utilizing a Fluorescent Dye that Determines Accurate Surviving Fractions of Cells, J. Immunol. Methods **1994**, 172(2), 255-264.

[37] www.probes.com, product information B-1170

[38] H.S. Rye, J.M. Dabora, M.A. Quesada, R.A. Mathies, Fluorometric Assay using Dimeric Dyes for Double- and Single-Stranded DNA and RNA with Picogram Sensitivity, Anal. Biochem. **1993**, 208, 144-150.

[39] J.R. Lakowicz, Principles of Fluorescence Spectroscopy, 2nd Ed. Kluwer/Plenum, New York **1999**.

5. Experimental Part

5.1. Materials and Methods

5.1.1. Chemicals, Solvents, Proteins, and Oligonucleotides

All chemicals and solvents used were purchased from Aldrich (Steinheim, Germany), Fluka (Buchs, Switzerland), Merck (Darmstadt, Germany), Acros Organics (Geel, Belgium) or Sigma (Steinheim, Germany). All chemicals were of analytical grade and were used as received. Anhydrous DMF was prepared following standard procedures [1]. The polymer Hydromed D4 (formerly known as *Hydrogel D4*) was received from Cardiotech Inc. (Woburn, MA, USA; www.cardiotech-inc.com) on request.

Water was doubly destilled. *Phosphate buffer* (PB) of pH 7.2, 22 mM: 5.67 g of $Na_2HPO_4 \cdot 12\ H_2O$ and 0.96 g of $NaH_2PO_4 \cdot 2\ H_2O$ are dissolved in 1 L of doubly distilled water. *Bicarbonate buffer* (BCB) of pH 9.0, 50 mM: 2.1 g of $NaHCO_3$ are dissolved in 500 mL of doubly destilled water. *Triethylammonium acetate* (TEAA) of pH 7.1, 0.1 M: 13.8 mL of triethylamine and 5.76 mL of acetic acid are mixed and diluted to 1 L with water. *5x sample buffer* with SDS: 330 mM Tris, 5% SDS, 10% β-mercaptoethanol, 25% glycerin, 2.5 mM EDTA, and a few crystals of bromothymol blue are dissolved in 1 L of doubly distilled water and adjusted to a pH of 6.8. *1x sample buffer* without SDS: 66 mM Tris, 2% β-mercaptoethanol, 5% glycerin, 0.5 mM EDTA are dissolved in 1 L of doubly distilled water and adjusted to a pH of 6.8. *5x saline sodium citrate* (SSC) of pH 7.5 is prepared by dissolving 22 g (75 mmol/L) trisodium citrate dihydrate and 43.8 g (750 mmol) sodium chloride in 1 L of doubly distilled water. *1x SSC buffer* of pH 7.5 is prepared by dilution of 5x SSC buffer 1:5 (v/v) with doubly distilled water. The 10 mM *Tris/HCl buffer* of pH 7.5 (used in the beacon experiment) is prepared by dissolving 0.788 g of tris(hydroxymethyl)aminomethane·HCl, 1.86 g KCl and 0.119 g $MgCl_2$ in doubly distilled water. The buffers are adjusted to the corresponding pH value with 1 N HCl and 1 N NaOH, respectively. The pH measurements were performed with a Schott pH meter with temperature compensation.

The dyes ATTO 550, ATTO TR-X (from ATTO-TEC, www.atto-tec.com), the Bodipy dyes (from Invitrogen, www. probes.com), sulforhodamine G, sulforhodamine B, fluorescein, Chromeon546, Chromeon482, and Chromeon642 (here named as C546, C482 and C642, from Chromeon, www.chromeon.de) were used in FRET assays (chapter 4.2.), in

pre-staining experiments (chapter 4.1.1.) and in photostability tests (chapter 3.1.). The structures and spectral properties of C546 and C642 were published [2]. The structure and spectral data of C482 are shown in fig. 5.1.

λ_{max}^{abs} 482 nm

λ_{max}^{em} 506 nm

molar absorbance 15 000 L cm^{-1} mol^{-1}
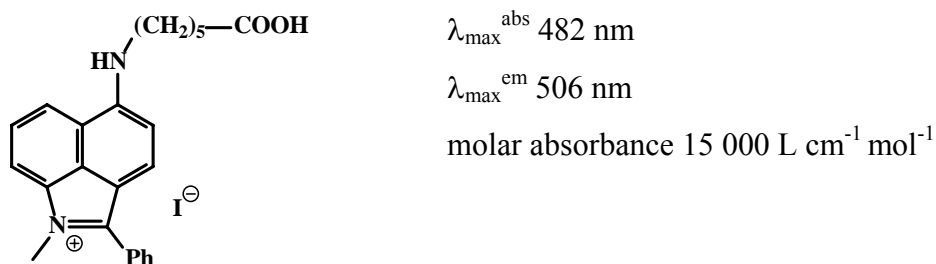
Fig. 5.1.   Structure and spectral data of C482.

Proteins were obtained as lyophilized crystalline powders from Sigma-Aldrich (www.sigma-aldrich.com) and from Merck (www.merckbiolab.com). The stock concentrations of the proteins were determined by spectrophotometry at 280 nm in PB of pH 7.2 using the following molar absorbances and molecular weights: bovine serum albumin (BSA), 66 kDa, 44 000 L cm^{-1} mol^{-1}; lysozyme, 14.4 kDa, 37 770 L cm^{-1} mol^{-1}; human serum albumin (HSA), 66 kDa, 35 000 L cm^{-1} mol^{-1}; anti human serum albumin (anti-HSA), 160 kDa, 200 000 L cm^{-1} mol^{-1}, pepsin, 36 kDa, 46 200 L cm^{-1} mol^{-1}; γ-globulin, 160 kDa, 213 900 L cm^{-1} mol^{-1}; apoferritin, 480 kDa (as calculated from data in the Sigma-Aldrich product information and after establishing a calibration plot for the protein in PB of pH 7.2 versus absorbance at 280 nm). The *low range protein standard* from Sigma (Dalton Mark VII-L, standard mixture, 14-66 kDa, for SDS PAGE, seven proteins) used for pre-staining contains bovine albumin (M$_r$ 66 kDa), ovalbumin (M$_r$ 45 kDa), glyceraldehyde-3-phosphate dehydrogenase (M$_r$ 36 kDa), carbonic anhydrase (M$_r$ 29 kDa), trypsinogen (M$_r$ 24 kDa), trypsin inhibitor (M$_r$ 20 kDa), α-lactalbumin (M$_r$ 14 kDa). 1 mg of this lyophilized powder was dissolved in 1.5 mL of 1x sample buffer without SDS. The *standard protein mix Protemix* contains: myosin (M$_r$ 220 kDa), 80 ng/band; β-galactosidase (M$_r$ 116 kDa), 50 ng/band; glycogen phosphorylase (M$_r$ 97 kDa), 150 ng/band; albumin (M$_r$ 66 kDa), 250 ng/band; glutamate dehydrogenase (M$_r$ 55.6 kDa), 80 ng/band; lactate dehydrogenase (M$_r$ 36.5 kDa), 80 ng/band; carbonic anhydrase (M$_r$ 29 kDa), 80 ng/band; trypsin inhibitor (M$_r$ 20 kDa), 250 ng/band; lysozyme (M$_r$ 14 kDa), 700 ng/band; aprotinin (M$_r$ 6.1 kDa), 180 ng/band.

The *bovine serum* used for quantification and recovery experiments was obtained from bovine blood (from a local source). It was allowed to stand at room temperature for 2 h and was then centrifuged at 2000 rpm for 20 min. *Bovine plasma* was obtained by adding 1 mL of ACD solution (0.47 g citric acid mono hydrate, 1.6 g sodium citrate, and 2.5 g D-glucose in

100 mL distilled water) to 4 mL of fresh blood, followed by centrifugation at 2000 rpm for 20 min. *Adult bovine serum* (ABS) was obtained from PAA Laboratories (www.paa.at) and had a specified total protein concentration of 68 g L^{-1} of total protein (59.1% albumin, 40.9% of $\alpha-$, β-, γ-globulin).

DNA oligonucleotide syntheses were carried out by Metabion (Martinsried, Germany). The sequences summarized in table 5.1.were used.

Table 5.1. List of the different used oligonucleotides, their sequences and modifications.

name	sequence and modification	complementary to
oligo-1	amino-C6-5'-CCG GCA GCA AAA TGT-3'	oligo-3
oligo-2	amino-C6-5'-CCG GCA GCA AAA TGT-3'-biotin	oligo-3
oligo-3	5'-ACA TTT TGC TGC CGG-3'-C6-amino	oligo-1 oligo-2
oligo-4	5'-CCG GCA GCA AAA TGT-3'	oligo-3
oligo-5	5'-ACA TTT TGC TGC C<u>AA</u>-3'	<u>mismatch</u> to oligo-1
oligo-6	5'-ACA TTT TGC TGC <u>T</u>G<u>C</u>-3'	<u>mismatch</u> to oligo-1
oligo-7	amino-C6-5'-CCC ACC CGG CAG CAA AAT GTG GGG G-3'	oligo-8
oligo-8	5'-GTT ACA TTT TGC TGC CGG GTA TT-3'	oligo-7

5.1.2. Chromatography

For analytical thin-layer chromatography RP-18 (TLC) F$_{254s}$ aluminum sheets and silica gel 60 F$_{254}$ aluminum sheets (thickness 0.2 mm each) from Merck (Darmstadt, Germany) were used. Column chromatography was carried out using silica gel 60 (40-63 μm) as the stationary phase for non-polar substances and silica gel 60 RP-18 (40-63 μm) or LiChroprep RP-18 (40-63 μm) as the stationary phase for polar substances (all from Merck). HPLC was performed on a Knauer HPLC 64 apparatus. A Hibar pre-packed column RT (250 x 4 mm) packed with LiChrosorb RP 18 (10 μm) was used as the stationary phase.

Labeled protein was separated from unlabeled dye by gel permeation chromatography using Sephadex G-25 from Sigma as the stationary phase (2 x 12 cm column) and a 22 mM PB of pH 7.2 as the eluent.

5.1.3. Melting Points

Melting points (m.p.) were measured with a melting point apparatus "Dr. Tottoli" from Büchi. They were determined in open capillary tubes and are not corrected.

5.1.4. Spectra and Imaging

^{1}H-NMR spectra were recorded with a 300 MHz PFT-NMR spectrometer (ARX 300 from Bruker) or a 400 MHz PFT-NMR spectrometer (ARX 400 from Bruker). The internal or external standard was tetramethylsilan (TMS) or the solvent (TMS external). The chemical shifts are given in ppm. The following abbreviations were used to describe the signals: s = singlet, d = doublet, dd = doublet of doublets, dt = doublet of triplets, t = triplet, q = quartet, quin = quintet, m = multiplet, br. = broad. Mass spectra were recorded with a Thermoquest TSQ 7000 (electro-spray ionization, ESI).

Absorption spectra in standard quartz cuvettes (1 x 1 x 3 cm) were acquired on a Cary 50 Bio UV-visible spectrophotometer from Varian (www.varian.com), fluorescence spectra on an Aminco Bowman AB2 luminescence spectrometer (www.thermo.com) equipped with a 150-W continuous wave xenon lamp as the excitation source. Absorption data in microplates were acquired on a Sunrise absorbance reader (from Tecan; www.tecan.com). Fluorescence emission intensities of solutions in microplates were measured on either a Fluoroskan Ascent (www.thermo.com), or on a Tecan Genios Plus microplate reader (Tecan) with ten flashes, respectively. Decay times of fluorescent labels in 96-well microplates were determined under standard conditions using a LF 401 NanoScan HT microplate reader (from IOM; www.iom-berlin.de). The device pulses the excitation beams at a repetition rate of 50 Hz. Excitation wavelengths were set to 485, 505 or 530 nm, resp., and emission wavelengths were set to 630($\pm$25) nm, respectively. The signals for single data points were averaged over 16, 32, or 64 laser pulses, depending on the signal-to-noise ratio. The resolution of the reader is $\pm$ 80 ps at a decay time of 0.5 ns, 50 ps at 1.5 ns, and 40 ps at 2.5 ns. A 96-well plate can be scanned within 110 s (when averaged over 16 pulses per well), and a 384-well plate within 300 s. The imaging of fluorescent protein bands on SDS gels were measured on a standard laser based scanner from Tecan (FL200, www.tecan.com, excitation at 542 nm (He-Ne laser); emission filter set to 630 nm).

The transparent 96-well microplates (polystyrene) with either round or flat bottom (flat bottom for photometry) were from Greiner Bio-One (www.greinerbioone.com), the black 96-well microplates form Nunc (type 96F; www.nunc.de), and black with streptavidin coated 96-well microplates were from Pierce (product no. 15119; www.perbio.com).

5.2. Synthesis and Purification of the Dyes

5.2.1. Syntheses of Dyes with a 2,6-Dimethyl-Pyrylium Group

5.2.1.1. Synthesis Procedure for Monomethine Dyes (Py-7 and Py-8)

The quaternized indole or quinole and 2,6-dimethyl-gamma-pyrone are dissolved in acetic anhydride and 0.2% (v/v) perchloric acid. The reaction mixture is refluxed for several hours, the solvent reduced in vacuum and the raw product purified via column chromatography and recrystallization.

i) Synthesis of Py-7
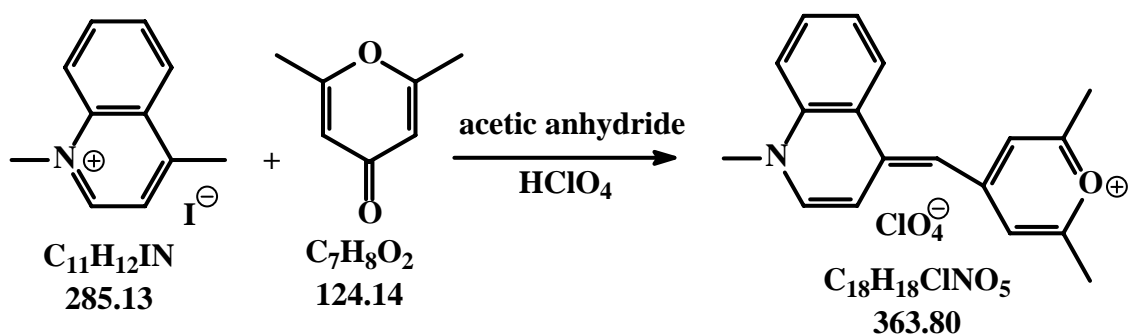
570.3 mg (2 mmol) of 1,4-dimethyl-quinolinium iodide [3, 4] and 248.3 mg (2 mmol) of 2,6-dimethyl-gamma-pyrone are dissolved in 10 mL of acetic anhydride and 20 µL of perchloric acid. The reaction mixture is heated to 140 °C for 12 h. The solvent is reduced to a few milliliters on a rotary evaporator. The dye solution is added to a saturated aqueous $NaClO_4$ solution. The product precipitates within several hours to several days and can be washed with water.

Yield: 70 mg (0.2 mol, 10%), brown powder, $C_{18}H_{18}ClNO_5$ (363.80 g/mol); m.p. >250 °C.
R_f (silica gel, chloroform:methanol 80:20 v/v): 0.53.
ESI-MS: m/e (M^+, cation) for $C_{18}H_{18}NO$, calculated 264.1, found 263.8 and 264.9.

ii) Synthesis of Py-8

C$_9$H$_{10}$INS
291.15

C$_7$H$_8$O$_2$
124.14

acetic anhydride

HClO$_4$

C$_{16}$H$_{16}$ClNO$_5$S
369.82
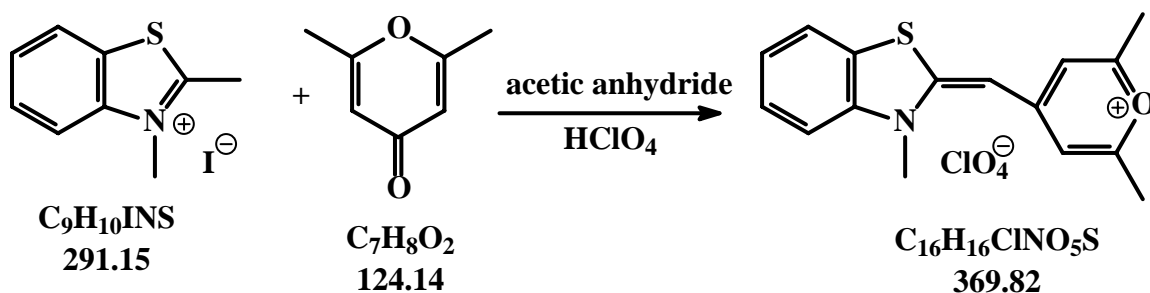
300 mg (1.03 mmol) of 2,3-dimethyl-benzothiazol-3-ium iodide [3, 4] and 136.6 mg (1.1 mmol) of 2,6-dimethyl-gamma-pyrone are dissolved in 10 mL of acetic anhydride and 20 µL of perchloric acid. The reaction mixture is refluxed for 6 h. The solvent is reduced in vacuum. The raw product is purified via column chromatography using silica gel 60 as the stationary phase and a chloroform/methanol mixture (gradient from 100:0 to 90:10 v/v) as the eluent.

Yield: 37 mg (0.1 mmol, 10%) brown powder, C$_{16}$H$_{16}$ClNO$_5$S (369.82 g/mol); m.p. 190 °C.

R$_f$ (silica gel, chloroform:methanol 80:20 v/v): 0.63.

^{1}H-NMR (d4-methanol, TMS external): 8.4-7.8 (m, 5H), 7.1 (s, 2H), 4.18 (s, 3H), 2.33 (s, 6H).

ESI-MS: m/e (M$^+$, cation) for C$_{16}$H$_{16}$NOS, calculated 270.1, found 269.8.

5.2.1.2. Synthesis of Py-1

i) Preparation of 2,3,6,7-Tetrahydro-1H,5H-pyrido[3,2,1-ij]quinoline-9-carbaldehyde

C$_{12}$H$_{15}$N
173.26

DMF
POCl$_3$

C$_{13}$H$_{15}$NO
201.27
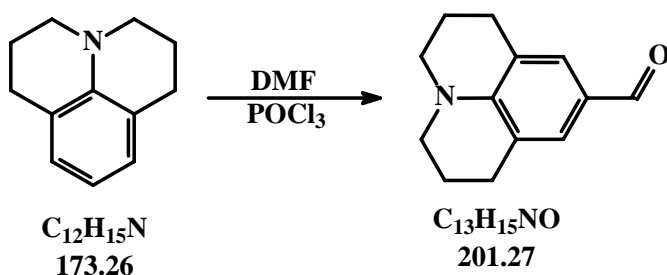
1.13 mL (12.1 mmol) of POCl$_3$ are added to 6 mL of dry and cold dimethylformamide. A solution of 2.1 g (12.1 mmol) of 2,3,6,7-Tetrahydro-1H,5H-pyrido[3,2,1-ij]quinoline (trivial name julolidin, from Aldrich) in DMF is added to the oxide chloride solution and the reaction mixture is heated to 100 °C for 2 h. The solution is cooled down to room temperature and poured into 60 mL of ice water. A pH value of 6-8 is adjusted with a saturated sodium acetate solution. The aldehyde crystallizes, is sucked off and washed with water. The residue is

recrystallized from acetone and triturated with hexane. The julolidin-9-carbaldehyde is dried in a desiccator and used without further purification [5].

Yield: 1.7 g (8.4 mmol, 69%) brown powder $C_{13}H_{15}NO$ (201.27 g/mol).

ii) Preparation of Py-1

$C_{13}H_{15}NO$
201.27

$C_8H_{11}BF_4O$
209.98

$C_{21}H_{24}BF_4NO$
393.23
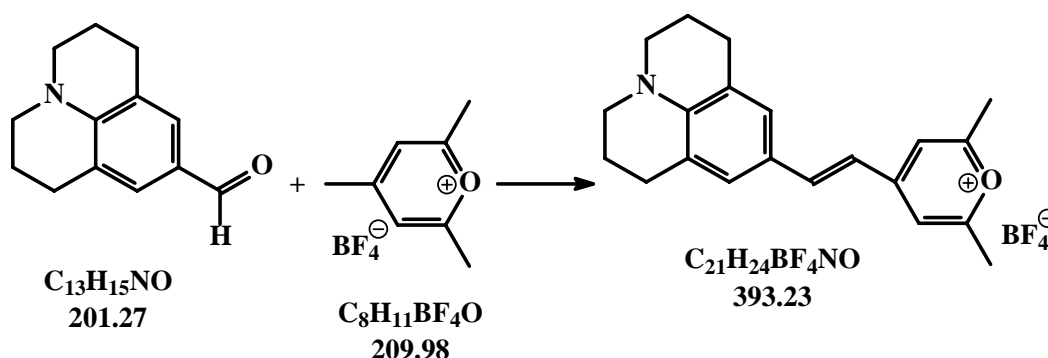
200 mg (0.99 mmol) of julolidin-9-carbaldehyde (2,3,6,7-tetrahydro-1*H*,5*H*-pyrido[3,2,1-ij]quinoline-9-carbaldehyde) and 300 mg (1.43 mmol) of 2,4,6-trimethylpyrylium tetrafluoroborate are dissolved in 5 mL methanol. The reaction mixture turns immediately deep blue. The reaction mixture is refluxed for 10 minutes and the solvent is removed. The raw product is purified via column chromatography using silica gel 60 as the stationary phase and a chloroform/methanol mixture (80:20 v/v) as the eluent.

Yield: 270 mg (0.69 mmol, 65%) of blue crystals, $C_{21}H_{24}BF_4NO$ (393.23 g/mol); m.p. 205 °C.

R_f (silica gel, chloroform:methanol 80:20 v/v): 0.60.

^{1}H-NMR (d$_4$-methanol/d$_1$-chloroform 1:1 v/v, TMS): δ 7.95 (d, 1H), 7.33 (broad peak, 2H), 6.73 (d, 1H), 3.5 (t, 4H), 2.77 (t, 4H), 2.51 (s, 6H), 2.0 (4H, m), two pyrylium protons give no peak in this spectrum; they exchange with the solvent.

ESI-MS: m/e (M$^+$, cation) for $C_{21}H_{24}NO$, calculated 306.19, found 306.0 and 307.0.

5.2.1.3. Synthesis of Py-2

i) Preparation of (1,3,3-trimethyl-1,3-dihydro-indol-2-ylidene)-acetaldehyde

C$_{12}$H$_{15}$N
173.26

C$_{13}$H$_{15}$NO
201.27
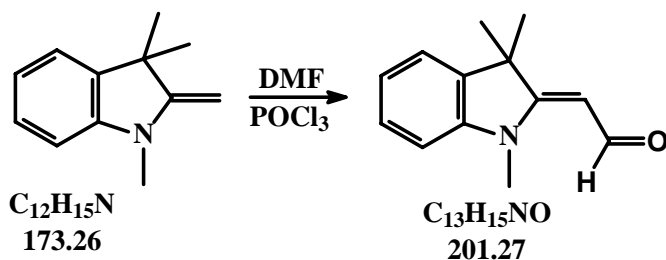
1.38 g (0.824 mL, 9 mmol) of POCl$_3$ are added to 3 mL of dry and cold DMF. A solution of 1.5 g (8.7 mmol) of 1,3,3-trimethyl-2-methylene-2,3-dihydro-1H-indole (from Aldrich) in 3.5 mL DMF is heated to 70 °C and the oxide chloride solution is added. The reaction mixture is refluxed for 1 h. The solution is cooled down to room temperature and poured into a cold solution of 1.26 g of NaClO$_4$ dissolved in 25 mL of methanol. The product crystallizes from the solution within 12 h at 4 °C, is sucked off and dried in a desiccator. The raw product is refluxed in a mixture of 30 mL of chloroform and 10 mL of 20% sodium hydroxide in aqueous solution for 17 h. The organic phase is washed three times with distilled water, dried with sodium sulfate and the solvent is removed on a rotary evaporator. The remaining red oil is triturated with diethylether and used without further purification [5].

Yield: 1.3 g (5.5 mmol, 74%) red oil C$_{13}$H$_{15}$NO (201.27 g/mol).

ii) Preparation of Py-2

C$_{13}$H$_{15}$NO
201.27

C$_8$H$_{11}$BF$_4$O
209.98

C$_{21}$H$_{24}$BF$_4$NO
393.23
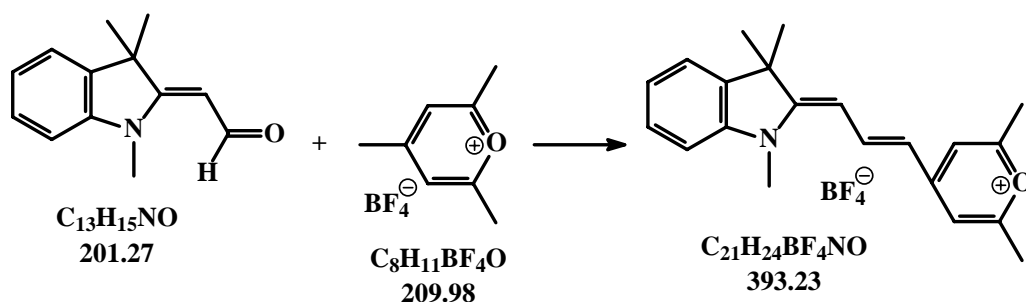
900 mg (4.47 mmol) of (1,3,3-trimethyl-1,3-dihydro-indol-2-ylidene)-acetaldehyde and 965 mg (4.6 mmol) of 2,4,6-trimethylpyrylium tetrafluoroborate are dissolved in 10 mL of acetic acid anhydride and 3 mL of pyridine. The reaction mixture is refluxed for 10 min, the solvent removed under reduced pressure and the dye recrystallized out of ethanol.

Yield: 865 mg (2.2 mmol, 50%) violet powder $C_{21}H_{24}BF_4NO$ (393.23 g/mol); m.p. 137 °C.

R_f (silica gel, chloroform:methanol 80:20 v/v): 0.56.

^{1}H-NMR (d$_1$-chloroform, TMS external): δ 8.36 (t, 1H), 7.68 (m, 1H), 7.52 (m, 1H), 7.36 (m, 2H), 7.17 (s, 1H), 6.47 (s, 1H), 6.31 (d, 1H), 6.17 (d, 1H), 3.73 (s, 3H), 2.08 (s, 6H), 1.7 (s, 6H).

5.2.1.4. Synthesis of Py-3

$C_9H_{11}NO$
149.19

$C_8H_{11}BF_4O$
209.98

$C_{17}H_{20}BF_4NO$
341.16

350 mg (2.35 mmol) of 4-dimethylamino-benzaldehyde (from Fluka) and 500 mg (2.38 mg) of 2,4,6-trimethylpyrylium tetrafluoroborate are dissolved in 50 mL of methanol and heated to 60 °C for 2 h. The dye was recrystallized from ethanol and triturated with diethylether.

Yield: 320 mg (0.9 mmol, 40%), blue crystals, $C_{17}H_{20}BF_4NO$ (341.16 g/mol); m.p. 172 °C.

R_f (silica gel, chloroform:methanol 80:20 v/v): 0.73.

ESI-MS: m/e (M$^+$, cation) for $C_{17}H_{20}NO$, calculated 254.15, found 253.9.

5.2.1.5. Synthesis of Py-4

i) Preparation of (3-Methyl-3H-benzothiazol-2-ylidene)-acetaldehyde

$C_9H_{10}INS$
291.15

$C_{10}H_9NOS$
191.25
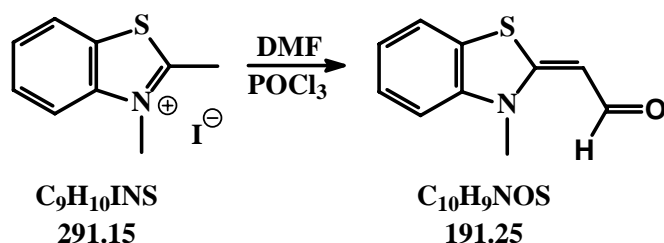
522.7 mg (3.4 mmol) of POCl$_3$ are added to 1 mL of dry and cold dimethylformamide. A solution of 1 g (3.43 mmol) of 2,3-dimethyl-benzothiazol-3-ium iodide [3, 4] in 3.5 mL DMF is heated to 70 °C and the oxide chloride solution is added. The reaction mixture is refluxed for 1 h. The solution is cooled down to room temperature and poured into a solution of 570 mg of NaClO$_4$ dissolved in 15 mL cold methanol. After a crystallizing for at least 2 h at 4 °C

the product is sucked of and dried in a desiccator. 970 mg of the raw product are refluxed in a mixture of 10 mL chloroform and 5 mL 20% sodium hydroxide in aqueous solution for 17 h. The organic phase is washed three times with distilled water, dried with sodium sulfate and the solvent removed on a rotary evaporator. The remaining red oil is triturated with petrol ether to get a brick red powder [5].

Yield: 325 mg (1.7 mmol, 50%) red powder $C_{10}H_9NOS$ (191.25 g/mol).

ii) Preparation of Py-4

$C_{10}H_9NOS$
191.25

$C_8H_{11}BF_4O$
209.98

$C_{18}H_{18}BF_4NOS$
383.21
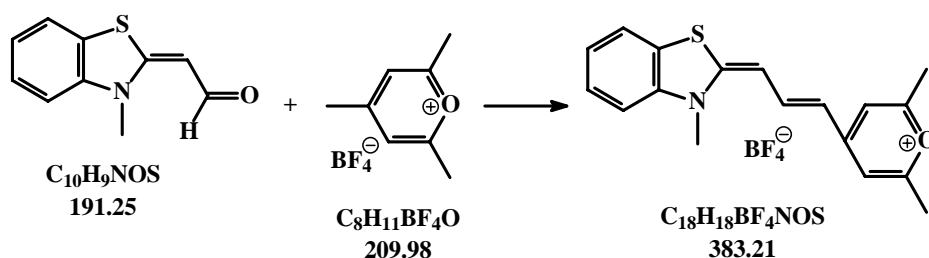
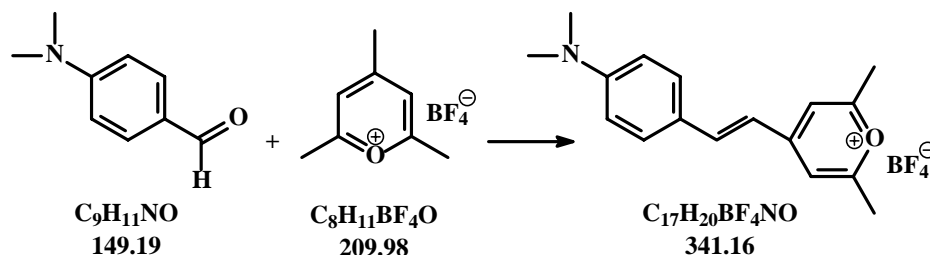50 mg (0.26 mmol) of (3-methyl-3*H*-benzothiazol-2-ylidene)-acetaldehyde and 52 mg (0.26 mmol) of 2,4,6-trimethylpyrylium tetrafluoroborate are dissolved in 5 mL of acetic acid anhydride and 3 mL of pyridine. The reaction mixture is refluxed for 10 min, cooled to room temperature and the solvents are removed under reduced pressure. The dye is recrystallized from ethanol.

Yield: 69.7 mg (0.18 mmol, 70%) violet crystals $C_{18}H_{18}BF_4NOS$ (383.21 g/mol); m.p. 169 °C.

R_f (silica gel, chloroform:methanol 80:20 v/v): 0.44.

^{1}H-NMR (d$_3$-acetonitrile, TMS external): δ 8.08 (t, 1H), 7.95 (d, 1H), 7.52-7.73 (d, m, t, 3·1H), 6.97 (s, 1H), 6.6 (d, 1H), 6.3 (s, 1H), 5.94 (d, 1H), 4.41 (s, 3H), 2.27 (s, 3H), 2.22 (s, 3H).

5.2.1.6. Synthesis of Py-5

C$_{11}$H$_{13}$NO
175.23

C$_8$H$_{11}$BF$_4$O
209.98

C$_{19}$H$_{22}$BF$_4$NO
367.19
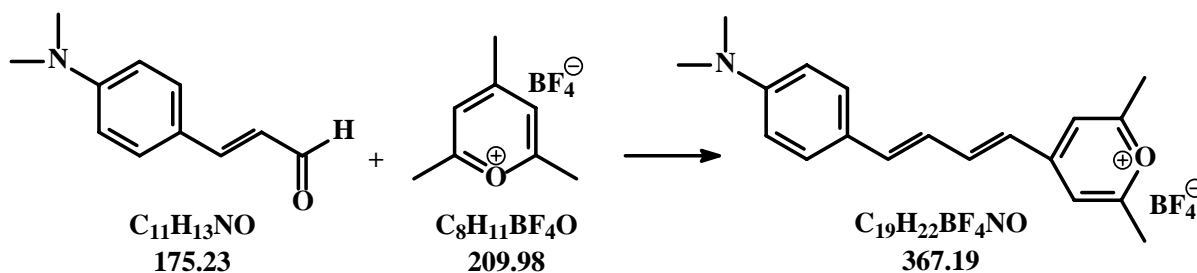
400 mg (2.28 mmol) of 3-(4-dimethylamino-phenyl)-propenal (from Merck) and 630 mg (3 mmol) of 2,4,6-trimethylpyrylium tetrafluoroborate are dissolved in 5 mL of methanol and refluxed for 10 min. The solvent is removed and the raw dye purified via column chromatography using silica gel 60 as the stationary phase and a chloroform/methanol mixture (gradient from 100:0 to 90:10 v/v) as the eluent.

Yield: 335 mg (0.9 mmol, 40%), blue crystals, C$_{19}$H$_{22}$BF$_4$NO (367.19 g/mol).

R$_f$ (silica gel, chloroform:methanol 80:20 v/v): 0.49.

^{1}H-NMR (d$_4$-methanol, TMS external): δ 8.18 (dd, 1H), 7.6 (d, 2H), 7.52 (s, 2H), 7.44 (d, 1H), 7.16 (dd, 1H), 6.8 (d, 2H), 6.5 (d, 1H), 3.12 (s, 6H), 2.64 (s, 6H).

5.2.1.7. Synthesis of Py-6

i) Preparation of 1,1,2,3-tetramethyl-1H-benzo[e]indolium iodide

C$_{15}$H$_{15}$N
209.29

CH$_3$I
141.94

C$_{16}$H$_{18}$IN
351.23
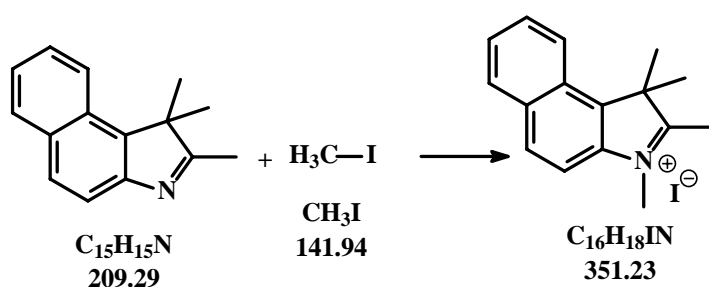
2 g (9.5 mmol) of 1,1,2-trimethyl-1*H*-benzo[e]indole (from Acros) and 4 g (1.8 mL, 20mmol) of methyl iodide are dissolved in 10 mL of toluene. The reaction mixture is heated to 100 °C in a sealed tube under argon atmosphere for 5 h. The reaction mixture is dissolved in water/ether (50/50, v/v). The water fraction is collected and the water is removed. The grey residue is washed with ether and the product is dried in a desiccator [3, 4].

Yield: 950 mg (2.7 mmol, 30%).

ii) Preparation of [1,1,3-trimethyl-1,3-dihydro-benzo[e]indol-(2Z)-ylidene]-acetaldehyde

$C_{16}H_{18}IN$
351.23

DMF
$POCl_3$

$C_{17}H_{17}NO$
251.33
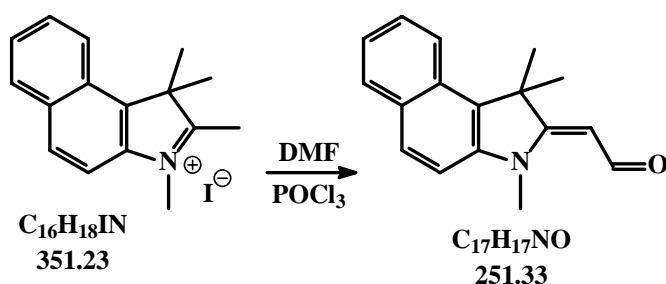
1 g (2.8 mmol) of 1,1,2,3-tetramethyl-1*H*-benzo[e]indolium iodide is dissolved in 3.5 mL of DMF and heated to 70 °C. 460 mg (0.27 mL, 3 mM) of $POCl_3$ dissolved in 0.5 mL of cold DMF are added dropwise to this solution. The reaction mixture is refluxed for 1 h, cooled to room temperature and poured into an ice cold solution of 0.42 g of sodium perchlorate in 10 mL of methanol. The raw product crystallizes out of this solution within 24 h at 4 °C. The dried crystals are dissolved in a mixture of 5 mL of sodium hydroxide solution in water (20%) and 10 mL of chloroform and are refluxed for 17 h. The organic phase is washed three times with water, dried with sodium sulfate and the chloroform is removed on a rotary evaporator. The residue is triturated with diethylether, the product sucked off and dried in a desiccator. The product is used without further purification [5].

Yield: 141 mg (0.56 mmol, 20%) black needles.

iii) Preparation of Py-6

$C_{17}H_{17}NO$
251.33

$C_8H_{11}BF_4O$
209.98

$C_{25}H_{26}BF_4NO$
443.29
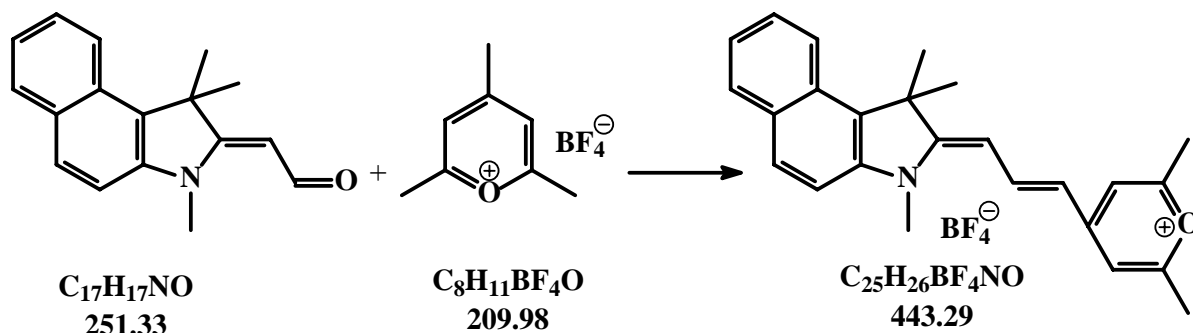
67 mg (0.27 mmol) of [1,1,3-trimethyl-1,3-dihydro-benzo[e]indol-(2Z)-ylidene]-acetaldehyde and 67.2 mg (0.32 mmol) of 2,4,6-trimethylpyrylium tetrafluoroborate are dissolved in 2 mL of acetic anhydride and 0.5 mL of pyridine and refluxed 10 min at 100 °C. The product precipitates upon adding 5 mL diethylether, is sucked off and purified via column chromatography using silica gel 60 as the stationary phase and a chloroform/methanol mixture (gradient from 100/0 to 90/10, v/v) as the eluent. The blue-violet fraction is collected. The dye can be recrystallized from ethanol.

Yield: 96 mg (0.2 mmol, 80%), black shining powder, $C_{25}H_{26}BF_4NO$ (443.29 g/mol); m.p. 105-110 °C.

R_f (silica gel, chloroform:methanol 80:20 v/v): 0.47.

^{1}H-NMR (d_4-methanol, TMS external): δ 8.48 (dd, 1H), 8.26 (d, 1H), 8.04 (m, 2H), 7.7 (m, 2H), 7.53 (m, 1H), 7.27 (s, 1H), 6.55 (s, 1H), 6.46 (d, 1H), 6.15 (d, 1H), 3.82 (s, 3H), 1.99 (s, 6H), 1.27 (s, 6H).

5.2.1.8. Synthesis of Py-20

i)   Preparation   of   3-butoxy-4-[1,3,3-trimethyl-1,3-dihydro-indol-(2Z)-ylidenemethyl]-cyclobut-3-ene-1,2-dione
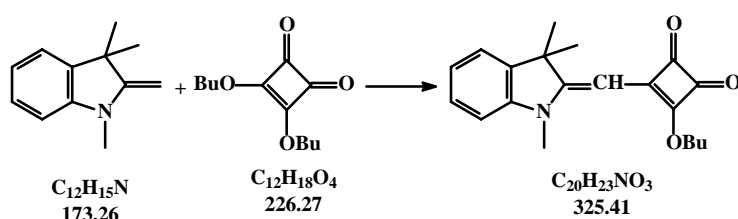
200 µL (316 mg, 1.82 mmol) of 1,3,3-trimethyl-2-methylene-2,3-dihydro-1H-indole (from Aldrich) and 420 µL (441 mg, 1.95 mmol) of 3,4-dibutoxy-cyclobut-3-ene-1,2-dione (from Acros) are dissolved in 20 mL of ethanol and 1 mL of triethylamine. The reaction mixture is refluxed for 4 h. The solvent is removed and the raw product triturated with diethyl ether. The intermediate is sucked off and completely used for the next reaction step [6, 7].

ii) Preparation of Py-20
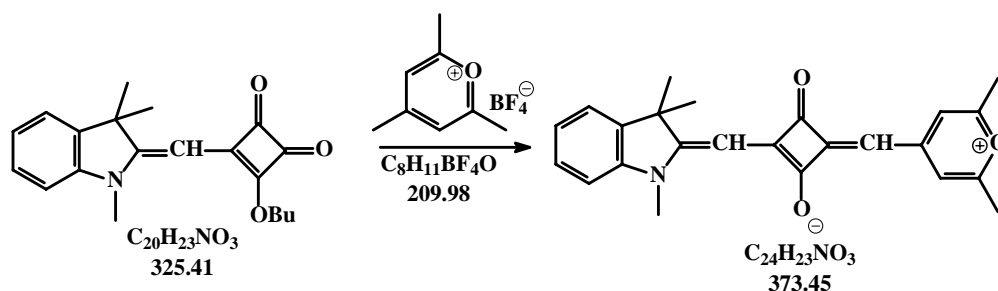
The raw 3-butoxy-4-[1,3,3-trimethyl-1,3-dihydro-indol-(2Z)-ylidenemethyl]-cyclobut-3-ene-1,2-dione is dissolved in a butanol/toluene mixture and 462 mg (2.2 mmol) of 2,4,6-trimethylpyrylium tetrafluoroborate is added and the reaction mixture is refluxed for 12 h. The solvent is removed and the dye purified via column chromatography using silica gel 60 as the stationary phase and a chloroform/methanol mixture (gradient from 100:0 to 80:20 v/v) as the solvent [6, 7].

Yield: 68 mg (0.18 mmol, 10%), blue crystals, $C_{24}H_{23}NO_3$ (373.45 g/mol).

R_f (silica gel, chloroform:methanol 80:20 v/v): 0.88.

^{1}H-NMR (d_1-chloroform, TMS external): δ 8.33 (d, 1H), 7.3 (m, 2H), 7.2 (t, 1H), 7.05 (d, 1H), 6.15 (d, 1H), 5.9 (s, 1H), 5.75 (s, 1H), 3.6 (s, 3H), 2.26 (s, 3H), 2.19 (s, 3H), 1.74 (s, 6H).

ESI-MS: m/e (M-H$^+$, cation) for $C_{24}H_{24}NO_3$, calculated 374.2, found 374.1.

5.2.2. Syntheses of Py-Dyes with a Sterically Hindered Pyrylium Moiety

5.2.2.1. Syntheses of Pyrylium Derivatives

i) Preparation of 2,6-di-tertbutyl-4-methylpyranylium trifluoro-methanesulfonate
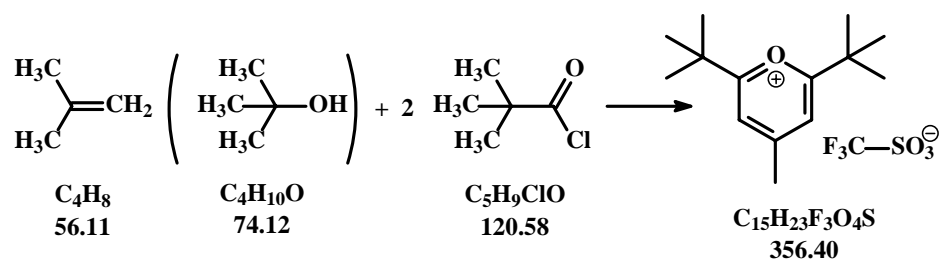
A three necked flask with intensive reflux condenser (-20 °C) and a stop-cock for flushing nitrogen is filled with 11.8 mL (12.1 g, 100 mmol) of 2,2-dimethylpropanic acid chloride (from Fluka) and 1.85 g (25 mmol) of iso-butanol. The flask is rinsed carefully with nitrogen and the reaction mixture is heated to 85 °C. 7.5 mL of trifluormethane sulfonic acid are added dropwise within 15 min and the reaction is finished within 10 min. The mixture is cooled in ice water and triturated with cold ether. The white crystals are sucked off and dried [8].

Yield: 3.4 g (9.54 mmol, 38%); m.p. 165 °C.

^{1}H-NMR (d_4-methanol, TMS external): δ 8.04 (s, 2H), 1.52 (s, 18H); the protons of the 4-methyl group exchange with the solvent.

ii) Preparation of 4-methyl-2,6-diphenyl-pyrylium aluminium tetrachloride

C$_4$H$_9$Cl
92.57

C$_7$H$_5$ClO
140.57

AlCl$_3$
133.34

C$_{18}$H$_{15}$AlCl$_4$O
416.11
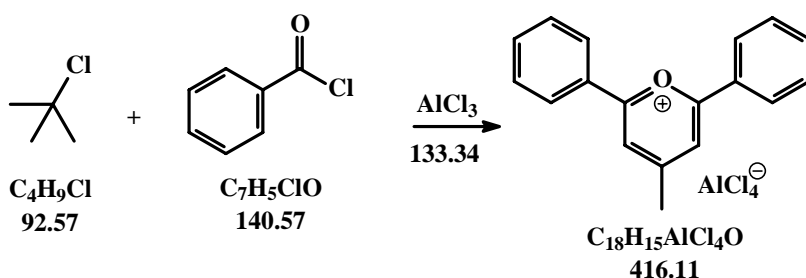
A three necked flask with intensive reflux condenser, a dropping funnel and a stop cock with a plastic tube is filled with 14.05 g (11.6 mL, 0.1 mol) of benzoyl chloride. The flask is rinsed carefully with nitrogen. The reaction is very sensitive against water. 7 g (0.05 mol) aluminium chloride is poured through the plastic tube to the benzoyl chloride at 0-10 °C under stirring and nitrogen atmosphere. Most of the aluminium chloride is dissolved. 4.5 g (0.05 mol) tert.-butyl chloride (from Fluka) are slowly added to the reaction mixture. The reaction mixture is stirred at 20 °C for 3-4 h. After that time all educts have to be dissolved and the development of hydroxide chloride stops. The reaction is stirred another 12 h at room temperature, then poured onto crashed ice. The aqueous phase is extracted with diethyl ether to remove the impurities. The water evaporated to a few mL and the brown-green product is sucked off, washed with ether and dried [8].

Yield: 840 mg (2.0 mmol, 4%) brown-green powder, C$_{18}$H$_{15}$AlCl$_4$O (416.11 g/mol); m.p. >260 °C.

ESI-MS: m/e (M$^+$, cation) for C$_{18}$H$_{15}$O, calculated 247.11, determined 246.8 and 247.8.

5.2.2.2. Syntheses of Py-9, Py-11, Py-12, Py-13 and Py-18

i) Preparation of the acetyl-phenyl-amino-butadienyl-intermediate
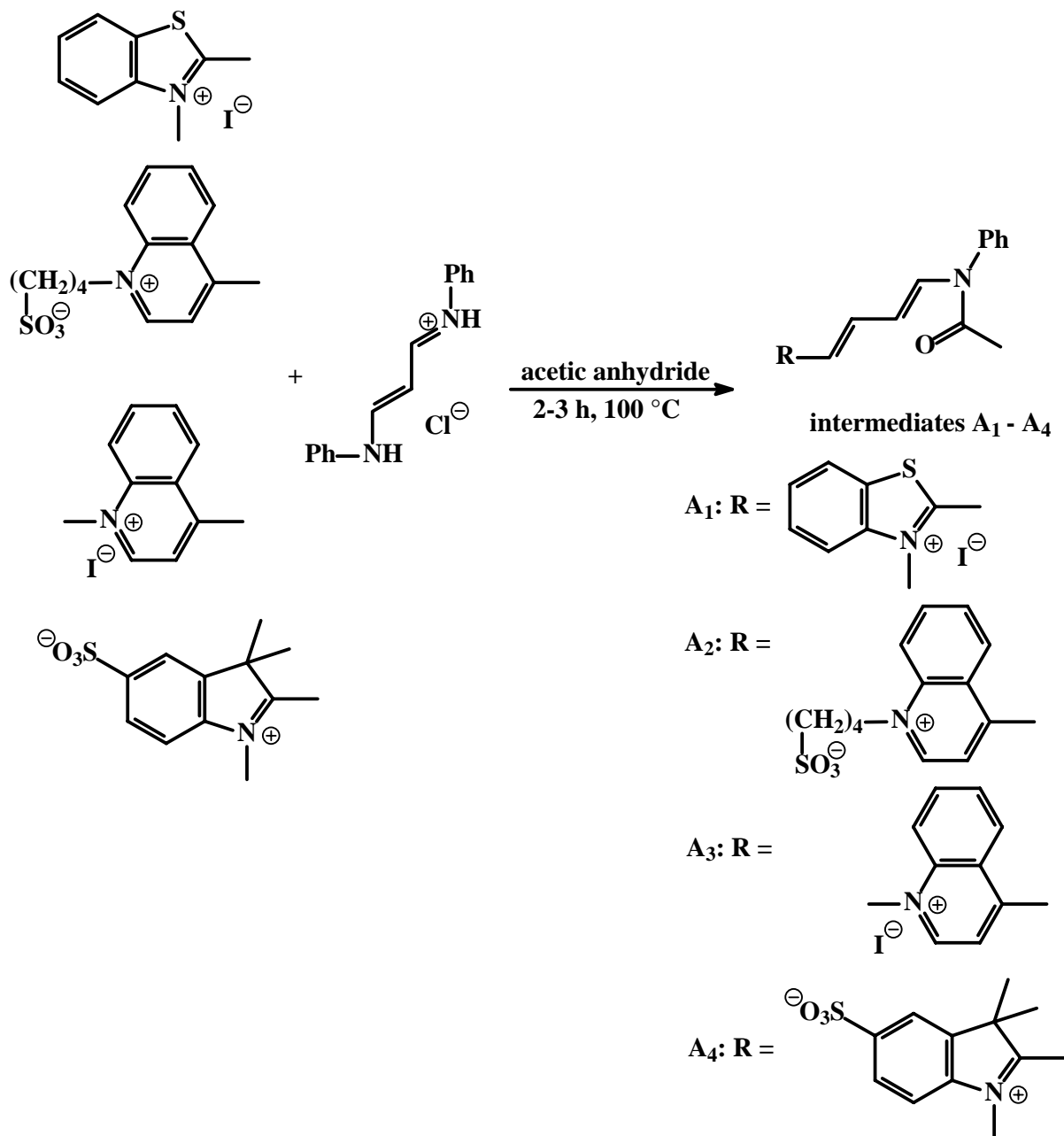
A$_1$) 300 mg (1.03 mmol) of 2,3-dimethyl-benzothiazol-3-ium iodide [3, 4] and 266.6 mg (1.03 mmol) of malondialdehyde bis(phenylimine) monohydrochloride (from Aldrich) are dissolved in 7 mL of acetic anhydride and heated for 3 h to 100 °C. The solvent is removed under reduced pressure and the product dried in a desiccator [3, 9].

A$_2$) 200 mg (0.72 mmol) of 1-(butyl-4-sulfonic acid)-4-methyl-quinolinium (synthesis in analogy to [3, 5]) and 185 mg (0.72 mmol) of malonaldehyde bis(phenylimine) monohydrochloride (from Aldrich) are dissolved in 5 mL of acetic anhydride and refluxed for 1-2 h. The solvent is removed and the product dried in a desiccator [3, 9].

A$_3$) 200 mg (0.70 mmol) of 1,4-dimethyl-quinolinium iodide [3] and 181 mg (0.70 mmol) of malonaldehyde bis(phenylimine) monohydrochloride (from Aldrich) are dissolved in 5 mL of acetic anhydride and refluxed for 1-2 h. The solvent is removed and the product dried in a desiccator [3, 9].

A$_4$) 200 mg (0.79 mmol) of 1,2,3,3-tetramethyl-3H-5-indoliumsulfonate (synthesis in analogy to [3, 4]) and 204 mg (0.79 mmol) of malonaldehyde bis(phenylimine) monohydrochloride (from Aldrich) are dissolved in 5 mL of acetic anhydride and refluxed for 3 h. The solvent is removed and the product dried in a desiccator [3, 9].

ii) Preparation of the Py dyes
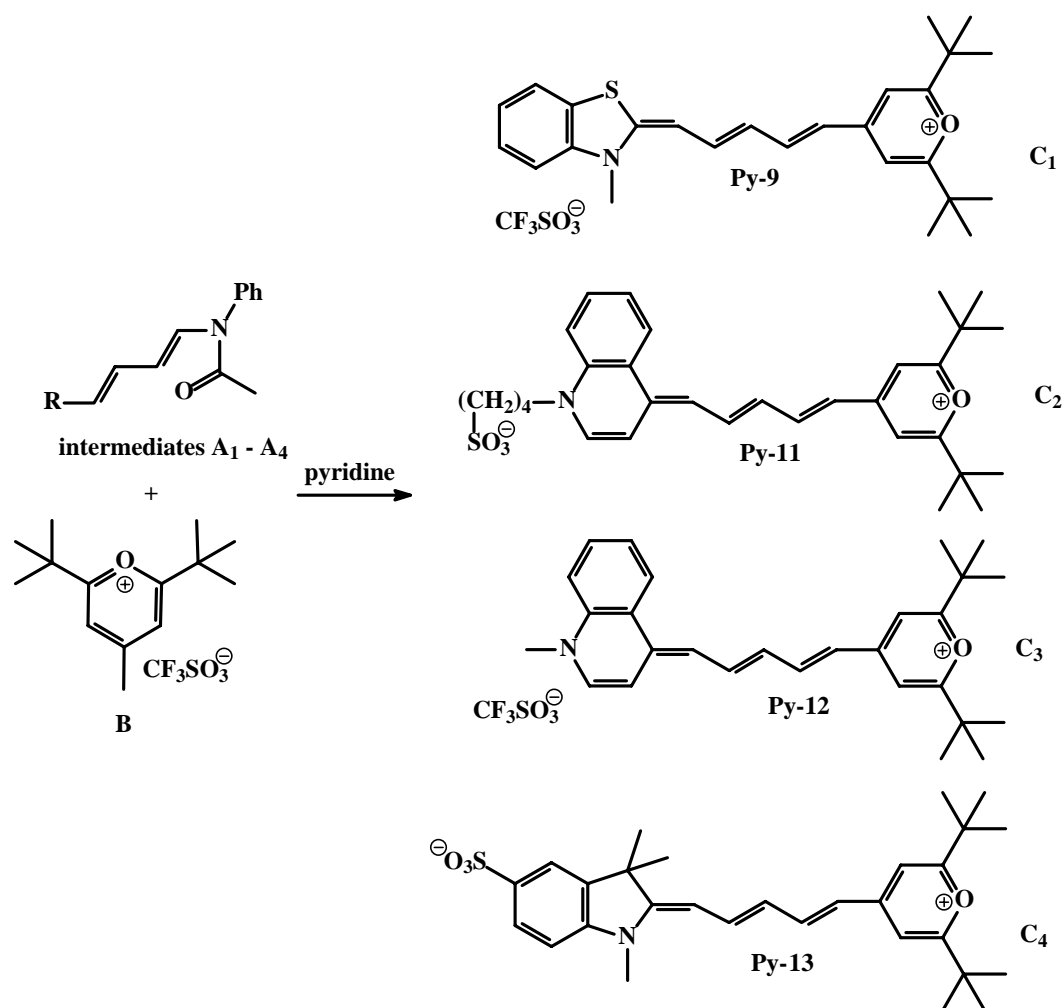
Py-9 (C_1): The intermediate (A_1) and 367.1 mg (1.03 mmol) of 2,6-di-tertbutyl-4-methyl-pyrylium trifluoromethane sulfonate (B) are dissolved in 5 mL of pyridine and refluxed for 1 h at 100 °C. The solvent is removed and the raw product is purified via column chromatography using silica gel 60 as the stationary phase and a chloroform/methanol mixture (80:20 v/v) as the eluent [3, 9].

Yield: 280 mg (0.5 mmol, 49%) blue powder, $C_{27}H_{32}F_3NO_4S_2$ (555.17 g/mol); m.p. 260 °C.

R_f (silica gel, chloroform:methanol 80:20 v/v): 0.67.

^{1}H-NMR (d_1-CDCl$_3$, TMS external): δ 8.0 (d, 1H), 7.9 (d, 1H), 7.84 (d, 1H), 7.76 (d, 1H), 7.69 (dd, 1H), 7.58 (t, 1H), 6.83 (d, 1H), 6.71 (s, 1H), 6.55 (t(dd), 1H), 6.22 (s, 1H), 5.9 (d, 1H), 4.02 (s, 3H), 1.33 (s, 9H), 1.28 (s, 9H).

Py-11 (C_2): The intermediate (A_2) and 255 mg (0.72 mmol) of 2,6-di-tertbutyl-4-methyl-pyrylium trifluoromethane sulfonate (B) are dissolved in 5 mL of pyridine and heated to 100 °C for 1 h. The solvent is removed and the dye is purified via column chromatography using silica gel RP-18 and a methanol/water mixture (80:20 v/v) as the eluent [3, 9].

Yield: 21 mg (0.040 mmol, 6%), blue crystals, $C_{31}H_{39}NO_4S$ (521.71 g/mol).

R_f (silica gel RP-18, methanol:water 80:20 v/v): 0.21.

^{1}H-NMR (d4-methanol, TMS external): δ 8.7 (d, 1H), 8.61 (d, 1H), 8.3 (d, 1H), 8.1 (d, 1H), 7.97 (d, 2H), 7.84 (t, 1H), 7.47 (t, 1H), 7.35 (d, 1H), 6.6 (dd, 1H), 6.45 (s, 1H), 5.99 (s, 1H), 5.78 (d, 1H), 4.5 (br.s, 2H), 2.88 (t, 2H), 2.17 (m, 2H), 1.9 (m, 2H), 1.29 (s, 9H), 1.25 (s, 9H).

Py-12 (C_3): The intermediate (A_3) and 180 mg (0.5 mmol) of 2,6-di-tertbutyl-4-methyl-pyrylium trifluoromethane sulfonate (B) are dissolved in 5 mL of pyridine and heated to 100 °C for 1 h. The solvent is removed and the raw product is purified via column chromatography using silica gel 60 and a chloroform/methanol mixture (90:10 v/v) as the eluent [3, 9].

Yield: 69 mg (0.13 mmol, 18%), blue powder, $C_{29}H_{34}F_3NO_4S$ (549.65 g/mol); m.p. 230 °C.

R_f (silica gel, chloroform/methanol 80:20 v/v): 0.91

^{1}H-NMR (d1-chloroform, TMS external): δ 9.46 (d, 1H), 8.37 (d, 1H), 8.0-7.8 (m, 2H), 7.87 (m, 2H), 7.75 (m, 1H), 7.42 (t, 1H), 7.03 (d, 1H), 6.47 (dd, 1H), 6.4 (s, 1H), 5.89 (s, 1H), 5.71 (d, 1H), 4.45 (s, 3H), 1.30 (s, 9H), 1.24 (s, 9H).

ESI-MS: m/e (M$^+$, cation) for $C_{28}H_{34}NO$, calculated 400.26, determined 400.2 and 401.2.

Py-13 (**C$_4$**): The intermediate (**A$_4$**) and 282 mg (0.79 mmol) 2,6-di-tertbutyl-4-methyl-pyrylium trifluoromethane sulfonate (**B**) are dissolved in 5 mL of pyridine and heated to 100 °C for 1 h. The solvent is removed and the raw product is purified via column chromatography using silica gel RP-18 as the stationary phase and a methanol/water mixture (80:20 v/v) as the eluent [3, 9].

Yield: 80 mg (0.16 mmol, 20%), blue crystals, $C_{29}H_{37}NO_4S$ (495.7 g/mol); m.p. 245 °C.
R$_f$ (silica gel RP-18, methanol/water 80:20 v/v): 0.38.
^{1}H-NMR (d$_4$-methanol, TMS external): d 8.29-8.13 (m, 2H), 7.95 (d, 1H), 7.9 (m, 2H), 7.38 (d, 1H), 6.63 (t, 2H), 6.4 (d, 1H), 6.2 (d, 1H), 3.67 (s, 3H), 1.75 (s, 6H), 1.38 (s, 18H).
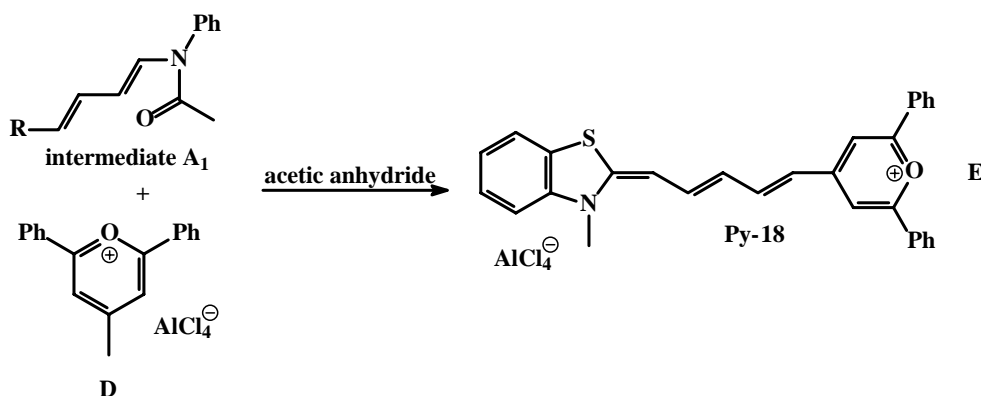
Py-18 (**E**): The intermediate (**A$_1$**) and 430 mg (1.03 mmol) of 4-methyl-2,6-diphenyl-pyrylium aluminium tetrachloride (**D**) are dissolved in 5 mL of acetic acid anhydride and refluxed for 1 h. The solvent is removed on a rotary evaporator and the product is purified via column chromatography using silica gel 60 as the stationary phase and a chloroform/methanol mixture (90:10 v/v) as the eluent [3, 9].

Yield: 76 mg (0.12 mmol, 12%), blue crystals, $C_{30}H_{24}AlCl_4NOS$ (615.38 g/mol).
R$_f$ (silica gel, chloroform/methanol 95:5 v/v): 0.52.
ESI-MS: m/e (M$^+$, cation) for $C_{30}H_{24}NOS$, calculated 446.16, determined 446.1.

5.2.2.3. Synthesis of Py-17

i) Preparation of 3-(5-carboxy-pentyl)-2-methyl-benzothiazol-3-ium bromide
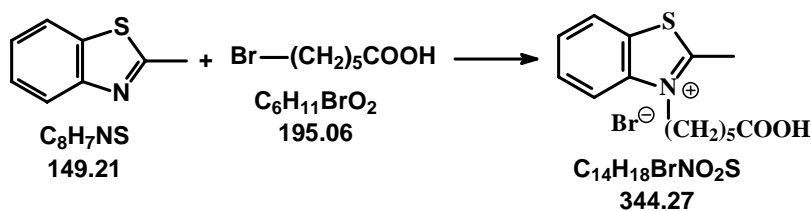
3 g (20 mmol) of 2-methyl-benzothiazole (from Aldrich) and 3.9 g (20 mmol) of 6-bromo-hexanoic acid are heated in a sealed tube to 140 °C for 18 h. The raw product is diluted in 10 mL of acetone and 10 mL water, the solvent removed on a rotary evaporator and the product washed with diethylether [3, 4].

Yield: 5.8 g (0.017 mmol, 85%), fawn powder, $C_{14}H_{18}BrNO_2S$ (344.27 g/mol); m.p. 215 °C.

^{1}H-NMR (d_1-chloroform, TMS external): δ 8.3 (m, 2H), 7.9 (m, 1H), 7.8 (m, 1H), 4.76 (t, 2H), 3.22 (s, 3H), 2.34 (t, 2H), 2.0 (m, 2H), 1.7 (m, 2H), 1.55 (m, 2H).

ii) Preparation of 2-[(1E,3Z)-4-(acetyl-phenyl-amino)-buta-1,3-dienyl]-3-(5-carboxy-pentyl)-benzothiazol-3-um bromide
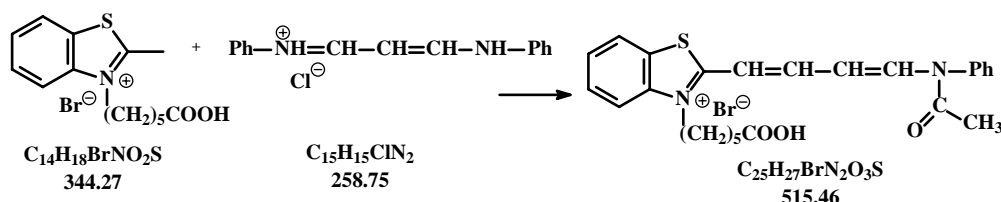
200 mg (0.58 mmol) of 3-(5-carboxy-pentyl)-2-methyl-benzothiazol-3-ium bromide and 125 mg (0.6 mmol) of malondialdehyde bis(phenylimine) monohydrochloride (from Aldrich) are heated in acetic anhydride to 100 °C for 3 h. The solvent is removed in vacuum and the residue is dried in a desiccator. The product is used without further purification [3, 9].

iii) Preparation of Py-17
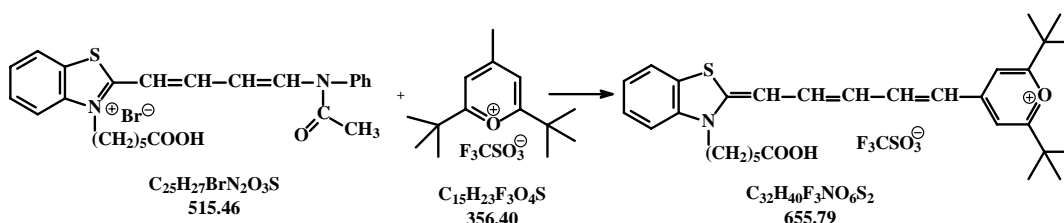
The dye intermediate and 214 mg (0.6 mmol) of 2,6-di-tert-butyl-4-methyl-pyranylium trifluoro-methanesulfonate are dissolved in 5 mL of pyridine and heated to 100 °C for 1 h.

The solvent is removed in vacuum and the dye is purified via column chromatography using silica gel RP-18 and a methanol/water mixture (80:20 v/v) as the eluent [3, 9].

Yield: 50 mg (0.076 mmol, 13%), blue crystals, $C_{32}H_{40}F_3NO_6S_2$ (655.79 g/mol); m.p. 155 °C.
R_f (silica gel, chloroform:methanol 80:20 v/v): 0.69.
^{1}H-NMR (methanol-d[4], TMS external): δ 7.69-7.49 (m, 5H), 6.80 (d, 1H), 6.68 (s, 1H), 6.52 (t, 2H), 5.88 (d, 1H), 6.19 (s, 1H), 4.48 (t, 2H), 2.26 (t, 2H), 1.85 (m, 2H), 1.65 (m, 2H), 1.49 (m, 2H), 1.27 (s, 18H).

iv) Preparation of Py-17-OSI Ester
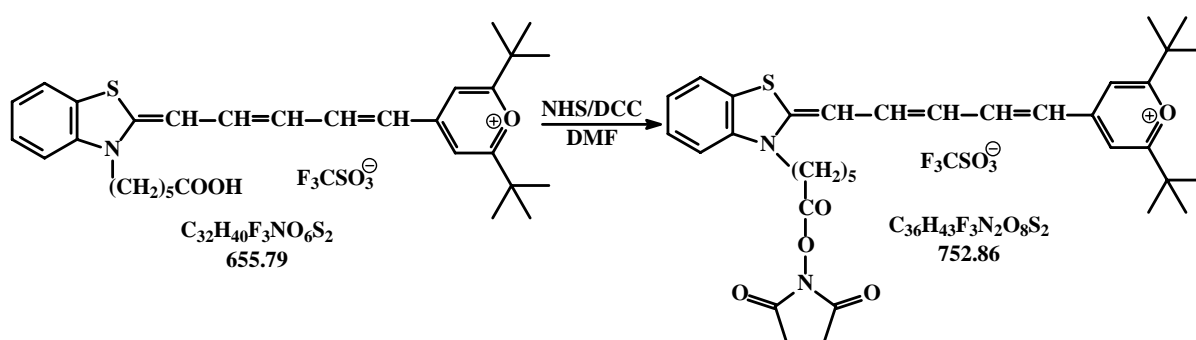
5 mg (7.6 mmol) of Py-17, 1.04 mg (9.1 mmol) of NHS, and 1.9 mg (9.1 mmol) of DCC are dissolved in 1 mL of dry DMF. The solution is stirred at room temperature for 12 h. The reaction is followed by TLC using silica gel 60 as the stationary phase and a chloroform/methanol mixture (80:20 v/v) as the eluent. When the fraction point of the acid has nearly disappeared on the TLC, 5 mL of diethylether are added into the reaction mixture, and the blue product precipitates. The product is centrifuged for 10 min at 15,000 RPM and washed with diethylether. The activated dye (OSI ester) is not separated from the remaining acid and used for coupling experiments without further purification [10, 11].
R_f (silica gel, chloroform:methanol 80:20 v/v): 0.45.

5.3. General Procedure for Labeling Py Dyes to Primary Aliphatic Amines

The pyrylium moiety of Py labels react with primary amino groups of proteins, oligonucleotides and organic compounds. The products of the labels coupled to primary amines with aliphatic residues were used for the determination of molar absorbances of Py conjugates, introduction of new reactivities, or addition of a spacer between the label and a biomolecule. The Py labels are exceptional labels since they undergo a significant change in color following conjugation to a primary amino group. Therefore they are termed chameleon

labels. The color change is due to the fact that labeling causes a major change in the electronic structure of the fluorophore as shown in fig. 5.2.
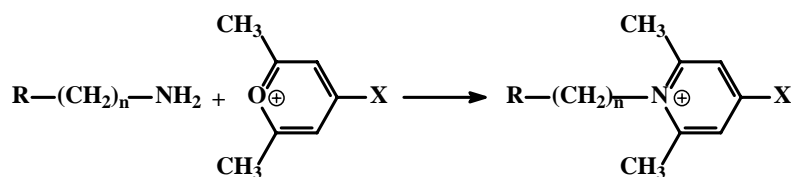
Fig. 5.2.   Labeling chemistry of the Py labels. *X* stands for the respective chromogenic/fluorgenic group, R stands for an aliphatic or aromatic group.

Standard protocol: 5-10 mg of the Py label is predissolved in 200 µL of DMF and diluted with 2 mL of methanol. The amine is dissolved in a 1.2-fold molar excess over the label in methanol, acetonitrile or DMF, one drop of triethylamine is added to ensure deprotonation of the amino groups. The two solutions are mixed and heated to 60 °C for several minutes up to 4 h. The reaction is followed by TLC. The product appears as a fluorescent red spot on the TLC. The solvent is removed on a rotary evaporator. The product is separated from impurities by column chromatography and dried in a desiccator. The yields are between 30 and 90%.

Py-1_propyl: Py-1 and propylamine are reacted in methanol and triethylamine for 1 h at 60 °C, and purified via a column chromatography using silica gel 60 as the stationary phase and a chloroform/methanol mixture (gradient from 100:0 to 95:5 v/v) as the eluent.
Yield: 38%.
^{1}H-NMR (d_1-chloroform, TMS external): δ 7.41 (s, 2H), 7.38 (d, 1H), 7.05 (s, 2H), 6.56 (d, 1H), 4.27 (t, 2H), 3.27 (t, 2·2H), 2.7 (br.s, 6H), 1.7 (m, 4H), 1.25 (t, 3H), 1.1 (m, 2H), 0.85 (m, 4H).

Py-1_acid: Py-1 is dissolved in methanol and added dropwise to a hot solution of aminohexanoic acid in methanol and triethylamine. The reaction mixture is refluxed for 2 h, the solvent is removed and the raw product washed with water. To a solution of the dye in methanol, chloroform is added and the dye precipitates at 4 °C within 24 h.
Yield: 50%.
^{1}H-NMR (d_4-methanol, TMS external): δ 7.67 (s, 2H), 7.63 (d, 1H), 7.12 (s, 2H), 6.83 (d, 1H), 4.33 (t, 2H), 3.26 (d, 4H), 2.77 (s, 6H), 2.73 (d, 2H), 2.35 (m, 4H), 1.96 (m(dd), 4H), 1.85 (m, 2H), 1.70 (m, 2H), 1.55 (m, 2H).
ESI-MS: m/e (M-H$^+$, cation) for $C_{27}H_{35}N_2O_2$, calculated 419.27, found 419.2 and 420.2.

Py-2_propyl: Py-2 and propylamine are reacted in methanol and triethylamine for 4 h at 60 °C and purified via column chromatography using silica gel 60 as the stationary phase and a chloroform/methanol mixture (gradient from 100:0 to 95:5 v/v) as the eluent.

Yield: 40%.

^{1}H-NMR (d$_1$-chloroform, TMS external): δ 7.9 (dd, 1H), 7.3-7.2 (s, 2H, dd, 2H), 7.0 (t, 1H), 6.79 (d, 1H), 6.06 (d, 1H), 5.61 (d, 1H), 4.24 (t, 2H), 3.27 (s, 3H), 2.73 (s, 6H), 1.77 (m, 2H), 1.67 (s, 6H), 1.09 (t, 3H).

Py-2_acid: The dye Py-2 is dissolved in methanol and added dropwise to a solution of aminohexanoic acid in methanol with triethylamine. The reaction mixture is heated to 60 °C for 1 h and the product purified via column chromatography using silica gel 60 as the stationary phase and a chloroform/methanol mixture (gradient from 100:0 to 80:20 v/v with 0.1% v/v of 15% HCl).

Yield: 50%.

^{1}H-NMR (d$_4$-methanol, TMS external): δ 8.04 (dd, 1H), 7.48 (s, 2H), 7.32-7.23 (m, 2H), 7.0-6.93 (m, 2H), 7.2 (d, 1H), 5.78 (d, 1H), 4.28 (t, 2H), 3.23 (s, 3H), 2.75 (s, 6H), 2.28 (t, 2H), 1.84 (m, 2H), 1.73 (m, 2H), 1.67 (s, 6H), 1.51 (m, 2H).

Py-2_OH: The dye Py-2 is dissolved in methanol and added dropwise to a solution of aminohexanol in methanol. The reaction mixture is heated to 60 °C for 30 min and the product purified via column chromatography using silica gel RP-18 as the stationary phase and a methanol/choloform mixture (gradient from 100:0 to 80:20 v/v with 0.1% v/v of 15% HCl).

Yield: 30%.

^{1}H-NMR (d$_4$-methanol, TMS external): δ 8.98 (dd, 1H), 7.26-7.13 (2·d, 2·1H), 7.95 (d, 1H), 6.87 (d, 1H), 6.14 (d, 1H), 5.89 (s, 1H), 5.71 (d, 1H), 5.4 (s, 1H), 4.23 (t, 2H), 3.6 (t, 2H), 3.58 (s, 3H), 2.1 (m, 2H), 1.61 (s, 6H), 1.55 (m, 2H), 1.23 (s, 6H), 0.85 (m, 2H).

ESI-MS: m/e (M$^+$, cation) for C$_{27}$H$_{37}$N$_2$O, calculated 405.29, found 405.2 and 406.2.

Py-3_propyl: Py-3 and propylamine are reacted in methanol and triethylamine for 4 h at 60 °C. The product is purified via column chromatography using silica gel 60 as the stationary phase and a chloroform/methanol mixture (gradient 100:0 to 95:5 v/v) as the eluent.

Yield: 20%.

^{1}H-NMR (d$_1$-chloroform, TMS external): δ 7.75-6.6 (m, 8H), 4.3 (t, 2H), 3.06 (s, 6H), 2.76 (s, 6H), 1.14 (m, 2H), 0.89 (t, 3H).

Py-4_propyl: Py-4 and propylamine are reacted in methanol and triethylamine for 4 h at 60 °C. The product is purified via column chromatography using silica gel 60 as the stationary phase and a chloroform/methanol mixture (gradient 100:0 to 95:5 v/v) as the eluent.
Yield: 50%.
^{1}H-NMR (d$_4$-methanol, TMS external): δ 7.65 (dd, 1H), 7.5 (d, 1H), 7.31 (m, 2H), 7.17 (d, 1H), 7.1 (t(dd), 2H), 6.05 (d, 1H), 5.88 (d, 1H), 4.15 (t, 2H), 3.49 (s, 3H), 2.65 (s, 6H), 1.83 (m, 2H), 1.08 (t, 3H).

Py-4_acid: The dye Py-4 is dissolved in DMF and added dropwise to a solution of aminohexanoic acid in BCB of pH 9. The reaction mixture is stirred for 4 h at RT. 10 mL doubly distilled water with one drop 15% HCl and 10 mL chloroform are added. The product is extracted into the organic phase and separated. The organic phase is dried over K$_2$SO$_4$ and removed under vacuum.
Yield: 50%.
ESI-MS: m/e (M$^+$, cation) for C$_{25}$H$_{31}$N$_2$O$_2$S, calculated 423.2, determined 423.2.

Py-4_C18: The dye Py-4 is dissolved in methanol and added dropwise to a solution of octadecylamine in methanol with triethylamine. The reaction mixture is heated to 60 °C for 4 h, and the product purified via column chromatography using silica gel 60 as the stationary phase and a chloroform/methanol mixture (gradient from 100:0 to 95:5 v/v).
Yield: 70%.
ESI-MS: m/e (M$^+$, cation) for C$_{36}$H$_{55}$N$_2$S, calculated 547.41, found 547.6, 548.6, 549.6 .

Py-6_propyl: Py-6 and propylamine are reacted in methanol and triethylamine for 4 h at 60 °C. The product is purified via column chromatography using silica gel 60 as the stationary phase and a chloroform/methanol mixture (gradient 100:0 to 95:5 v/v) as the eluent.
Yield: 71%.
^{1}H-NMR (d$_1$-chloroform, TMS external): δ 8.09 (d, 1H), 8.03 (dd, 1H), 7.83 (t, 2H), 7.52 (t, 1H), 7.34 (t, 1H), 7.25 (s, 2H), 7.15 (d, 1H), 6.06 (d, 1H), 5.64 (d, 1H), 4.25 (t, 2H), 3.39 (s, 3H), 2.75 (s, 6H), 1.25 (s, 6H), 1.12 (m, 2H), 0.88 (t, 3H).

Py-6_acid: Py-6 is dissolved in methanol and added to a solution of aminohexanoic acid in methanol at 60 °C. The reaction mixture is refluxed for 3 h. The raw product is purified via column chromatography using silica gel RP-18 as the stationary phase and methanol (with 1 drop of 1 M HCl per 100 mL methanol) as the eluent.

Yield: 50%.

ESI-MS: m/e (M^+, cation) for $C_{31}H_{37}N_2O2$, calculated 469.29, found 469.3.

Py-8_propyl: Py-8 and propylamine are reacted in methanol and triethylamine for 4 h at 60 °C, and purified via column chromatography using silica gel 60 as the stationary phase and a chloroform/methanol mixture (gradient from 100:0 to 95:5 v/v) as the eluent.

Yield: 50%.

^{1}H-NMR (d_4-methanol, TMS external): δ 7.85-7.21 (m, 6H), 5.99 (s, 1H), 4.2 (t, 2H), 3.71 (s, 3H), 2.71 (s, 6H), 1.1 (m, 2H), 0.9 (t, 3H).

5.4. General Procedure for Staining Proteins in a SDS-PAGE

Protocol for pre-staining

5 µL of the protein standard mixture from Sigma (Dalton Mark VII-L, standard mixture, 14-66,000 D, for SDS PAGE, seven proteins, and see chapter 5.1.1.) were diluted with 5 µL of BCB pH 9. 0.2 mg of the different amino reactive dyes (Py-2 (1), Py-4 (2), Py-6 (3), Py-1 (4), ATTO 550 (5), Bodipy (6), Chromeon546 (7)) were dissolved in 100 µL of DMF ([dye] = 2 g/L), respectively, and 1 µL of each dye solution was reacted with the 10 µL standard protein solution. In the second part of the experiment the seven dye solutions in DMF were diluted 1:10 v/v with DMF ([dye] = 0.2 g/L) and added to the protein standard solutions. After a reaction time of 30 min the protein labeling solutions were diluted with 10 µL of 5x sample buffer (containing SDS) and heated to 100 °C for 3 min. These fourteen labeled protein standard samples (two different concentrations of each dye) were loaded onto the SDS gel. The gel has 17 pockets to be filled with a protein mixture. In line 1, 9 and 17 the protein standard without pre-labeling is separated. In line 2 to 8 the standard protein mixtures labeled with the concentrated dye solutions and in line 10 to 16 proteins stained with the diluted dye solutions were separated. The electrophoresis was performed in a vertical polyacrylamide gel system (electrophoresis device Multigel TYP G44 was from biometra, pharmacia, www.biometra.de), consisting of a separating (12.5%, m/v) and a stacking gel (5%, m/v). The

electrophoresis buffer consisted of the tris-glycine system, containing 25 mM Tris, 192 mM glycin, and 0.1% SDS.

The fluorescent protein bands on the gel were first detected on a UV-transilluminator (from Stratagen, Amsterdam, model transiluminator 2040 EV) equipped with a camera (Herolab Laborgeräte, type E.A.S.Y 429 K), and a fluorescence scanner (from Tecan). Afterwards the gel was stained with Coomassie Brilliant Blue, following a standard protocol described in [12], dried and scanned. The results are shown in chapter 4.1.1.2.

Protocol for staining after gel electrophoreses

The gels are commercially available as 4 - 12% tris-glycine-gradient-geles (Anamed GmbH, Darmstadt, www.anamed-gele.de). Its 10 lines were loaded with a series of different dilutions of the protein standard Protemix (Anamed, Darmstadt, protein composition see chapter 5.1.1). Then the electrophoresis was done with: a Tris/HCl (450 mM) as the probe buffer containing glycerol (12%), SDS (4%), Coomassie Brilliant Blue G (0.0025% in water), phenol red (0.0025%), pH 8.45; running buffer (pH 8.3): consisting of Tris/HCl (25 mmol/L), glycine (192 mmol/L), and SDS (0.1%); 125 V, amperage from 80 mA (at the beginning) to 40 mA (at the end of the run; 90 min); vertical cell. The serial dilution factors of this mixture from line 1 to ten (fig. 4.1.) are as follows 0.0, 1.3, 1.7, 2.0, 2.5, 5.0, 10.0, 12.5, 16.7, 20.0.

After electrophoresis the gel was first incubated in a solution containing 50% methanol, 10% acetic acid, and 40% distilled water (3 min), washed with 50% aqueous methanol, and then fixed twice with a mixture of 50% triethylamine/acetate (TEAA) buffer of pH 10 and 50% methanol. Staining was performed with a freshly prepared 0.004% solution of Py-1 in a 1:1 mixture of methanol and TEAA buffer (Py-1 can be predissolved in minute quantities of DMF). The staining time depends on the thickness and percentage of the gel. Once the optimal signal is achieved, additional staining (over night) does not enhance or degrade the signal. The gel was rinsed (a) briefly in a washing solution of 50% methanol and 50% TEAA buffer, (b) several times with a destaining solution containing 5% methanol, 7% acetic acid and 88% distilled water, and subsequently scanned or dried. Gels are stable in the washing solution for at least two days.

For the detection of the fluorescent protein bands on the gel a fluorescence scanner from Tecan FL200 (excitation at 542 nm; emission filter set to 630 nm) was used. The results are shown in chapter 4.1.1.1.

5. 5.   General Procedure for the Determination of Amines and Proteins in Solution

The reagent solutions were used in the staining experiments and in the general protein assay:

Stock Solution: This was prepared by dissolving 4 mg of Py-1 in 1 mL of dimethylformamide (DMF) and diluting this solution with methanol to a total volume of 100 mL. The stock solution for Py-6 was obtained analogously, except that 4.4 mg of Py-6 were used. The stock solutions are stable at 4 °C for at least 1 month if protected from light.

Reagent Solution: It is obtained by diluting 1 mL of the Py-1 or Py-6 methanol stock solution with 9 mL of doubly distilled water and has to be used at once. The reagent solutions have an maximum absorbance of 0.63 cm^{-1} for Py-1 and 0.35 cm^{-1} for Py-6, respectively.

Recommended general protocol

Photometric Assay. The protein sample is diluted with BCB to a concentration between 10 and 50 µg/mL (lower ranges are possible but resulting in smaller absorbances). 200 µL thereof are placed in the wells of a 96-well microplate. To this are added 20 µL of the dye stock solution in methanol. After 30 min incubation the absorbance at 492 nm is measured and the value is related to the protein concentration using a dillution series and a calibration graph established in the identical way (see fig. 4.6.).

Fluorimetric Assay. The protein sample is diluted with BCB to a concentration between 5 and 10 µg/mL (lower ranges are possible but result in weaker fluorescence intensities and larger signal-to-noise ratios), and 100 µL are placed in the wells of a 96-well microplate. 100 µL of reagent solution is added to each well. After shaking for 1 h at 25 °C fluorescence intensity is measured at excitation/emission wavelengths of 485/635 nm and related to the protein concentration using a dilution series and a calibration graph established in the identical way (see fig. 4.9.).

5.6. General Labeling Procedures for Proteins and Oligonucleotides

5.6.1. General Procedure for Labeling Proteins and Determination of Dye-to-Protein Ratios

Preparation of Labeled Biotin and Proteins

Labeled proteins were prepared by labeling proteins with solutions of the respective dyes DMF. In order to obtain HSA of varying dye-to-protein ratio, varying quantities of dye solution (2, 5, 7.5, 10, 12 μL of a solution of 1 mg Py-1 or Py-6, respectively, in 100 μL of DMF) were added to solutions of 3 mg HSA in 1 mL of BCB. After a reaction time of 30 min, the protein-dye conjugates were separated from excess of label by size exclusion chromatography on a Sephadex G-25 medium column with phosphate buffer as the eluent. The dye-to-protein ratios were determined via the ratio of the absorbances of dyes and conjugates (see table 3.2.; the molar absorbance of labeled propylamine was used in these calculations), and from the intrinsic absorbance of HSA at 280 nm ($\varepsilon_{280 \text{ nm}}$ = 35,000 L/(cm·mol)).

Labeled biotin (Bt*) was obtained by dissolving 5 mg (13.6 μmol) of biotin ethylenediamine (from Sigma) in 5 mL methanol containing 1 μL of triethylamine. The labels (the OSI ester of C546 or the Py labels) were first dissolved in a 1.5-fold molar excess over biotin in DMF and added to a stirred solution of biotin ethylenediamine. The mixture was refluxed for 2 h and the solvent removed under vacuum. The labeled biotin was separated from unlabeled biotin and excess of label by column chromatography using a 7 cm column filled with silica gel RP-18 as the stationary phase and a methanol/chloroform mixture (1:1, v/v) as the eluent. The labeled biotins were characterized by ESI mass spectroscopy.

Labeled streptavidin was obtained by dissolving 1 mg of streptavidin (from Sigma) in 500 μL of BCB. Thereafter, 0.1 mg of the label (the C546 OSI ester or the respective Py dye) were first dissolved in 10 μL of DMF and then slowly added to the protein solution. After a reaction time of 1 h at room temperature, the conjugate was purified by size exclusion column chromatography using Sephadex G25 (from Sigma) as the stationary phase and PB as the eluent. The concentrations of the labeled streptavidin was determined via its absorption at 280 nm ($\varepsilon_{280 \text{ nm}}$ = 176,000 L/(cm·mol)), after correction for the intrinsic absorbance of the dye which amounts to around 6,000 – 9,000 L/(cm·mol). Labeled biomolecules are marked with an asterisk in chapter 4.3.

Procedure for Labeled Proteins bound to the surface of a microtiter plate

Microplates whose wells were coated with labeled streptavidin were obtained from streptavidin-coated microplates (being blocked with non-proteomic blocking buffer; product no. 15119; from Pierce; www.perbio.com). Their binding capacity is specified by the manufacturer as being ~5 pmol of biotin per well. Each well was washed three times with PB, once with BCB, and then loaded with 100 µL of BCB. In parallel, 1 mg of the amino-reactive label was dissolved in 100 µL of DMF. Then, different quantities of the dye solution were added to the wells (typically 1 µL, 2 µL, and 5 µL). After an incubation of 1 h, excess label was washed out with PB to give microwells where the streptavidin on the bottom of each well is labeled at different dye-to-protein ratios (see fig. 4.24.).

Microplates whose wells were coated with labeled goat-anti-mouse IgG were obtained by attaching biotinylated goat-anti-mouse IgG to the streptavidin coated microplate and label the anti-body after that. Each well was washed three times with PB of pH 7.2, and then loaded with 100 µL of the biotinylated anti-IgG dissolved in PB (10 µg/mL). After an incubation time of 1 h (RT and slow motion), the wells were washed once with PB and BCB and filled with 100 µL of BCB. In parallel, 1 mg of label Py-1 was dissolved in 100 µL of DMF. Then, 1 µL of the dye solution was added to the wells and incubated for 1 h. Excess of label was washed out with PB to give microwells, where the streptavidin on the bottom of each well was coated via a biotin binding with anti-IgG, which is labeled with Py-1 (see fig. 4.25.).

Determination of Dye-to-Protein Ratios

The dye-to-protein ratio (DPR) can be determined with the help of the following formula, which is derived from the Lambert-Beer law:

$$\frac{D}{P} = \frac{A^{max} \cdot \varepsilon_P^{280\,nm}}{A^{280\,nm} \cdot \varepsilon_F^{max} - A^{max} \cdot \varepsilon_F^{280\,nm}}$$

with $\varepsilon_P^{280\,nm}$ = molar absorption coefficient of the protein at 280 nm,

         $\varepsilon_F^{280\,nm}$ = molar absorption coefficient of the dye at 280 nm,

         ε_F^{max} = molar absorption coefficient of the free dye at its maximum,

         A^{max} = absorbance of the dye-protein solution at its maximum,

         $A^{280\,nm}$ = absorbance of the dye-protein solution at 280 nm.

This formula is valid assuming that at long-wavelengths only the label absorbs and that there are no spectral differences between the free dye and the covalently bound dye. For Py labels the spectral properties of the label bound to a primary amine (propylamine) are used.

5.6.2. General Procedure for Labeling Oligonucleotides

The amino modified oligonucleotides are listed in table 5.1. The coupling reactions are carried out as follows. 20 nmols of the oligonucleotide are dissolved in 10 µL of sterile water, and diluted with 200 µL BCB (pH 9). 1 mg of the reactive dye is pre-dissolved in 100 µL DMF, and 10 µL of the dye solution is added to the oligonucleotide. The solution is incubated for 4 h at room temperature. 1.5 mL of ice-cold ethanol are added. The solution is mixed well and placed at -18°C for 2 h. The solution is centrifuged at 15,000 RPM for 10 min. The supernatant containing unreacted dye is removed carefully and the pellet containing labeled and unlabeled oligonucloetide is rinsed twice with cold ethanol. The pellet is dissolved in 0.1 M triethylammonium acetate (TEAA) buffer of pH 7.1. Non-labeled oligonucleotide is removed by reversed-phase (RP18 column) HPLC using a gradient of 10-65% acetonitrile in 0.1 M aqueous TEAA buffer. The dissolved pellet is loaded onto the column; the run takes over 30 min. Reaction yields of 50% were achieved. In all cases, the unlabeled oligonucleotide migrates fastest, followed by the labeled oligonucleotide. The solvent of the HPLC fraction is removed on a rotary evaporator.

The residue is dissolved in 100 µL of doubly distilled water and the oligonucleotides were precipitated with ice-cold ethanol and diethylether. The solution is centrifuged after 2 h at -18 °C for 10 min at 15,000 RPM. The supernatant is removed carefully and the pellet containing the purified labeled oligonucleotides can either be stored at -18 °C or dissolved in 100 mM Tris/HCl buffer (pH 7.5) for storage, or diluted in the corresponding SSC buffer for further experiments. Labeled oligonucleotides in Tris/HCl buffer of pH 7.5 can be stored at 4 °C for several weeks, and solution of oligonucleotide in the SSC buffer, as the working buffer, should be measured within a few days.

A Cary 50 Bio UV-Visible spectrophotometer from Varian (Australia, www.varian.com) was used to investigate the absorption characteristics and to adjust the dye-labeled oligonucleotide concentration. All experiments are done at 25 °C unless otherwise stated.

5.7. General Procedures for Energy Transfer Measurements in Hybridization Studies

Determination in cuvettes. Varying quantities (typically 5-200 µL) of acceptor solution of a certain concentration (typically 10^{-6}-10^{-7} mol/L of oligonucleotides) are diluted with 1x SSC buffer of pH 7.5 to a final volume of 200 µL. 50 µL of donor solution with the same concentration are added. After incubation of 30 min at room temperature fluorescence is measured at 25 °C (see fig. 4.14. and 4.15.).

Determination in microplates. Varying quantities (typically 5-150 µL) of acceptor solution of a certain concentration (typically 10^{-6}-10^{-7} mol/L of oligonucloetides) are diluted with 1x SSC buffer of pH 7.5 to a final volume of 150 µL. 50 µL of donor solution with the same concentration are added. After incubation of 30 min at room temperature fluorescence is measured at 25 °C (see fig. 4.16.).

5.8. Procedures for Hybridization Lifetime Assays in Microplates

Homogeneous Hybridization Assays. Oligo-1 was labeled with Py-1 (oligo-1*) and diluted to a concentration of $1 \cdot 10^{-7}$ mol/l in 1x SSC buffer. Varying quantities (typically 5 to 100 µL) of oligo-3 solution ($2 \cdot 10^{-7}$ mol/l) in 1x SSC buffer were diluted in the wells of a black microplate to a final volume of 100 µL. Then, 50 µL of oligo-1* solution were added. After an incubation for 30 min at room temperature, both fluorescence intensity and fluorescence lifetime were measured (at excitation 505 nm, emission 630 nm).

Homogeneous hybridization assays. Detection of mismatches. Oligo-1 was labeled with Py-1 (to give oligo-1*). Oligo-1*, oligo-1, oligo-3, oligo-5, and oligo-6 were diluted to a concentration of $1 \cdot 10^{-6}$ mol/l in 5x SSC buffer. Quantities between 5 to 150 µL of these solutions were diluted with 5x SSC buffer to a final volume of 150 µL. Then, 50 µL of oligo-1* solution were added to give a final volume of 200 µL. After an incubation of 30 min at room temperature, fluorescence lifetimes were measured (at excitation 505 nm, emission 630 nm).

Hybridization assay using a mono-labeled molecular beacon (MB). Oligo-7 was labeled with Py-1 (to give oligo-7*) and diluted with Tris/HCl buffer pH 7.5 to a concentration of $1 \cdot 10^{-6}$ mol/L. Quantities of 2.5 to 100 µL of oligo-8 (concentration $2 \cdot 10^{-6}$ mol/L) were diluted to a final volume of 100 µL in cups with safe lock. Thereafter, 50 µL of oligo-7* solution were added. The final volume in the cup was 150 µL. The samples were incubated for 5 minutes at 70°C, slowly cooled to room temperature and then transferred to the wells of a microplate. Fluorescence intensity and lifetimes were then determined at 23 °C (at excitation 505 nm, emission 630 nm).

Hybridization Assay on Lifetime Plates (LPs). Microplates with wells coated with fluorescently labeled oligonucleotides were obtained from streptavidin-coated microplates (being blocked with non-proteomic blocking buffer; product no. 15119; from Pierce; www.perbio.com). Their binding capacity is specified by the manufacturer as being ~5 pmol of biotin per well. Each well was washed three times with PB of pH 7.2. Thereafter, 50 µL of Py-1 labeled oligo-2 (= oligo-2*, concentration $1 \cdot 10^{-6}$ mol/L in PB) were added to the wells. Incubation was performed at room temperature for 1 h under shaking. Excess oligo-2* was washed away with 1x SSC buffer to give wells where the streptavidin on the bottom of each well was occupied with the biotinylated oligo-2*. Oligo-3 is complementary to oligo-2*. Oligo-3 was diluted to a concentration of $1 \cdot 10^{-7}$ mol/L in 1x SSC buffer. Different quantities of this solution (typically 5 to 150 µL) were added into the coated wells of the microplate (final volume 200 µL). After incubation of 30 min the plate was washed with 1x SSC buffer and filled again with 100 µL of this buffer. Then, fluorescence lifetimes were determined as mentioned above.

5.9. Determination of Z'-Value

Z' is a parameter applied to statistically assess data obtained in high-throughput screening and reflects the robustness of the signal changes measured [13, 14]. A Z'-value bigger than 0.5 is considered to be indication for a reliable assay. Z' is defined as

$$Z' = 1 - \frac{3\sigma \text{ positive control} + 3\sigma \text{ negative control}}{\text{mean positive control} - \text{mean negative control}}$$

where σ is the standard deviation, the "negative control" is the background signal, and the "positive control" is the signal after the assay has gone into saturation (i.e., the receptor is fully titrated).

5.10. Determination of Quantum Yields

The quantum yields (QYs) of the dyes and the conjugates, respectively, were measured in phosphate buffer (22 mM, pH 7.2) relative to a reference fluorophore with a known quantum yield. This references were cresyl violet with a specified quantum yield of 0.56 in methanol for dyes absorbing from 510 to 550 nm, fluorescein with a specific quantum yield of 0.92 in buffer of pH 9 for dyes absorbing from 480 to 500 nm and Cy5 (Amersham) with a quantum yield of 0.28 in buffered solution for dyes absorbing from 630 to 670 nm [15, 16]. The quantum yields were determined using the following formula:

$$\phi_X = \phi_R \frac{A_R \cdot I_X \cdot n_X^{\,2}}{A_X \cdot I_R \cdot n_R^{\,2}}$$

where ϕ_R is the quantum yield of the reference, A_R and A_X are the absorbances of the reference (R) and the dye (X), respectively, at the excitation wavelength, I_R and I_X are the integrated areas under the corrected emission spectra of the reference and the dye, respectively, and n_R and n_X are the refractive indices of the solvent of the reference and the dye, respectively.

5.11. References

[1] Organikum, 19. Aufl., Dt.Verl. der Wiss. Leipzig **1993**.

[2] M. Gruber, B. Wetzl, B. Oswald, J. Enderlein and O. S. Wolfbeis, New Long-Wavelength Absorbing Fluorophores and Their Application to Oligonucleotide Labeling and Fluorescence Resonance Energy Transfer (FRET) Hybridization Studies, J. Fluoresc. **2005**, 15(3), 2007-2014.

[3] R.B. Mujumdar, L.A. Ernst, S.R. Mujumdar, C.J. Lewis, A.S. Waggoner, Cyanine Dye Labeling Reagents: Sulfoindocyanine Succinimidyl Esters, Bioconjugate Chem. **1993**, 4, 105-111.

[4] M. Gruber, FRET Compatible Long-Wavelength Labels and their Application in Immunoassays and Hybridization Assays, Dissertation, University of Regensburg (Germany) **2002**.

[5] M. Probst, Synthese und Charakterisierung von Reaktiven Diodenlaserkompatiblen Fluoreszenzfarbstoffen, Diploma Thesis, University of Regensburg (Germany) **1999**.

[6] E. Terpetschnig, H. Szmacinski, J. R. Lakowicz, Synthesis, Spectral Properties and Photostabilities of Symmetrical and Unsymmetrical Squaraines; a New Class of

Fluorophores with Long-Wavelength Excitation and Emission, Anal. Chim. Acta **1993**, 282, 633-641.

[7]   E. Terpetschnig, J.R. Lakowicz, Synthesis and Characterization of Unsymmetrical Squaraines: a New Class of Cyanine Dyes, Dyes and Pigments **1993**, 21, 227-234.

[8]   Houben-Weyl, Methoden der organischen Chemie, 4. Edition, **1985**.

[9]   O. Mader, K. Reiner, H.-J. Egelhaaf, R. Fischer, R. Brock, Structure Property Analysis of Pentamethine Indocyanine Dyes: Identification of a New Dye for Life Science Applications, Bioconjugate Chem. **2004**, 15, 70-78.

[10]   B. Oswald, L. Patsenker, J. Duschl, H. Szmacinski, O.S. Wolfbeis, E. Terpetschnig, Synthesis, Spectral Properties, and Detection Limits of Reactive Squaraine Dyes, a New Class of Diode Laser Compatible Fluorescent Protein Labels, Bioconj. Chem. **1999**, 10, 925-931.

[11]   G. T. Hermanson, Bioconjugate Techniques, Academic Press, San Diego **1996**.

[12]   M. Holtzhauer, Biochemische Labormethoden, 2. Auflage, Springer Labor Manual, Heidelberg **1995**.

[13]   J.H. Zhang, T.D. Chung, K.R. Oldanburg, A Simple Statistical Parameter for use in Evaluation and Validation of High-throughput Screening Assays, J. Biomol. Screen. **1999**, 4, 67-73.

[14]   www.qiagen.com; Qiagen News, Issue No. 4, **2002**.

[15]   J.N. Demas, G.A. Crosby, Measurements of Photoluminescence Quantum Yields, J. Phys. Chem. **1971**, 75, 991 – 1024.

[16]   J.R. Lakowicz, Principles of Fluorescence Spectroscopy, 2nd ed., Kluwer Academic, New York **1999**.

6. Summary

6.1. In English

The aim of this work was the synthesis and the spectral and analytical characterization of pyrylium dyes. These can be used as labels, in hybridization assays, as stains in electrophoresis, and in general protein assays. The pyrylium group is introduced as a new amine-reactive group for fluorescent labels. Each dye contains only one pyrylium group and belongs either to the cyanine dyes or to the squaraines. Unlike in other labels, the reactive group is part of the chromophoric system. Thus, labeling also causes large spectral shifts.

The Py dyes were characterized by absorption and emission spectra, molar absorbance, fluorescence quantum yield and fluorescence decay time. Three different pyrylium derivatives (2,6-dimethyl, 2,6-di-tert-butyl and 2,6-diphenyl pyrylium) were tested with respect to their reactivity to proteins. Only the pyrylium derivative with the sterically smallest residues (2,6-dimethyl) gives fast reaction rates with primary amines and only these dyes (Py-1 to Py-8 and Py-20) were used as covalent labels for proteins.

The Py labels react easily with proteins but also with any other organic compounds containing a primary nucleophilic amino group. The oxonium atom in the pyrylium ring is exchanged by nitrogen to result in a pyridinium group. The Py labels undergo a significant shortwave shift of the absorption bands upon conjugation. They are virtually nonfluorescent before reaction with a primary amine but become highly fluorescent upon labeling.

The representatives of the new dye class with a sterically hindered pyrylium moiety (Py-9, Py-11, Py-12, Py-13, and Py-18) showed a strong (noncovalent) association to HSA, but no distinct spectral difference between label and conjugate. The absorption maxima shift a few nm, only, and the increase in quantum yield (QY) upon conjugation is much smaller than detected upon covalent linkage.

The spectral shift (which occurs upon conjugation of a Py label to a primary amine) and the increase of fluorescence intensity were used for qualitative and quantitative determination of proteins. Py-1 shows a short-wave shift in absorbance of over 100 nm and an increase in QY from <1% to 40-50% dependent on the dye-to-protein ratio (DPR). These properties were used for general photometric and fluorimetric protein assays. Proteins in a gel matrix (here SDS gels) can be detected very sensitively by covalent attachment of Py-1 to the protein bands separated via SDS PAGE before or if pre-stained and detected on a fluorescence scanner, after electrophoresis.

FRET-based binding studies were performed using fluorescently labeled oligonucleotides with either a Py label as a donor or acceptor, or in both positions. FRET is a self-referenced method, in which the ratio of two fluorescence intensities at one excitation wavelength can be related to the analyte. The concept of FLAA (fluorescence lifetime affinity assay) was introduced and represents a new self referenced method for detection of binding events of proteins or oligonucleotides. This affinity assay is based on the measurement of fluorescence lifetime in the ns time domain, and requires only one of the binding partners to be labeled. The decay times of the labels are dependent on their environment and therefore binding events can be detected by the change of the lifetimes. The assay was tested for the systems biotin – streptavidin, streptavidin – biotinylated BSA, IgG – anti-IgG, and complementary oligonucleotides. Assays were performed in solution and on solid supports. The labeled binding partner was attached to the well of a microplate and the analyte was added, which causes an increase in decay time. In addition, homogeneous hybridization assays with a Py-1 labeled oligonucleotide enabled the distinction of complementary oligonucleotides without, with a double or with a triple mismatch in their sequences. The label was also attached to the terminus of a hairpin oligonucleotide (a molecular beacon). The synthesis of MB with only one label is simple which is in contrast to FRET assays. Both intensity and the lifetime of the fluorescent label were found to be affected when hybridization to a complementary oligonucleotide occurred.

Py-4_acid and Py-4_C18 were used for flow cytometric measurements and in a toxicity test. The dyes showed no toxicity compared to a toxic standard reagent (staurosporin). In addition, microscopic tests of cells stained with the two dyes showed that Py-4_acid is exclusively located in the cell nucleus.

6.2. In German

Ziel dieser Arbeit war die Synthese und die spektrale und analytische Untersuchung von Pyryliumfarbstoffen (Py-Farbstoffen), die man als kovalente Biomarker und in proteinanalytischen Assays benutzen kann. Die Pyryliumgruppe wurde als neue amin-reaktive Gruppe in die Struktur von fluoreszierenden Farbstoffen eingeführt.

Jeder der hier gezeigten Farbstoffe besitzt nur eine Pyryliumgruppe und gehört entweder zur Farbstoffklasse der Cyanine oder Quadratsäurefarbstoffe. Neu an diesen Py-Farbstoffen ist, dass die reaktive Gruppe Teil des chromophoren Systems ist, wodurch sie sich von den meisten anderen Biomarkern unterscheiden. Die Farbstoffe wurden durch ihre Absorptions-

und Emissionsspektren, molaren Extinktionskoeffizienten, Quantenausbeuten und Abklingzeiten charakterisiert. Drei verschiedene Pyryliumderivate (2,6-Dimethyl, 2,6-Di-tert-butyl und 2,6-Diphenyl Pyrylium) wurden auf ihre Reaktivität mit Proteinen getestet. Nur das Pyryliumderivat mit dem sterisch kleinsten Rest (2,6-Dimethyl) zeigte eine schnelle Reaktion mit primären Aminen und nur die Farbstoffe, mit diesem Pyryliumrest (Py-1 bis Py-8 und Py-20) konnten zur kovalenten Markierung von Proteinen verwendet werden.

Py-Farbstoffe reagieren sehr einfach und schnell mit Proteinen, aber ebenso mit jedem anderen organischen Molekül, dass eine primäre Amino-Gruppe trägt. Der Sauerstoff des Pyryliumrest wird dabei durch den Stickstoff des primären Amines ausgetauscht, d.h. aus einem Pyrylium- wird ein Pyridiniumrest im chromogenen System des Farbstoffes. Aus diesem Grund ändern Py-Farbstoffe ihre spektralen Eigenschaften durch Konjugation an Amine. Das Absorptionsmaximum der Farbstoffe wird kurzwelliger, und aus einem gering fluoreszierenden reaktiven Farbstoff wird ein stark fluoreszierendes Konjugat. Die Quantenausbeuten hängen von dem jeweiligen Reaktionspartner und, im Fall von Proteinen, von dem Farbstoff-zu-Proteinverhältnis ab.

Die in der Arbeit gezeigten Vertreter der neuen Farbstoffklasse mit einem sterisch abgeschirmten Sauerstoff im Pyryliumring (Py-9, Py-11, Py-12, Py-13, Py-18) zeigen eine starke nichtkovalente Bindung an HSA. Der spektrale Unterschied zwischen Farbstoff und Konjugat, wie ihn die reaktiven Py-Farbstoffe zeigen, tritt hier jedoch nicht auf. Das Absorptionsmaximum des Farbstoffes an HSA bleibt nahezu unverändert. Die Quantenausbeute steigt zwar an, allerdings geringer verglichen mit kovalent markierten HSA-Konjugaten.

Die spektralen Unterschiede der freien Py-Farbstoffe und deren Konjugate an primären Aminen und der Anstieg der Fluoreszenz bei der Konjugation wurden zur qualitativen und quantitativen Bestimmung von Proteinen genutzt. Py-1 zeigt eine kurzwellige Verschiebung des Absorptionsmaximums von über 100 nm und einen Anstieg der Quantenausbeute, von <1% auf über 40% (abhängig von Bindungspartner und DPR) nach Konjugation. Deshalb wurde dieser Farbstoff zur photometrischen und fluorimetrischen Bestimmung von Proteinen in Lösung und in Gelen benutzt.

FRET-Messungen an fluoreszenzmarkierten Oligonukleotiden wurden entweder mit einem Py-Farbstoff als Donor oder als Akzeptor oder an beiden Positionen durchgeführt. FRET ist eine selbstreferenzierte Methode bei der das Verhältnis der beiden Fluoreszenzintensitäten (von Donor und Akzeptor) bei einer Anregungswellenlänge auf die Konzentration des Analyten bezogen werden kann.

Der FLAA stellt eine neue Methode zur Erkennung von Bindungsereignissen dar. Dieser Bindungsassay basiert auf der Messung von Fluoreszenzabklingzeiten im ns Bereich und erfordert, dass nur ein Bindungspartner fluoreszenzmarkiert ist. Die Abklingzeit der getesteten Marker ist stark abhängig von ihrer Umgebung und deshalb sehr sensitiv hinsichtlich neuer Bindungspartner. Der Assay wurde mit den Systemen Biotin - Streptavidin, Streptavidin - biotiniliertem BSA, IgG – anti-IgG, und an komplementären Oligonukleotiden getestet. Neben der Durchführung der Assays in Lösung wurden auch Assays an Festphase (Boden der Mikrotiterplatte) getestet, wobei der fluoreszenz-markierte Bindungspartner im Well immobilisiert und der Analyt zugegeben wurde. Aufgrund der Bindung des Analyten an das Fängermolekül, welches gleichzeitig zur Detektion dient, konnte eine Abklingzeitänderung des Py-Farbstoffes gemessen werden. Zudem war es in homogenen Hybridisierungsassays mit Py-1 als Marker an einem Oligonucleotid möglich, vollständig komplementäre Gegenstränge und Gegenstränge mit zwei Basen-Mißmatches voneinander zu unterscheiden. Py-1 wurde zudem an das Ende eines Oligonucleotides, das mit sich selbst die Form einer *Haarnadel* bildet, gebunden. Die Herstellung dieses *molecular beacon* (MB heißt wörtlich übersetzt molekulares Blinklicht) mit nur einem Fluoreszenzmarker ist vergleichsweise sehr einfach im Gegensatz zu zweifach markierten FRET MBs. Bei diesem einfach markierten MB konnte eine Bindung an einen komplementären Gegenstrang und damit ein Auffalten der Haarnadelform des MB, durch die Änderung der Fluoreszenzintensität und der Abklingzeit nachgewiesen werden.

Py-4_acid und Py-4_C18 wurden zu Messungen im Flow-Cytometer und für Toxizitätsuntersuchungen benutzt. Diese Farbstoffe zeigten keine Zelltoxizität. Zusätzlich wurde durch mikroskopische Aufnahmen von gefärbten Zellen gezeigt, dass sich Py-4_acid ausschließlich in den Zellkern einlagert.

7. Acronyms, Abbreviations and Nomenclature of the Dyes

7.1. Acronyms and Abbreviations

anti-HSA	polyclonal anti-human serum albumin
BCA	2,2'-bicinchoninic acid
BCB	bicarbonate buffer
BCECF AM	2',7'-bis(2-carboxyethyl)-5-(and-6-)carboxyfluorescein acetoxymethyl ester; the AM is membrane-permeant and nonfluorescent, but converts to the fluorescent BCECF by action of intracellular esterases and is therefore an indicator of cell viability
Bt	biotin
CBB	Coomassie Brilliant Blue
DCC	dicyclohexylcarbodiimide
DMF	dimethylformamide
DMSO	dimethoxysulfoxid
dsDNA	double stranded DNA
DPR	dye-to-protein ratio
em	emission maximum
ESI	electro-spray ionization
exc	excitation maximum
FACS	fluorescence-activated cell sorter
FL1	green fluorescence; signal received by the photomultiplier tube (PMT), FL1 (515-545 nm)
FL2	orange-red fluorescence; signal received by the photomultiplier tube, FL2 (564-606 nm)
FL3	red fluorescence; signal received by the photomultiplier tube, FL3 (above 670 nm)
FL4	red-range fluorescence; signal received by the photomultiplier tube, FL4 (653-669 nm)
Folin-Ciocalteu	$Na_2MoO_4 + Na_2WoO_4 + H_3PO_4$
FRET	fluorescence resonance energy transfer

FSC   forward scatter, a parameter measuring light scattered less than 10 degrees as a
              cell passes through the laser beam; the FSC measurement is related to cell size

HSA   Human Serum Albumin

m.p.   melting point

NHS   N-hydroxysuccinimide

λ_{max}^{abs} absorption maximum

λ_{max}^{em} emission maximum

OSI   oxysuccinimidyl

PB   phosphate buffer

RPM   rounds per minute

SA   streptavidin

SDS   sodium dodecyl sulfate

SSC   side scatter also called 90° scatter or right angle scatter; light scattered at a 90
              degree angle as a cell passes through the laser beam; this measurement is
              related to the internal granularity or complexity of a particle

SSC   saline sodium citrat

ssDNA   single stranded DNA

TEAA   triethylammonium acetate

TMS   trimethylsilane

TRET   time resolved energy transfer

v/m   rate of volume to mass

v/v   rate of volumes

7.2. Nomenclature of the Dyes

Py-1   2,6-dimethyl-4-[(E)-2-(2,3,6,7-tetrahydro-1*H*,5*H*-pyrido[3,2,1-ij]quinolin-9-yl)-vinyl]-
       pyranylium tetrafluoro borate

Py-2   2,6-dimethyl-4{(E)-3-[1,3,3-trimethyl-1,3-dihydro-indol-(2Z)-ylidene]-propenyl}-
       pyranylium tetrafluoro borate

Py-3   4-[(E)-2-(4-dimethylamino-phenyl)-vinyl]-2,6-dimethyl-pyranylium tetrafluoroborate

Py-4   2,6-dimethyl-4-{(E)-3-[3-methyl-3*H*-benzothiozol-(2E)-ylidene]-propenyl}-
       pyranylium tetrafluoro borate

Py-5   4-[(1E,3E)-4-(4-dimethylamino-phenyl)-buta-1,3-dienyl]-2,6-dimethyl-pyranylium
       tetrafluoro borate

Py-6   2,6-dimethyl-4-{(E)-3-[1,1,3-trimethyl-1,3-dihydro-benzo[e]indol-(2Z)-ylidene]-propenyl}-pyranylium tetrafluoro borate

Py-7   2,6-dimethyl-4-[1-methyl-1H-quinolin-(4E)-ylidenemethyl]-pyranylium perchlorate

Py-8   2,6-dimethyl-4-[3-methyl-3H-benzothiazol-(2E)-ylidenemethyl]-pyranylium perchlorate

Py-9   2,6-di-tert-butyl-4-{(1E,3E)-5-[3-methyl-3*H*-benzothiazol-(2E)-ylidene]-penta-1,3-dienyl}-pyranylium trifluoro-methanesulfonate

Py-11 2,6-di-tert-butyl-4-{(1E,3E)-5-[1-(1-sulfonyl-butyl)1*H*-quinolin-(4E)-ylidene]-penta-1,3-dienyl}-pyranylium

Py-12 2,6-di-tert-butyl-4-{(1E,3E)-5-[1-methyl-1*H*-quinolin-(4E)-ylidene]-penta-1,3-dienyl}-pyranylium trifluoro-methanesulfonate

Py-13 2,6-di-tert-butyl-4-{(1E,3E)-5-[1,3,3-trimethyl-5-sulfonyl-1,3-dihydro-indol-(2Z)-ylidene]-penta-1,3-dienyl}-pyranylium

Py-17 2,6-di-tert-butyl-4-{(1E,3E)-5-[3-(5-carboxy-pentyl)3*H*-benzothiazol-(2Z)-ylidene]-penta-1,3-dienyl}-pyranylium trifluoro-methanesulfonate

Py-18 4-{(1E,3E)-5-[3-methyl-3*H*-benzothiazol-(2E)-ylidene]-penta-1,3-dienyl}-2,6-diphenyl-pyranylium aluminium tetrachloride

Py-20 2,6-dimethyl-4-{(1-methyl-3,3-dimethyl-3H-2-indoliumyl]methylidene}-3-oxo-1-cyclobuten-1-olate}- pyranylium

8. Curriculum Vitae

Personal Data

Surname	Höfelschweiger, nee Wetzl
First name	Bianca Katharina
Date of Birth	16.12.1976
Place of Birth	Mainburg, Bavaria
Nationality	German
Address	Narzissenweg 1, 84098 Hohenthann

Education

09/1983 - 07/1987	Grund- und Teilhauptschule Rudelzhausen
09/1987 - 06/1996	Gabelsberger Gymnasium in Mainburg
06/1996	Abitur

Studies

11/1996 – 03/2001	Chemistry (Diploma) at the University of Regensburg
05/2001 – 02/2002	Diploma Work at the Institute of Analytical Chemistry, Chemo- and Biosensors, supervisor: Prof. O. S. Wolfbeis
	Subject: " New Rhodamines and Squarylium Dyes for Biological Applications"
03/2002	Academic degree of a Diplomchemikerin
since 06/2005	Ph.D. Work at the Institute of Analytical Chemistry, Chemo- and Biosensors (head: Prof. Wolfbeis)
	Subject: "The Pyrylium Dyes: A New Class of Biolabels. Synthesis, Spectroscopy, and Application as Labels and in General Protein Assay"

Extracurricular Activities

07/1996 - 04/2001	student trainee at Hydroisotop Schweitenkirchen
04/2002 - 08/2004	freelancer for Chromeon GmbH Regensburg
10/2003-09/2004	Participation at the DFG Graduate College *Sensory Photoreceptors in Natural and Artificial Systems*

9. List of Papers and Posters

9.1. Papers Published, Accepted or Submitted

B. Wetzl, M. Gruber, B. Oswald, A. Duerkop, B. Weidgans, M. Probst, O. S. Wolfbeis, Set of Fluorochromophores in the Wavelength Range from 450 to 750 nm and Suitable for Labeling Proteins and Amino-Modified DNA, J. Chromatogr. B **2003**, 793, 83-92.

B. K. Wetzl, M. Gruber and O. S. Wolfbeis, Fluoreszenter Marker für Proteine in SDS PAGE Gelen, LaborWelt **2003**, Nr. 6, Vol. 4, 41-42.

B. K. Wetzl, S. M. Yarmoluk, D. B. Craig and O. S. Wolfbeis, Chameleon Labels for Staining and Quantifying of Proteins, Angew. Chem. Int. Ed. **2004**, 43, 5400-5402; Angew. Chemie **2004**, 116, 5515-5517.

M. Gruber, B. Wetzl, B. Oswald, J. Enderlein and O. S. Wolfbeis, New Long-Wavelength Absorbing Fluorophores and Their Application to Oligonucleotide Labeling and Fluorescence Resonance Energy Transfer (FRET) Hybridization Studies, J. Fluoresc. **2005**, 15(3), 2007-2014.

L. Pfeifer, K. Stein, U. Fink, A. Welker, B. Wetzl, P. Bastian, O. S. Wolfbeis, Improved routine bio-medical and bio-analytical online fluorescence measurements using fluorescence lifetime resolution, J. Fluoresc. **2005**, accepted.

D. B. Craig, B. K. Wetzl, A. Duerkop and O. S. Wolfbeis, Determination of Picomolar Concentrations of Proteins Using Novel Amino Reactive Chameleon Labels and Capillary Electrophoresis Laser-Induced Fluorescence Detection, Electrophoresis **2005**, 26, 2208-2213.

B. K. Wetzl, L. Pfeifer, O. S. Wolfbeis, Screening Scheme Based on Measurement of Fluorescence Lifetime in the Nanosecond Domain, J. Biomol. Screening **2005**, accepted.

B. K. Hoefelschweiger, A. Duerkop, O. S. Wolfbeis, General Protein Assay Using a Chromogenic and Fluorogenic Amine-Reactive Probe, Anal. Biochem. **2005**, submitted.

B. K. Wetzl and O. S. Wolfbeis, Hybridization Assay in Homogeneous Solution and at Interfaces Based on Measurement of Fluorescence Intensity and on Fluorescence Decay Time in the Nanosecond Time Domain, Nucleic Acids Research **2005**, submitted.

9.2. Posters

B. K. Wetzl, O. S. Wolfbeis, CHROMINOBLUE: A FLUORESCENT CHAMELEON LABEL FOR PROTEINS. 8th *International Conference on Methods and Applications of Fluorescence (MAF),* August 24-27, **2003**, Prag, Czech Republic.

A. Karasyov, B. Wetzl, M. Gruber, O. S. Wolfbeis, New Benzoindole Fluorophores as alternatives to Fluorescein. 8th *International Conference on Methods and Applications of Fluorescence (MAF),* August 24-27, **2003**, Prag, Czech Republic.

B. Wetzl, R. Kromas, M. Gruber, A. Dürkop, B. Stoelcker, O. Wolfbeis, G. Brockhoff, New Long Wavelength Fluorochromes for Cytometric Analysis. *16th Heidelberger Cytometry Smposium (HCS)*, Oktober 16-18, **2003**, Heidelberg, Germany.

B. Wetzl, M. Gruber, L. Pfeifer, P. Bastian, K. Stein, O. S. Wolfbeis, Homogenous Bioassays based on Measurement of Fluorescence Lifetime. *7th MipTec Enabling Technologies for Drug Discovery*, May 3-6, **2004**, Basel, Switzerland.

B. K. Wetzl, D. B. Craig and O. S. Wolfbeis, Py-1: A Fluorescent Chameleon Label for General Protein Determination and Capillary Electrophoresis. *Deutsches Biosensor Symposium 2005 (DBS 2005)*, March 13-16, 2005, Regensburg, Germany.

Erklärung

Hiermit versichere ich, dass ich die vorliegende Arbeit selbst verfasst und keine anderen als die angegebenen Quellen und Hilfsmittel verwendet habe.

Hohenthann,

Bianca Höfelschweiger